CLIMATIC VARIABILITY AND CHANGES IN GREENNESS AND PRIMARY PRODUCTIVITY IN THE SOUTHEASTERN UNITED STATES

by

SERGIO BERNARDES

(Under the Direction of Marguerite Madden)

ABSTRACT

The Southeastern United States is home to more than 80 million people, to key agricultural areas and to numerous unique ecosystems, ranging from diverse Appalachian Mountain forests to the swamps and prairies of the Everglades. The region has been experiencing high precipitation and temperature variability, including climate extremes. Following 2006, the Southeast witnessed an exceptionally severe drought, with below-normal precipitation being recorded for multiple years. As a result, water levels fell to record lows and local terrestrial ecosystems were affected by water stress and wildfires. Droughts in the region have been frequently exacerbated by increased temperatures. Wet periods and associated floods have also affected the Southeast in the recent past (e.g., in 2003 and in 2009). Under a climate-change scenario, with increased probability of extreme events affecting unique ecosystems and society, it is critical to expand our capacity to identify, understand and act upon the biosphere's responses to future climates. In particular, the capacity to characterize vegetation responses to severe and extreme droughts and wet periods, including impacts to photosynthetic potential and primary productivity, as well as tipping points when systems collapse, are fundamental in order to develop adaptation strategies in face of a new climatic reality. This dissertation used a multi-scale, multi-temporal approach involving in-situ, remotely sensed and modeled data to characterize severe and extreme climate events (1896-2012) and vegetation status (2000-2013) over twelve states in the Southeast. Data processing included the generation of multiple descriptors (i.e., drought indices,

vegetation and water content indices, primary productivity metrics). Increased variability in the frequency of dry and wet periods were observed for several time periods analyzed (5, 10, 20 and 30 years), and multiple severe and extreme dry (1925, 1954, 1986, 2007) and wet (1973, 1983, 2003, 2009) events were identified in the region. Negative anomalies of greenness were observed following the onset of major droughts, including the 2007 drought. Primary productivity during the 21st century stayed below the region's potential for carbon uptake, and results suggest connections between reductions in productivity and water scarcity in the Southeast.

INDEX WORDS: Precipitation, Temperature, Drought, Extreme Events, Floods, Climate, Remote Sensing, Vegetation, Greenness, Plant Productivity, CO_2, Time Series Analysis

CLIMATIC VARIABILITY AND CHANGES IN GREENNESS AND PRIMARY PRODUCTIVITY IN THE SOUTHEASTERN UNITED STATES

by

SERGIO BERNARDES

BS, Viçosa Federal University, Brazil, 1991

MS, Brazilian National Institute for Space Research, Brazil, 1996

A Dissertation Submitted to the Graduate Faculty of The University of Georgia in Partial Fulfillment of the Requirements for the Degree

DOCTOR OF PHILOSOPHY

ATHENS, GEORGIA

2013

CLIMATIC VARIABILITY AND CHANGES IN GREENNESS AND

PRIMARY PRODUCTIVITY IN THE SOUTHEASTERN UNITED STATES

by

SERGIO BERNARDES

Major Professor:	Marguerite Madden
Committee:	Elgene Box Lisa Donovan Marshall Shepherd Thomas Jordan

Electronic Version Approved:

Maureen Grasso
Dean of the Graduate School
The University of Georgia
December 2013

DEDICATION

To Gabriel, Allison and Marlene

"*I do not know what I may appear to the world; but to myself I seem to have been only like a boy playing on the seashore, and diverting myself in now and then finding of a smoother pebble or a prettier shell than ordinary, whilst the great ocean of truth lay all undiscovered before me*."

Sir Isaac Newton

ACKNOWLEDGEMENTS

Multiple institutions and individuals contributed to the development of this research and I deeply appreciate their support. I thank the University of Georgia (UGA) for the opportunity and for financially supporting my studies. At UGA, I am grateful to the Graduate School, to the Department of Geography, to the Latin American and Caribbean Studies Institute (LACSI) and to the Office of the Vice-President for Research (OVPR). A very special thank you goes to the Center for Geospatial Research (CGR), my home at UGA. CGR provided me with the environment and opportunities to grow as a scientist. Hopefully, my contributions to the center will benefit others to come.

Thanks also to the National Aeronautics Space Administration (NASA) for granting me a NASA Space and Science Fellowship (NESSF), which funded most of this research. I am also grateful to the Coweeta Long Term Ecological Research Program and appreciate their support during my last year as a Ph.D. student. I would like to thank the American Society for Photogrammetry and Remote Sensing (ASPRS) and their award committee for their expressive financial contribution to this research. I also appreciate the financial support provided to this research by The United States Geospatial Intelligence Foundation (USGIF). Support was also received from the Partnerships for International Research and Education (PIRE) program, and I thank the University of Arizona and Dr. Scott Saleska for their financial assistance.

Thanks to the friends at the Center for Geospatial Research (CGR) and to the Safety Meeting Board. In particular, thanks to Hunter Allen, Ryan Lash, Shadrock Roberts and Dr. Sydney Bacchus.

I thank the staff at the department of Geography at UGA for their assistance and friendship. To Amy Bellamy, Audrey Hawkins, Dylan Tracy, Emily Coffee, Emily Duggar, Jane Worley, Jodie Guy, Kate Blane, Loretta Scott, Margaret Bolton, and Robert Phares.

I thank Dr. Thomas Mote and Dr. Marshall Shepherd for their suggestions while preparing my NESSF proposal. NESSF made this set of investigations possible and gave me multiple opportunities.

I would like to thank my committee members, Dr. Elgene Box, Dr. Lisa Donovan, Dr. Marshall Shepherd and Dr. Thomas Jordan for their patience, comments and suggestions. I am also grateful to Dr. Edward Gardiner, for his contributions during the development of this dissertation.

I thank Dr. Katia Fernandes, for the encouragement to initiate this journey, for the discussions, for the support and for the friendship.

I would like to express my gratitude to the legion of scientists, engineers and technicians who designed, implemented and maintain the data acquisition systems and the multiple data repositories used by this investigation. In particular, thanks to the United States Geological Survey (USGS) for their support and patience while I was slowing down their servers.

I am forever indebted to Dr. Marguerite Madden, my amazing advisor, who has the ability to see the positive when others cannot see. Thanks, Marguerite, for always being there to help, for your excitement and “wows”, and for believing that, yes, we should promote the crazy idea of week.

I am also thankful to my son, Gabriel Bernardes, who shared part of this journey with me while in Athens and now shares from a distance, for all his patience and love.

And last, but definitely not least, to Allison Howard, my sweet partner, for the support, for keeping me sane and for being there when I most needed.

TABLE OF CONTENTS

Page

APPENDICES

LIST OF TABLES

Page

LIST OF FIGURES

Page

CHAPTER 1

BACKGROUND AND RESEARCH SCOPE

1.1 Background

Increases in climate variability, including increases in drought frequency and severity, are expected to occur in various parts of the world under future climates. These changes can negatively affect plant metabolism, reduce primary productivity/carbon uptake, affect plant survival, change fire regimes, and limit services of entire ecosystems. Ecophysiologists have traditionally investigated plant responses to changes in water availability at fine spatial scales, particularly at the individual or stand levels. These studies often include plant responses to variations in soil moisture and may address the combined effects of reduced precipitation and high temperature on photosynthesis, productivity, phenology and others. Water stress is recognized as a primary limiting factor for plant growth, but the full extent of the interactions between changes in water availability and vegetation at landscape and regional scales is still poorly understood. In particular, we have very limited knowledge of how terrestrial ecosystems respond to stresses at different severity levels and recurrence intervals, including those responses associated with acclimation and adaptation.

The Southeastern United States (SEUS) is home to more than 80 million people, to key agricultural areas and to numerous unique ecosystems, from diverse Appalachian mountain forests to swamps and prairies in the Everglades. The region has experienced high precipitation and temperature variability over the past century, including climate extremes, and has recently witnessed an exceptionally severe drought, with below normal precipitation being recorded for multiple years. In 2007, water levels in the region fell to record lows and local terrestrial ecosystems were impacted by water stress and wildfires. Droughts in the region have been

frequently exacerbated by increased temperatures. Effects of these impacts can ripple through several connected biological systems in the Southeast, resulting in changes in primary productivity, redefinition of plant and animal geographic distribution, and massive die-back and extinction in one of the most diverse regions in the United States. Under a climate change scenario, with increased probability of extreme events affecting unique, vulnerable ecosystems and society, it is critical to expand our capacity to identify, understand and act upon environmental responses to these extremes. In particular, the capacity to characterize the biosphere's responses to droughts, floods and increased temperatures, including impacts to plant health, vigor and productivity are fundamental in order to develop adaptation strategies in the face of a new climatic reality. Further, this characterization is critical for the identification of tipping points when systems collapse. Due to its climatological history, to its diversity in land cover and to current climate projections for the 21st century, the SEUS is an ideal model system for regional studies involving the response of multiple vegetation types to climatic variability and climate extremes.

Variations in water availability to plants (including water deficit and surplus) and temperature may modify plant physiology, structure and morphology. These changes have the potential to alter how electromagnetic radiation interacts with plant material and may, therefore, be detected by sensors onboard aerial and orbital platforms. The use of remotely-sensed image data acquired at different regions of the electromagnetic spectrum, including the visible, near infrared and short wavelength infrared spectral regions, adds unique perspectives to studies involving the characterization of vegetation status. Orbital remote sensing, in particular, allows for high revisiting frequency of the area under investigation and has been used to collect data at spatial scales ranging from local to global. As a result, remote sensors have been frequently incorporated into ecophysiological studies involving the characterization of vegetated areas and the quantification of biophysical properties of vegetation.

Challenges in the use of remote sensing also exist, including those associated with the development and use of procedures for scaling-up field measurements to coarser spatial scales. Further, a recurrent concern in remote sensing is pixel contamination due to non-target sources sharing the field of view of the remote sensor. Since 2000, the availability of a series of image products derived from the Moderate Resolution Imaging Spectroradiometer (MODIS) sensor onboard NASA's Terra and Aqua satellites has invited the scientific community to address these challenges. MODIS products consider pixel contamination and image quality and have been widely used, together with field data, as part of scaling-up efforts of vegetation status, including numerical modeling.

1.2 Research Scope

This research incorporates climate, vegetation and remote sensing domains and is mainly concerned with severe and extreme events of climate, their effects on vegetation and the ability of remote sensing products and tools to detect and characterize these effects. Specifically, the studies reported by this dissertation emphasize the spatiotemporal variation of severe and extreme climate events in the SEUS, as depicted by the historical climatological record (1896-2012), including the analysis of vegetation status (greenness, water content and primary productivity) for multiple vegetation types in the Southeast. To investigate vegetation status, the studies use the entire time series (2000-2013) of several MODIS products and include carbon exchange data derived from eddy covariance techniques acquired at multiple field sites across the United States.

This dissertation document was divided into a literature review chapter, three chapters (manuscripts) reporting on individual investigations and a summary/conclusion chapter. The first manuscript (Chapter 3) describes a spatiotemporal analysis of severe and extreme dry and wet periods over 117 years in the SEUS. The second and third studies (Chapters 4 and 5) explore potential responses of vegetation to climatic events and involve different, but complementary, perspectives. In this context, the second manuscript uses orbital images to analyze changes in

vegetation greenness (photosynthetic potential) and vegetation water content descriptors over the Southeast. The third study reported by this dissertation includes a spatiotemporal analysis of changes in primary productivity over the 21st century, as well as associations between vegetation productivity and climatic events, including temporal linkages between these events and vegetation processes. The paragraphs below present an overview of each of these chapters.

Chapter 2 characterizes the area of study and synthesizes developments in scaling plant biophysical attributes and processes, emphasizing the spatial domain and considering local, regional and global levels. Different approaches exist for scaling-up, often involving modeling and the identification of relationships between biophysical variables and remotely sensed data. The text emphasizes the use of remote sensing as a tool associated with the scaling process.

Chapter 3 analyzes the historical record of water balance, considering precipitation and temperature data and investigates water availability at relatively short and long time scales. The investigation is mainly concerned with severe and extreme dry and wet climate events, thus representing both ends of the water availability gradient for the period 1896-2012. The spatiotemporal analysis includes the identification of areas and periods when these events were more severe and include trend analysis. The study supports the understanding of potential impacts of severe and extreme events on biota and ecosystem services.

Chapter 4 uses the Enhanced Vegetation Index (EVI) and the Normalized Difference Water Index (NDWI) descriptors, derived from images acquired by the MODIS sensor to investigate spatiotemporal changes in vegetation photosynthetic potential and water content in the SEUS. The study presents and discusses anomalies of greenness and water content over the region and period 2000-2013, identifying relationships between satellite-derived indices and changes in water availability represented by the Standardized Precipitation–Evapotranspiration Index (SPEI).

Chapter 5 uses a light-use efficiency model constrained by climate variables to estimate vegetation primary productivity for multiple biomes over the SEUS. The work incorporates

products derived from images acquired by the MODIS sensor during the period 2000-2013 and uses CO_2 exchange measurements from flux towers belonging to the Ameriflux network. Anomalies of productivity are identified and total carbon uptake is estimated for the region for each year during the period analyzed.

Chapter 6 summarizes this set of investigations by presenting a brief discussion on key findings for the three studies conducted as part of this dissertation work. General conclusions also are presented. Finally, the chapter introduces and discusses topics to be considered by future research dealing with estimations of biophysical properties of vegetation using remote sensing techniques.

1.3 Significance

This set of studies advances the understanding of terrestrial ecosystems and, in particular, increases our knowledge of vegetation responses to precipitation and temperature variability and severe and extreme climatic events in the SEUS. In this respect, the work contributes to the understanding of the role of the region in local, regional and global processes. Models of biosphere response to climate change require calibrated understanding of vegetation responses to both climate and disturbance, as these factors directly influence carbon fixation, energy balance and biogeochemical cycles.

Results from this dissertation contribute to the identification and understanding of future impacts of climate change on natural and managed ecosystems occurring in the SEUS. The investigation supports future research, policymaking and resource management by quantifying impacts on vegetation and by indicating critical areas and periods associated with these impacts. In this context, the work can be used to identify particularly vulnerable food and natural ecosystems and to support estimates of system vulnerabilities and risks of collapse.

This dissertation directly or indirectly contributes to answering the following critical questions:

- What are the spatial distribution, frequency and recurrence intervals of severe and extreme dry and wet climate events in the SEUS?
- How did photosynthetic potential (vegetation greenness) and plant water content indices change in the SEUS following dry and wet periods during the first years of the 21st Century?
- How did primary productivity of terrestrial systems change over the same region and period above?
- What are the temporal linkages between extreme events and responses of vegetation?
- How are growing seasons affected by extreme events of climate in the region?
- What are the effects of these events on individual natural vegetation types, on managed vegetation and on the entire region?
- What are the spatial variability, extent, frequency and magnitude of these effects?
- How does vegetation respond to normal conditions returning to the region following an extreme event?
- What are the vulnerabilities and risks to ecosystems in the region, resulting from these extreme events, particularly when considering future climates?
- What are the limits of detectability of different techniques, including remote sensing, regarding vegetation responses to extreme events? i.e., when can these responses first be identified?

1.4 Objectives

This series of studies aimed to explore spatiotemporal variations and linkages in carbon uptake, plant respiration, vegetation and drought indices using a multi-scale, multi-temporal approach involving in-situ, remotely sensed and modeled data. In particular, these investigations

had the objective to characterize the history of extreme climatic events in the SEUS and aimed to verify and quantify vegetation responses to precipitation and temperature variability in the region during the first years of the 21st Century.

As a secondary objective, efforts associated with the development of this dissertation aimed to generate a high-quality set of time series of climate and vegetation descriptors in support of future investigations. Time series generation aimed to address shortcomings of products currently available to the scientific community and incorporated quality control and recent developments in index formulation (e.g., the Standardized Precipitation-Evapotranspiration Index-SPEI). A further improvement over currently available products is represented by a refined version of MODIS primary productivity output, based on fine-resolution climate surfaces available for North America.

CHAPTER 2

LITERATURE REVIEW

This chapter introduces and reviews topics relevant to this dissertation, including the physiographic characterization of the Southeastern United States (SEUS). Remote sensing concepts are also introduced and interactions between radiation and different targets are presented. Finally, the text discusses scaling plant biophysical attributes and processes, emphasizing the spatial domain and considering local, regional and global scales. Emphasis is given to the use of remote sensing as a tool associated with the scaling process, particularly when applied to vegetation studies using products derived from the Moderate Resolution Imaging Spectroradiometer (MODIS) sensor, onboard NASA's Terra and Aqua satellites.

2.1 Physiography of the Southeastern United States

2.1.1 Land Cover

The Southeastern United States (SEUS, Figure 2.1), as considered by this dissertation, encompasses twelve states and includes Alabama, Arkansas, Florida, Georgia, Kentucky, Louisiana, Mississippi, North Carolina, South Carolina, Tennessee, Virginia, and West Virginia. The region totals approximately 1.4 million square kilometers and is physiographically defined by a variety of geological and geomorphological histories. Diversity in the Southeast translates into high landscape variability and complexity, including multiple physiographic regions in Eastern-Central United States (i.e., Atlantic Plain, Appalachian Highlands, Interior Highlands and Interior Plains). These regions are characterized by considerable internal geological and geomorphological variability, resulting in diverse textures of geomorphological features and numerous types of rock substrate, types of soils and geologic structures (Hunt, 1973). In this respect, important physiographic provinces in the Southeast include a vast low-relief coastal

plain, which extends from North Carolina to Louisiana and includes the Lower Mississippi Valley. Other notable features include the Piedmont Plateau, characterized by rolling hills topography, the mountains of the Blue Ridge, the Appalachian Plateaus, the Interior Low Plateaus and the Ozark Plateaus (Fenneman, 1946).

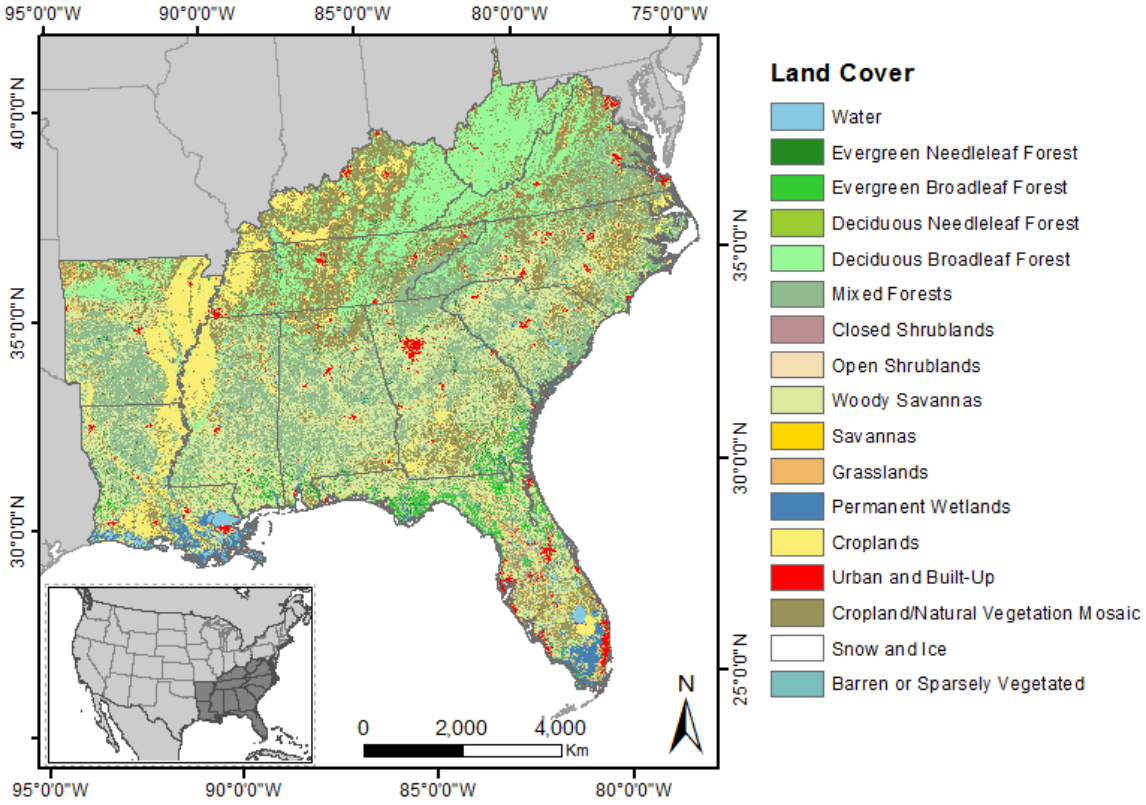

Figure 2.1: Spatial distribution of land cover classes over the Southeastern United States (data source: MOD12Q1, 2012, IGBP classification scheme).

Land cover, and particularly the vegetation cover in the region (Figure 2.1), reflects this large physiographic diversity. Multiple forest formations occur in the SEUS, including large areas of deciduous broadleaf and mixed forests (broadleaf deciduous + evergreen needleleaf forests), where oaks (*Quercus* spp.) and hickories (*Carya* spp.) are common associates. Common pine species in these regions include loblolly (*Pinus taeda*) and shortleaf pine (*Pinus echinata*), which may represent 50% of stands. Other forest expressions reflecting specific edaphic and topographic conditions and variability include mixed mesophytic hardwood forests. Evergreen broadleaf and evergreen needleleaf forests dominated by long-leaf pine (*Pinus palustris*) occur at

the south of the region of study, particularly in the coastal plain. Other well represented vegetation types include woody savannas and, to a lesser extent, permanent wetlands. The region harbors important areas for conservation, including the Southern Appalachian Mountains, one of the most biodiversity-rich temperate regions on the planet (Walker, 1991). Agriculture is an important economic activity in the SEUS and significant areas of croplands can be found in the northwest of the region, in the Mississippi Valley and along the coastal plain and in the Piedmont. The main cash crops in the region include rice, cotton, peanuts and corn (United States National Agricultural Statistics Service, 2009).

2.1.2 Climate and climatic variability

Figure 2.2 presents annual values of climatological normals for the SEUS. Monthly normals for precipitation, minimum, maximum and mean temperatures can be found in Appendix B. Normals are calculated from climate data provided by the PRISM Climate Group at Oregon State University (www.prism.oregonstate.edu, accessed on October 22, 2013). Rainfall in the SEUS ranges from 820 mm/year in the northeastern part of the region to over 2,200 mm/year in Southern Appalachia. Higher precipitation values can also be observed along the Gulf of Mexico, particularly on the western side of Florida's panhandle, as well as in the southern parts of Alabama, Mississippi and Louisiana. Most of the coastal plain receives around 1,300 mm of precipitation per year, equaling the mean precipitation for the entire SEUS. Although reductions in precipitation and dry spells occur along the year, the region has no well-defined dry season. Most of the SEUS is characterized by a humid climate, with a north-south gradient of winter temperature, from cold to mild winters. Significant spatiotemporal variability in minimum and maximum temperature occurs throughout the region and lowest temperatures can be observed at the northern section, over the highest elevations in the Appalachian Mountains. A warm extreme of the temperature gradient is represented by the tropical climate of the southern tip of the Florida peninsula, while minimum temperatures approach zero Celsius over northern-central Florida.

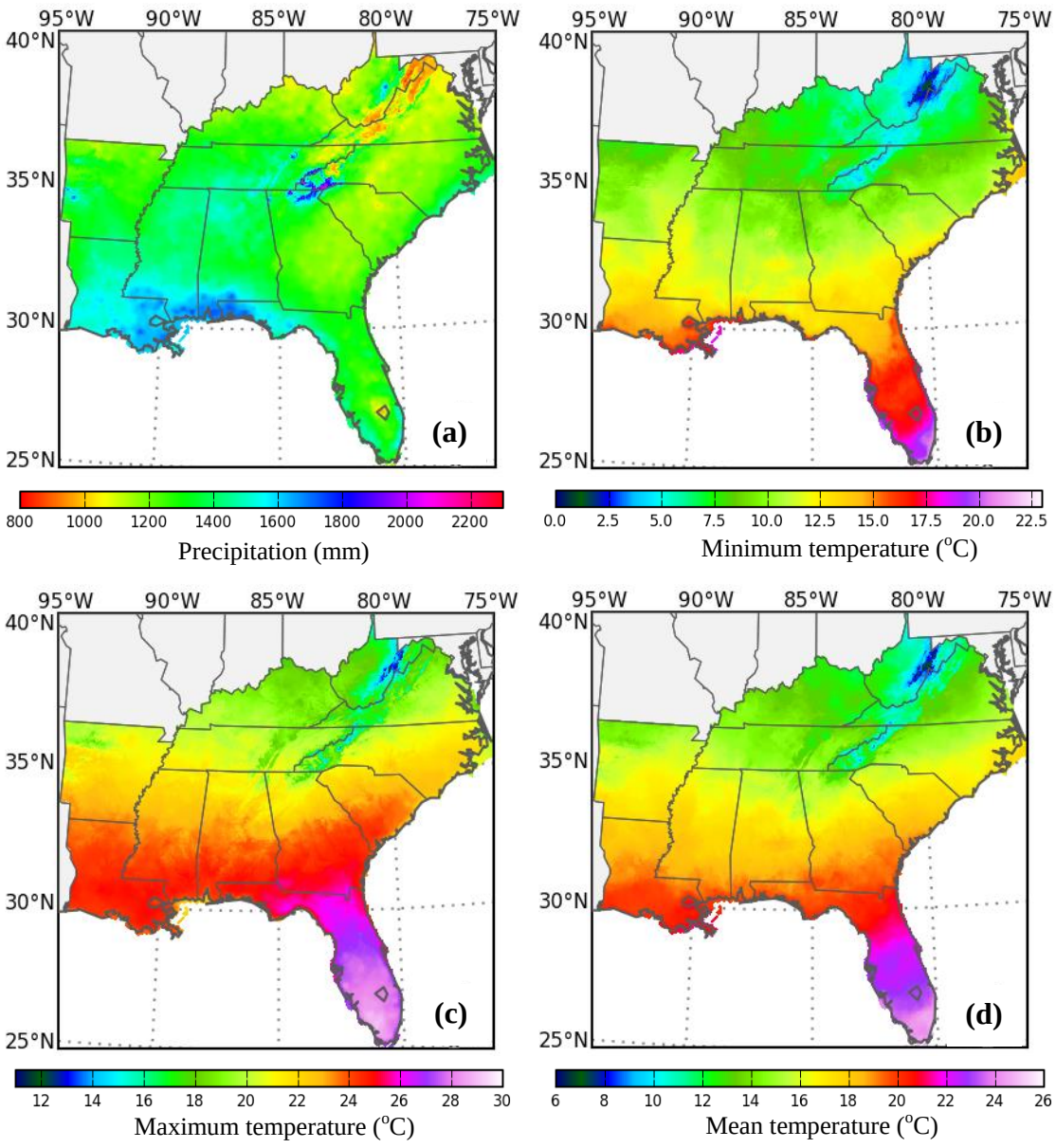

Figure 2.2: Climatological normals (annual values) for the SEUS and period 1981-2010 (a) precipitation (mm), (b) minimum temperature (°C), (c) maximum temperature (°C) and (d) mean temperatures (°C). Scale changes between maps. Data source: PRISM Climate Group.

Large-scale ocean-atmosphere dynamics acting at different time scales (i.e., interannual, decadal, to multi-decadal), have been linked to climatic variability in the SEUS, although the extent of these interactions and their effects on precipitation and temperature in the region are still not fully understood. In particular, changes in the climate system affecting moisture transport and convection, including variability in surface temperature, atmospheric pressure and the jet stream

have been correlated with climatic variability in the Southeast. Changes in atmospheric pressure in the North Atlantic and the North Atlantic Oscillation (NAO) have been demonstrated to affect the positioning of the jet stream as well as winter temperatures in the SEUS. Colder winters in the region tend to occur during the negative phase of NAO (Hurrell & VanLoon, 1997). In addition, anomalies of sea-surface temperature in the Atlantic, including the warm phase of the Atlantic Multidecadal Oscillation (AMO), have been linked to precipitation in Florida (warm phase=wet; cool phase=dry) (Enfield, Mestas-Nunez, & Trimble, 2001). Sea-surface temperature in the Atlantic has also been found to be correlated positively to the strengthening of tropical storms and to the number of severe hurricanes. Atlantic tropical cyclones play a significant role in bringing water to the Southeast and are particularly important in alleviating drought conditions in the region (Kam, Sheffield, Yuan, & Wood, 2013). In addition, the positioning of the North Atlantic Subtropical High has recently been reported to influence summer rainfall in the SEUS (Li, Li, Fu, Deng, & Wang, 2011). Through teleconnections, anomalies in sea surface pressure and temperature in the Tropical Pacific and the El Niño Southern Oscillation (ENSO) phenomenon also influence dry and wet conditions in the SEUS. Reductions in winter precipitation have been reported during the La Niña mode of ENSO, while increases in precipitation in the SEUS would be associated with the warm phase of the oscillation (Ropelewski & Halpert, 1986).

In addition to these quasi-periodic cycles involving ocean-atmosphere dynamics, internal atmospheric variability of the climate system and instances of persistent high pressure over regions in the SEUS have had strong impacts on the recent climate history of the region, including the 2007 drought (Seager, Tzanova, & Nakamura, 2009). In this respect, significant departures from normal precipitation and temperature conditions have been observed multiple times in the SEUS in recent decades. This “new normal” climatic status for the region includes intensified summer droughts (Wang, Fu, Kumar, & Li, 2010), persistent multi-year droughts (Seager et al., 2009), as well as instances of anomalous wet periods (data from the U.S. National Climatic Data Center-NCDC, http://www.ncdc.noaa.gov/cag/time-series/us, accessed on October

28, 2013). Climate projections suggest changes in precipitation during the 21st century, resulting in: (a) reduction in rainfall for most of the region during summer, winter and spring and (b) increase in precipitation during fall (Karl, Melillo, & Peterson, 2009). In addition, recent runs of general circulation models (GCMs) indicate substantial warming in temperature extremes during this century, suggesting increased likelihood that heat waves will become longer, more frequent and/or intense over most land areas (IPCC, 2012).

2.2 Remote sensing of biophysical properties of terrestrial landscapes

Remote sensing involves the acquisition of information from an object, area or phenomenon at a distance and without direct contact with the target being measured (Lillesand, Kiefer, & Chipman, 2008). Usually, remote sensors read radiant energy reflected or emitted by the target, allowing for inferences on the object's properties. Characteristics of remote sensors, including their synoptic view, their ability to periodically revisit study areas and their multispectral capabilities make these instruments powerful tools when describing the landscape. In particular, the majority of remote sensing systems have the ability to read and record radiation using regions of the electromagnetic spectrum beyond the sensitivity range of the human eye. As presented by the following section, interactions between radiation at different wavelengths and elements of the landscape (i.e., vegetation, background soil, water and others) are a function of the properties of these elements. This specificity increases our ability to discriminate and characterize different targets (Lillesand et al., 2008).

2.2.1 Interactions between electromagnetic radiation, vegetation, soils and water

Interactions between electromagnetic radiation and targets occur at multiple levels of organization and, for plants and vegetation, spectral responses are a function of physiological, anatomical and structural factors (Asner, 1998). Extrinsic factors also play a role in how these targets are perceived by remote sensors, particularly when involving target illumination and viewing geometry (Guyot, Guyon, & Riom, 1989).

To fully understand the descriptive power of remotely sensed products it is necessary to comprehend how electromagnetic energy interacts with pigments, leaves, canopies and other parts of the plant, including stems and exposed roots. It is also critical to understand radiation interactions with background features (potentially other plants, litter or soil). The following paragraphs describe these interactions.

The amount of energy penetrating a leaf and interacting with its internal structure depends on the characteristics of the leaf surface. The presence of epidermal outgrowths, for instance, may significantly increase the proportion of incident energy that is reflected by leaves, reducing the amount of radiation that is absorbed or transmitted by the plant. Some plants (e.g., *Encelia farinosa*, brittlebush) control their reflectance properties actively by increasing pubescence when illumination is more intense (Sandquist & Ehleringer, 2003). A waxy layer on the surface of the leaf may also contribute to higher reflectance. In addition, trichomes and waxy layers can contribute, respectively, to a more diffuse or specular reflection behavior of a leaf (Woolley, 1971). Other factors affecting the surface of a leaf may also contribute to alter its spectral behavior, including the presence of free water (Jensen, 2007).

In the visible part of the electromagnetic spectrum (from 0.4 μm to 0.7 μm) leaf reflectance is highly correlated to internal leaf pigment. In this region, chlorophyll a and chlorophyll b absorb energy in the blue and red parts of the spectrum (chlorophyll a presents peaks of absorption at 0.43 μm and 0.66 μm, while chlorophyll b has peaks at 0.45 μm and 0.65 μm). These pigments reflect energy in the green part of the spectrum and are the reason why we see vegetation as green. Other pigments (e.g., carotenes, xanthophylls and anthocyanins) are also present in the leaf and are usually masked by chlorophyll. Carotenes and xanthophylls absorb radiation in the blue part of the spectrum. When chlorophyll degrades during senescence, the contribution of these pigments becomes more significant and leaves gain tones of yellow and/or red (Pfündel, Agati, & Cerovic, 2006; Woolley, 1971).

In the near infrared (NIR) region (from 0.7 μm to 1.3 μm) the reflectance of leaves is dominated by the internal structure of the leaf and the multiple scattering resulting from the wall-air-water interfaces in the leaf mesophyll (primarily in the spongy mesophyll). Reflectance of healthy leaves in the NIR is particularly high (40-60%) and can be affected by the turgidity of the cells (Woolley, 1971). Although water is not the main agent interacting with radiation at this range of wavelengths, liquid water is responsible for keeping cells turgid and therefore affects leaf reflectance. Loss of water may result in a characteristic blue shift of the red-edge (interface between the red and NIR spectral region) (Jensen, 2007). The middle infrared (MIR) region of the spectrum (interval between 1.3 μm and 3 μm) is directly affected by the water content of the leaf (Woolley, 1971). Water absorbs MIR and several bands of absorption can be found in this spectral region, including those at 0.97 μm, 1.19 μm, 1.45 μm, 1.94 μm and 2.7 μm, the latter being the strongest absorption band. It is therefore expected that a decrease in water contents would increase leaf reflectance for these regions (Jensen, 2007).

The spectral response of canopies is a function, among other factors, of the amount of leaves in the canopy, which can be represented or quantified by the leaf area index (LAI) or specific leaf area (SLA). Canopy spectral response involves a succession of reflections and transmissions, where energy hitting the surface of a leaf is partially transmitted to the leaf below it. This second leaf would then reflect part of the energy back and transmit/absorb the remaining radiation (Panferov et al., 2001). In addition, spectral responses of canopies depend on leaf angle distribution, as the amount of energy reflected or transmitted by a leaf is a function of the angle between the leaf's surface and the incident energy (Guyot et al., 1989). Further, the spectral response of leaves and canopies are affected also by the viewing geometry and the spatial relationships between the source of illumination, the target (the leaf/canopy) and the sensor. Leaves and canopies are not Lambertian surfaces and therefore do not reflect radiation equally in all directions (Guyot et al., 1989).

Other elements in the field of view of the remote sensor may alter the quality and/or the amount of radiation acquired and recorded and, therefore, may affect the spectral characterization of the main target under investigation. The influence of shadows (internal to the canopy or not) and background soil on vegetation reflectance has been reported as important factors when considering the spectral responses of vegetation. Specific formulations of vegetation indices, such as the Soil Adjusted Vegetation Index (SAVI) and the Enhanced Vegetation Index (EVI), incorporate terms associated with background soil as a way to minimize this influence (Huete, Justice, & van Leeuwen, 1999). In particular, soils often affect the spectral response of vegetation directly, usually by contributing fractionally to the energy signal arriving at the sensor (Jensen, 2007). As a result, the knowledge of how soils interact with radiation assists in understanding how vegetation responses to electromagnetic energy change over different spatial and temporal scales.

In the visible part of the spectrum, factors affecting the color of the soil are the main contributors to soil spectral behavior. Among these factors, the soil's mineral composition plays an important role. For instance, the occurrence of iron (e.g., in oxisols rich in iron and aluminum sesquioxides) may result in a reddish or yellowish color, particularly when soil moisture is not high (Singh & Sirohi, 1994). The occurrence of salts, such as calcium carbonate may contribute to soils having a light tone, and therefore reflecting more equally in the visible part of the spectrum. Moisture content can change this behavior, as water tends to darken the soil, reducing reflectance (Singh & Sirohi, 1994).

The texture of soil, varying from fine, medium or coarse, also can affect reflectance. Texture is related to soil composition and finer soils have higher clay content, while coarser soils tend to have higher proportions of sand. Texture can, therefore, affect moisture content and how minerals are adsorbed to surfaces. For instance, the effect of texture/composition is particularly strong when observing the spectral response of white sands (very high reflectance). Texture can also affect how radiation is received by a sensor as it may increase specular (fine texture soil) or

diffuse reflection (coarse soil). In addition, organic matter content is also an important factor affecting soil reflectance. Organic matter darkens soils due to the organic matter itself, but also resulting from an associated increase in soil moisture (Jensen, 2007).

Soil minerals contribute to spectral responses also outside the visible region of the electromagnetic spectrum. Soil spectral curves will present mineral-specific absorption bands when these minerals are present, often assisting in the identification of rock and soil composition. Similarly to the effects of water on vegetation spectra, water absorption bands can also affect soil spectra, indicating soil moisture content (Baumgardner, Silva, Biehl, & Stoner, 1985).

2.3 Scaling vegetation biophysical properties and processes

Recent investigations have addressed the relationships and dependencies of several compartments of the geobiosphere, stressing their importance and the need for understanding the variables and processes involved at multiple spatial and temporal scales (e.g., Knapp et al., 2008; Marshall et al., 2008; Phillips et al., 2009). These studies have shown connections between different process levels, either by considering their associated spatial context (e.g., from cells to individuals; from regional to global scales) or by exploring their temporal relationships, considering very short time intervals, years and decades. This review synthesizes developments in measuring and representing plant biophysical attributes and processes at different scales, emphasizing the spatial domain and considering local, regional and global levels. Different approaches exist for scaling-up these processes, often involving modeling and the identification of relationships between biophysical variables and remotely sensed data. The text emphasizes the use of remote sensing as a tool associated with the scaling process.

Traditionally, plant-science investigations dedicated to understanding attributes and processes involving plants and vegetation have been conducted at the local or fine scale (Jarvis, 1995). As discussed by Osmond, Björkman, and Anderson (1980), these characteristics may have broad spatial and temporal ranges and have the potential to occur at a variety of structural or

organizational levels and times (Figure 2.3). Ideally, measurements of an attribute or process would be conducted accurately for the entire spatial and temporal extent of the phenomenon. This practice would eliminate the need for sampling populations or extrapolating results to other levels of occurrence in space or time (Osmond et al., 1980). Frequently, several factors prohibit these measurements, including large size of the area under investigation, remoteness of the areas (access difficulties), the impossibility of maintaining continuous measurements and limitations in instrumentation and procedures (Potapov et al., 2008).

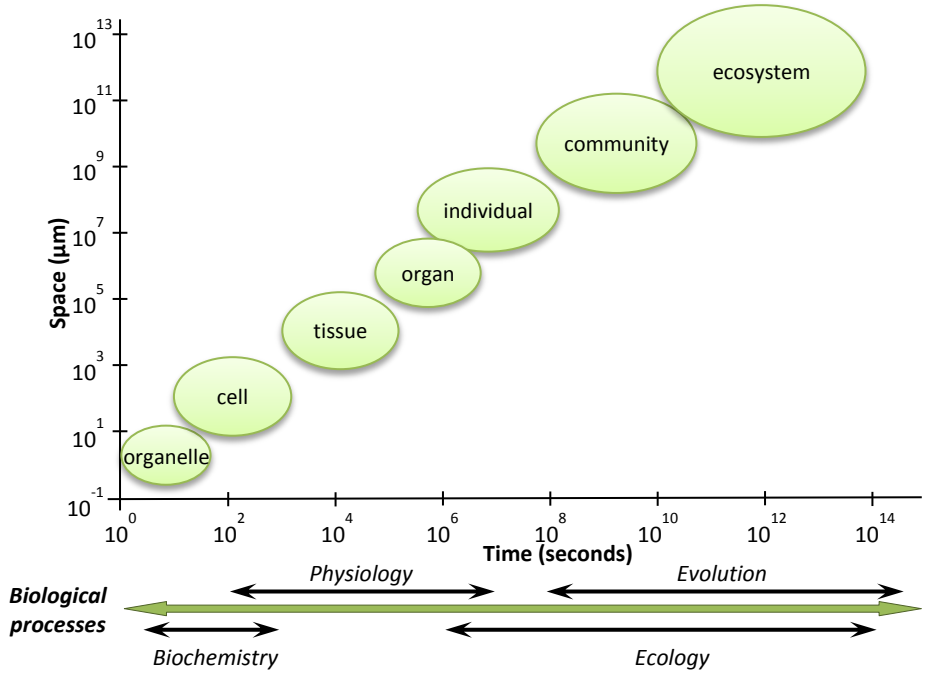

Figure 2.3: Spatial and time scales of biotic attributes and processes ranging from organelles to ecosystem (Osmond et al., 1980).

Strategies to deal with these measurement limitations consider the transformation and characterization of attributes and processes across different scales (Ehleringer & Field, 1993; Jarvis, 1995; Levin, 1992). Most frequently, scaling at the spatial level is concerned with up-scaling, or moving from a finer scale (leaf or plant) to a coarser scale (communities or even global) (Schulze, 2013). In particular, given that considerable effort has been associated with measuring quantities at a fine scale, estimating analogous quantities compatible with larger areas (e.g., region, country or globe), becomes then a problem of representation and extrapolation from

one scale to another (Jarvis, 1995). In this respect, scaling measurements requires the understanding of the variation of the quantity being scaled over the dimension considered. Measurements can vary over space, often following a gradient, with the resulting variability usually involving relationships of spatial dependency (e.g., autocorrelation) (de Knegt et al., 2009). In a similar fashion, scaling can be performed considering the time domain, for instance, through the conversion from quasi-instantaneous measurements to values representing periods of days, months or years (Levin, 1992; Schulze, 2013).

Scaling over time differs from spatial scaling, as aspects such as seasonalities, phenology and time lags may become more evident and relevant. In addition, the same phenomenon may have different expressions at different time scales. One such example is represented by differences between diurnal and weekly exchanges of CO_2 and water vapor for canopies, as factors conditioning these variations operate at different time scales (Baldocchi, Falge, & Wilson, 2001). However, although spatial and temporal scales can be seen, and treated, as separate entities, these scales are frequently interrelated, affecting each other (Caldwell, Matson, Wessman, & Gamon, 1993).

The problem of scale is thus complex, frequently incorporating both the diversity and nonlinearities of ecological processes (Field & Ehleringer, 1993). As a result, scaling-up processes often involve more than expanding or extrapolating the area (or time) where a particular attribute is verified or a process occurs. Scaling-up requires the understanding of a new dynamic involving these variables, which possibly incorporates a unique set of interactions and effects. For instance, scaling-up photosynthesis estimations from leaf to canopy level requires the consideration of particularities regarding gas exchange (e.g., boundary layer) and light attenuation, which are compatible with canopy level but which the leaf does not share (dePury & Farquhar, 1997). Moreover, the incorporation of new actors and interactions at new scale levels may result in emergent properties, increasing the complexity of the analysis. In this regard,

Schulze (2013) considers interactions between multiple scales and suggests that understanding processes at least one level lower than the scale of analysis is key to predictive modeling efforts.

2.3.1 Measuring and representing climate variables and biophysical attributes and processes at different scales

The scale dependency associated with measuring and representing biophysical attributes and processes can be explained by a series of interlinked stages or hierarchical levels (Figure 2.4). The incorporation of multiple scales into analyses then follows a sequence of connected levels of observations and strategies. When scaling-up, at each successive level the grid element associated with an observation becomes coarser and the area considered becomes larger, encompassing the previous level (Jarvis, 1995). Multiple strategies regarding the modeling and characterization of plants and vegetation are supported by data originating from these different scales. These strategies involve the resolution and understanding of a particular level, considering current target level knowledge, combined with measurements and predictions for the previous level (Jarvis, 1995; Schulze, 2013).

Approaches involving scaling a particular quantity or process, however, vary and both bottom-up and top-down methods have been employed (Caldwell et al., 1993), although not necessarily in equal proportions. The bottom-up approach usually involves the spatial generalization of locally collected/estimated measurements, often through modeling, being employed more frequently. The starting point for the scaling-up process (i.e., finest scale level considered) may vary according to the investigation conducted. Examples can be found associated with the estimation and modeling of CO_2 exchange at leaf (Chambers et al., 2004) and canopy level (Baldocchi, Falge, & Wilson, 2001; Baldocchi & Wilson, 2001; Hutyra et al., 2007), evapotranspiration (Juarez et al., 2008; F. H. Yang et al., 2006) and energy fluxes (da Rocha et al., 2004). The top-down approach supports the understanding of the problem at hand by using the coarser scale measurements (i.e., canopy, regional or global scales) in support of problem

identification and the testing of generalizations and relationships for specific cases. (Caldwell et al., 1993).

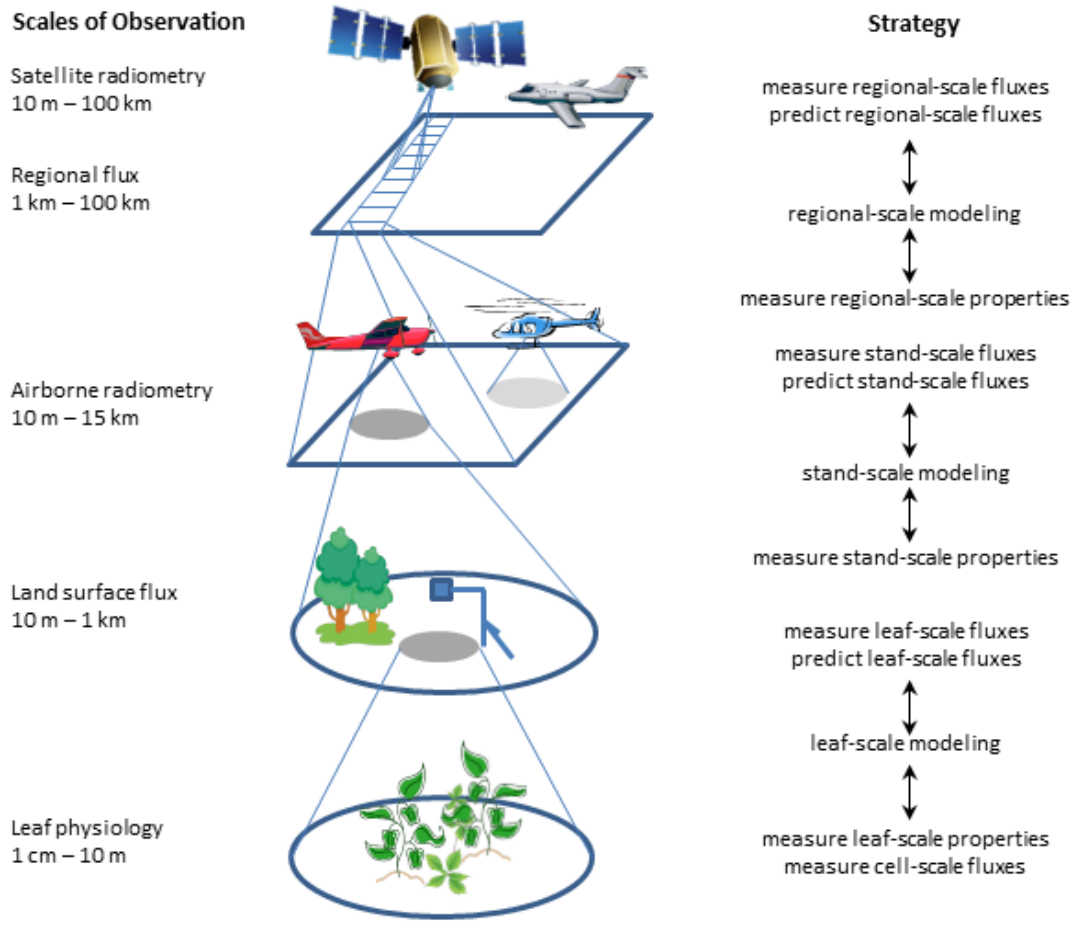

Figure 2.4: Strategies and scales of observation when scaling attributes and processes at the local, stand and regional levels (Jarvis, 1995).

2.3.2 Estimating photosynthesis and primary productivity at multiple scales

Methods to estimate photosynthetic activity at fine to landscape scales operate at the macroscopic level and can be used to analyze sections of leaves, entire leaves, plants and/or canopies. These methods often include the quantification of gas exchange (i.e., CO_2 or O_2) and make use of gas exchange systems, which can be coupled to leaves or installed above canopies and used to estimate CO_2 concentrations and gas flow, among other variables (Field, Ball, & Berry, 1989). In this respect, photosynthesis is not a quantity measured directly from leaves, but

calculated based on the concentration and flow of these gases (Field et al., 1989; Tamayo, Weiss, & Sánchez-Moreiras, 2003).

The estimation of photosynthetic activity at the level of individual plant or group of plants generally results from the quantification and modeling of photosynthesis at the scale of organelle and leaf, which can then be integrated at the level of single or multiple individuals. This procedure often involves scaling-up photosynthesis to groups of leaves, requiring the quantification of radiant energy reaching photosynthetic elements and the estimation of the photon flux density at different strata inside the canopy (dePury & Farquhar, 1997). In addition, the procedure requires the consideration of variations in physiology and photosynthetic capacity across the canopy (dePury & Farquhar, 1997; Kull, 2002). The representation of groups of leaves using a big-leaf model derives from this interpretation of photosynthetic activity and has been used widely (Dai, Dickinson, & Wang, 2004; Leuning, Kelliher, Depury, & Schulze, 1995). When employing this type of model, scaling photosynthesis up to canopy level is performed by considering the canopy as a single leaf with photosynthetic characteristics equivalent to the summation of the individual leaves for a plant or group of plants. Although convenient, it has been pointed out that this model may offer an oversimplification of the aspects regulating the photosynthetic process when migrating from single to multiple leaves (dePury & Farquhar, 1997; Kull, 2002).

An alternative technique for estimating photosynthesis for groups of plants or canopies incorporates the use of the eddy-covariance method. This technique involves measurements of gas exchange between canopies and the atmosphere, with gas fluxes being estimated by measuring the covariance between the mixing ratio of gases and fluctuations in the vertical velocity of the associated eddies (Baldocchi, 2008). When measuring these fluxes over vegetation stands, flux towers are frequently used to hold a series of instruments above the canopy. The instruments involved vary according to the purpose of the measurements but, when estimating photosynthesis, they often incorporate infrared gas analyzers (IRGA), responsible for measuring

the concentration of CO_2 in the air parcel, and three-dimensional sonic anemometers for measuring wind velocity (Baldocchi, Falge, Gu, et al., 2001). Eddy-covariance methods have been receiving great attention from the scientific community, and gas exchange estimates by flux towers have been considered as ground reference data when establishing relationships with other data sources (e.g., remotely sensed data). Data derived from eddy covariance techniques have been used extensively when scaling gas exchange, gross productivity and respiration up to regional, country and continental levels (Kim et al., 2006; Reichstein et al., 2007; Xiao et al., 2008). Eddy covariance methods are, however, affected by non-ideal acquisition conditions and have limited regional representation, being valid only for the area within the footprint of the flux tower (Chen et al., 2009; Xiao et al., 2008). These observations have direct implications to the scaling-up of quantities derived from flux towers, as these quantities become dependent on the spatial distribution of towers over a region, as well as on the representativeness of different ecosystems under study.

Remote sensing has been widely used to scale these biophysical measurements from local to coarser levels, often involving the identification of relationships between ground reference data and remotely sensed products. Among multiple other applications, this approach has been used to scale-up gas exchange measurements acquired by eddy covariance techniques (Chen et al., 2009; Kim et al., 2006). Validation efforts associated with the generalization of biophysical quantities and processes over larger areas using remote sensing involve the comparison of field measurements with the results of models or image derived products (e.g., Juarez et al., 2008; Morisette, Privette, & Justice, 2002). This approach is often affected by limited representativeness of the quantities measured by validation sites, including the reduced number and uneven spatial and thematic distribution of sites. Atkinson (1997) discusses the identification of these relationships and particularly addresses the implications of incomplete field sampling of the area seen by the remote sensor. It is noteworthy that temporal validation shares limitations with validation conducted over space, but may bring also new challenges, including the

non-availability of data for a certain period of time (Turner, Ollinger, & Kimball, 2004). This limitation involves conditions when the availability of ground reference and remotely sensed data are temporally out-of-phase and may include factors affecting the quality and usability of the acquired data.

Since the launch of NASA's Terra satellite, in 1999, several products derived from the Moderate Resolution Imaging Spectroradiometer (MODIS) sensor have been used to investigate vegetation biophysical properties and processes at regional and global levels. MODIS products have been widely used in scaling-up these properties, often employing local data collection for evaluation and validation (Justice et al., 2000; Justice et al., 1998). Due to the relevance of MODIS datasets to the investigations reported by this dissertation, descriptions of these efforts are provided below, including details about the methodology involved in the generation of these datasets.

Vegetation indices (VIs) derived from MODIS have been widely used over a range of biomes to characterize multiple vegetation biophysical attributes, including health, vigor, leaf area index and biomass (Baret & Guyot, 1991; Gao, Huete, Ni, & Miura, 2000; Tucker, 1979). These indices are also used as data input to several workflows in the generation of other MODIS products. MODIS VIs include the Normalized Difference Vegetation Index (NDVI) and the Enhanced Vegetation Index (EVI), which involve relationships between reflectance measured in the red and in the near infrared regions of the electromagnetic spectrum. The formulation of NDVI is presented below:

$$NDVI = \frac{\rho NIR - \rho Red}{\rho NIR + \rho Red}$$

where ρNIR and ρRed are reflectances in the near-infrared and red spectral regions, respectively. MODIS NDVI is considered a continuity index and the index has been reported to saturate under high biomass and leaf area conditions, with implications to the quality of analyses conducted over densely vegetated areas. To compensate for this increased sensitivity of NDVI to leaf mass,

as well as to account for contributions from residual atmospheric contamination and from canopy background, adjustment coefficients were incorporated into the formulation of EVI (Huete et al., 2002; Huete et al., 1999). EVI is presented below:

$$EVI = G \times \frac{(\rho NIR - \rho Red)}{\rho NIR + (C1 \times \rho Red - C2 \times \rho Blue) + L}$$

where ρNIR, ρRed and $\rho Blue$ are reflectance values in the spectral regions of the near infrared, red and blue, respectively. Coefficients added to EVI include a gain or scale factor (G = 2.5), a canopy background adjustment factor (L = 1) and two coefficients for the aerosol resistance term (C1 = 6 and C2 = 7.5), which corrects for aerosol influences in the red band by using the sensor's blue band.

Besides the VIs above, other MODIS-derived descriptors have been used in the characterization of vegetation; Two of these products, Leaf area index (LAI) and the fraction of photosynthetically active radiation (FPAR) absorbed by canopies, are closely related to vegetation processes associated with light use, including photosynthetic activity and primary productivity. In particular, FPAR tends to increase with higher LAI values and, due to their close relationship, these two variables are estimated by the same MODIS workflow. LAI and FPAR are derived from Bidirectional Reflectance Factor (BRF) images resulting from seven MODIS bands. The methodology employs a six-biome land cover classification and a look-up table to derive FPAR and LAI values. The procedure computes BRF's using a canopy radiative transfer model and considers a variety of canopy structures and background soil combinations. Modeled BRF values associated with different LAI/FPAR scenarios are compared to calculated BRF for 1 km resolution cells. When multiple possible solutions are found, the set of solutions is then averaged resulting in the final LAI/FPAR value. Under certain conditions the algorithm may fail to produce a result and an alternative method is used. Empirical relationships between NDVI and biome specific LAI/FPAR are then used as a backup algorithm (Myneni et al., 2002; W. Z. Yang et al., 2006).

The FPAR values generated above are input to the computation of gross and net primary productivity, with results validated against *in situ* measurements, including flux tower data (Reichstein et al., 2007; Turner et al., 2006; Turner et al., 2005). Gross primary productivity (GPP) results from a semi-empirical model based on radiation-use efficiency proposed by Monteith (1972). The method considers productivity of plants with an adequate supply of water and nutrients as being a linear function of the absorbed photosynthetically active radiation. The computation of GPP then incorporates MODIS FPAR, a land cover layer and a biome based look-up table with values of radiation conversion efficiency by vegetation. Primary productivity for each pixel of the image results from the identification of the biome for the pixel and the application of the conversion efficiency for a given FPAR. Environmental constraints, represented by non-optimal temperatures and reduced water availability, are incorporated into the methodology resulting in reduction in light conversion efficiency and GPP. The algorithm also incorporates the calculation of Net Primary Production (NPP) by subtracting growth and maintenance respiration from GPP (Running et al., 2004). A framework for the validation of MODIS products was presented by Morisette et al. (2002) employing field measurements at various locations around the globe.

References

Asner, G. P. (1998). Biophysical and biochemical sources of variability in canopy reflectance (vol 64, pg 234, 1997). *Remote Sensing of Environment, 65*(2), 225-226.

Atkinson, P. M. (1997). Scale and spatial dependence. In P. R. Van Gardingen, G. M. Foody & P. J. Curran (Eds.), *Scaling-up: From cell to landscape.* (pp. 35-60). Cambridge: Cambridge University Press.

Baldocchi, D. (2008). Breathing of the terrestrial biosphere: lessons learned from a global network of carbon dioxide flux measurement systems. *Australian Journal of Botany, 56*(1), 1-26. doi: Doi 10.1071/Bt07151

Baldocchi, D., Falge, E., Gu, L. H., Olson, R., Hollinger, D., Running, S., . . . Wofsy, S. (2001). FLUXNET: A new tool to study the temporal and spatial variability of ecosystem-scale carbon dioxide, water vapor, and energy flux densities. *Bulletin of the American Meteorological Society, 82*(11), 2415-2434. doi: Doi 10.1175/1520-0477(2001)082<2415:Fantts>2.3.Co;2

Baldocchi, D., Falge, E., & Wilson, K. (2001). A spectral analysis of biosphere-atmosphere trace gas flux densities and meteorological variables across hour to multi-year time scales. *Agricultural and Forest Meteorology, 107*(1), 1-27.

Baldocchi, D., & Wilson, K. (2001). Modeling CO2 and water vapor exchange of a temperate broadleaved forest across hourly to decadal time scales. *Ecological Modelling, 142*(1-2), 155-184. doi: Doi 10.1016/S0304-3800(01)00287-3

Baret, F., & Guyot, G. (1991). Potentials and Limits of Vegetation Indexes for Lai and Apar Assessment. *Remote Sensing of Environment, 35*(2-3), 161-173. doi: Doi 10.1016/0034-4257(91)90009-U

Baumgardner, M. F., Silva, L. F., Biehl, L. L., & Stoner, E. R. (1985). Reflectance Properties of Soils. *Advances in Agronomy, 38*, 1-44. doi: Doi 10.1016/S0065-2113(08)60672-0

Caldwell, M. M., Matson, P. A., Wessman, C., & Gamon, J. (1993). Prospects for Scaling. In R. Jacques, R. E. James, J. R. E. Christopher B. FieldA2 - Jacques Roy & B. F. Christopher (Eds.), *Scaling Physiological Processes* (pp. 223-230). San Diego: Academic Press.

Chambers, J. Q., Tribuzy, E. S., Toledo, L. C., Crispim, B. F., Higuchi, N., dos Santos, J., . . . Trumbore, S. E. (2004). Respiration from a tropical forest ecosystem: Partitioning of sources and low carbon use efficiency. *Ecological Applications, 14*(4), S72-S88.

Chen, B. Z., Black, T. A., Coops, N. C., Hilker, T., Trofymow, J. A., & Morgenstern, K. (2009). Assessing Tower Flux Footprint Climatology and Scaling Between Remotely Sensed and Eddy Covariance Measurements. *Boundary-Layer Meteorology, 130*(2), 137-167. doi: DOI 10.1007/s10546-008-9339-1

da Rocha, H. R., Goulden, M. L., Miller, S. D., Menton, M. C., Pinto, L. D. V. O., de Freitas, H. C., & Figueira, A. M. E. S. (2004). Seasonality of water and heat fluxes over a tropical forest in eastern Amazonia. *Ecological Applications, 14*(4), S22-S32.

Dai, Y. J., Dickinson, R. E., & Wang, Y. P. (2004). A two-big-leaf model for canopy temperature, photosynthesis, and stomatal conductance. *Journal of Climate, 17*(12), 2281-2299. doi: Doi 10.1175/1520-0442(2004)017<2281:Atmfct>2.0.Co;2

de Knegt, H. J., van Langevelde, F., Coughenour, M. B., Skidmore, A. K., de Boer, W. F., Heitkönig, I. M. A., . . . Prins, H. H. T. (2009). Spatial autocorrelation and the scaling of species–environment relationships. *Ecology, 91*(8), 2455-2465. doi: 10.1890/09-1359.1

dePury, D. G. G., & Farquhar, G. D. (1997). Simple scaling of photosynthesis from leaves to canopies without the errors of big-leaf models. *Plant Cell and Environment, 20*(5), 537-557. doi: DOI 10.1111/j.1365-3040.1997.00094.x

Ehleringer, J. R., & Field, C. B. (1993). *Scaling physiological processes : leaf to globe*. San Diego: Academic Press.

Enfield, D. B., Mestas-Nunez, A. M., & Trimble, P. J. (2001). The Atlantic multidecadal oscillation and its relation to rainfall and river flows in the continental US. *Geophysical Research Letters, 28*(10), 2077-2080. doi: Doi 10.1029/2000gl012745

Fenneman, N. M. (1946). *Physical divisions of the United States* (Ed. of 1946. ed.). Washington, D.C.: Geological Survey.

Field, C. B., Ball, J. T., & Berry, J. A. (1989). Photosynthesis: principles and field techniques. In R. Pearcy, J. Ehleringer, H. Mooney & P. Rundel (Eds.), *Plant Physiological Ecology* (pp. 209-253): Springer Netherlands.

Field, C. B., & Ehleringer, J. R. (1993). Introduction: Questions of Scale. In R. Jacques, R. E. James, J. R. E. Christopher B. FieldA2 - Jacques Roy & B. F. Christopher (Eds.), *Scaling Physiological Processes* (pp. 1-4). San Diego: Academic Press.

Gao, X., Huete, A. R., Ni, W. G., & Miura, T. (2000). Optical-biophysical relationships of vegetation spectra without background contamination. *Remote Sensing of Environment, 74*(3), 609-620. doi: Doi 10.1016/S0034-4257(00)00150-4

Guyot, G., Guyon, D., & Riom, J. (1989). Factors affecting the spectral response of forest canopies: A review. *Geocarto International, 4*(3), 3-18. doi: 10.1080/10106048909354217

Huete, A. R., Didan, K., Miura, T., Rodriguez, E. P., Gao, X., & Ferreira, L. G. (2002). Overview of the radiometric and biophysical performance of the MODIS vegetation indices. *Remote Sensing of Environment, 83*(1-2), 195-213. doi: Pii S0034-4257(02)00096-2, Doi 10.1016/S0034-4257(02)00096-2

Huete, A. R., Justice, C. O., & van Leeuwen, W. (1999). MODIS vegetation index (MOD 13) algorithm theoretical basis document, version 3: USGS Land Process Distributed Active Archive Center.

Hunt, C. B. (1973). *Natural regions of the United States and Canada*. San Francisco,: W. H. Freeman.

Hurrell, J. W., & VanLoon, H. (1997). Decadal variations in climate associated with the north Atlantic oscillation. *Climatic Change, 36*(3-4), 301-326. doi: Doi 10.1023/A:1005314315270

Hutyra, L. R., Munger, J. W., Saleska, S. R., Gottlieb, E., Daube, B. C., Dunn, A. L., . . . Wofsy, S. C. (2007). Seasonal controls on the exchange of carbon and water in an Amazonian rain forest. *Journal of Geophysical Research-Biogeosciences, 112*(G3). doi: Artn G03008, Doi 10.1029/2006jg000365

IPCC. (2012). Managing the risks of extreme events and disasters to advance climate change adaptation (Vol. 1, pp. 582-582). Cambridge: Cambridge University Press.

Jarvis, P. G. (1995). Scaling Processes and Problems. *Plant Cell and Environment, 18*(10), 1079-1089.

Jensen, J. R. (2007). *Remote sensing of the environment : an earth resource perspective* (2nd ed.). Upper Saddle River, NJ: Pearson Prentice Hall.

Juarez, R. I. N., Goulden, M. L., Myneni, R. B., Fu, R., Bernardes, S., & Gao, H. (2008). An empirical approach to retrieving monthly evapotranspiration over Amazonia. *International Journal of Remote Sensing, 29*(24), 7045-7063. doi: Pii 905133892, Doi 10.1080/01431160802226026

Justice, C., Belward, A., Morisette, J., Lewis, P., Privette, J., & Baret, F. (2000). Developments in the 'validation' of satellite sensor products for the study of the land surface. *International Journal of Remote Sensing, 21*(17), 3383-3390. doi: Doi 10.1080/014311600750020000

Justice, C., Vermote, E., Townshend, J. R. G., Defries, R., Roy, D. P., Hall, D. K., . . . Barnsley, M. J. (1998). The Moderate Resolution Imaging Spectroradiometer (MODIS): Land remote sensing for global change research. *Ieee Transactions on Geoscience and Remote Sensing, 36*(4), 1228-1249. doi: Doi 10.1109/36.701075

Kam, J. H., Sheffield, J., Yuan, X., & Wood, E. F. (2013). The Influence of Atlantic Tropical Cyclones on Drought over the Eastern United States (1980-2007). *Journal of Climate, 26*(10), 3067-3086. doi: Doi 10.1175/Jcli-D-12-00244.1

Karl, T. R., Melillo, J. M., & Peterson, T. C. (2009). *Global climate change impacts in the United States : a state of knowledge report*. Cambridge England ; New York: Cambridge University Press.

Kim, J., Guo, Q., Baldocchi, D. D., Leclerc, M., Xu, L., & Schmid, H. P. (2006). Upscaling fluxes from tower to landscape: Overlaying flux footprints on high-resolution (IKONOS) images of vegetation cover. *Agricultural and Forest Meteorology, 136*(3-4), 132-146. doi: DOI 10.1016/j.agrformet.2004.11.015

Knapp, A. K., Beier, C., Briske, D. D., Classen, A. T., Luo, Y., Reichstein, M., . . . Weng, E. (2008). Consequences of More Extreme Precipitation Regimes for Terrestrial Ecosystems. *Bioscience, 58*(9), 811-821.

Kull, O. (2002). Acclimation of photosynthesis in canopies: models and limitations. *Oecologia, 133*(3), 267-279. doi: DOI 10.1007/s00442-002-1042-1

Leuning, R., Kelliher, F. M., Depury, D. G. G., & Schulze, E. D. (1995). Leaf Nitrogen, Photosynthesis, Conductance and Transpiration - Scaling from Leaves to Canopies. *Plant Cell and Environment, 18*(10), 1183-1200. doi: DOI 10.1111/j.1365-3040.1995.tb00628.x

Levin, S. A. (1992). The Problem of Pattern and Scale in Ecology: The Robert H. MacArthur Award Lecture. *Ecology, 73*(6), 1943-1967. doi: 10.2307/1941447

Li, W. H., Li, L. F., Fu, R., Deng, Y., & Wang, H. (2011). Changes to the North Atlantic Subtropical High and Its Role in the Intensification of Summer Rainfall Variability in the Southeastern United States. *Journal of Climate, 24*(5), 1499-1506. doi: Doi 10.1175/2010jcli3829.1

Lillesand, T. M., Kiefer, R. W., & Chipman, J. W. (2008). *Remote sensing and image interpretation* (6th ed.). Hoboken, NJ: John Wiley & Sons.

Marshall, J. D., Blair, J. M., Peters, D. P. C., Okin, G., Rango, A., & Williams, M. (2008). Predicting and understanding ecosystem responses to climate change at continental scales. *Frontiers in Ecology and the Environment, 6*(5), 273-280.

Monteith, J. L. (1972). Solar-Radiation and Productivity in Tropical Ecosystems. *Journal of Applied Ecology, 9*(3), 747-766. doi: Doi 10.2307/2401901

Morisette, J. T., Privette, J. L., & Justice, C. O. (2002). A framework for the validation of MODIS Land products. *Remote Sensing of Environment, 83*(1-2), 77-96. doi: Pii S0034-4257(02)00088-3, Doi 10.1016/S0034-4257(02)00088-3

Myneni, R. B., Hoffman, S., Knyazikhin, Y., Privette, J. L., Glassy, J., Tian, Y., . . . Running, S. W. (2002). Global products of vegetation leaf area and fraction absorbed PAR from year one of MODIS data. *Remote Sensing of Environment, 83*(1-2), 214-231. doi: Pii S0034-4257(02)00074-3, Doi 10.1016/S0034-4257(02)00074-3

Osmond, C. B., Björkman, O., & Anderson, D. J. (1980). *Physiological processes in plant ecology : toward a synthesis with Atriplex*. Berlin ; New York: Springer-Verlag.

Panferov, O., Knyazikhin, Y., Myneni, R. B., Szarzynski, J., Engwald, S., Schnitzler, K. G., & Gravenhorst, G. (2001). The role of canopy structure in the spectral variation of transmission and absorption of solar radiation in vegetation canopies. *Ieee Transactions on Geoscience and Remote Sensing, 39*(2), 241-253. doi: Doi 10.1109/36.905232

Pfündel, E. E., Agati, G., & Cerovic, Z. G. (2006). Optical Properties of Plant Surfaces *Annual Plant Reviews Volume 23: Biology of the Plant Cuticle* (pp. 216-249): Blackwell Publishing Ltd.

Phillips, O. L., Aragao, L. E. O. C., Lewis, S. L., Fisher, J. B., Lloyd, J., Lopez-Gonzalez, G., . . . Torres-Lezama, A. (2009). Drought Sensitivity of the Amazon Rainforest. *Science, 323*(5919), 1344-1347.

Potapov, P., Yaroshenko, A., Turubanova, S., Dubinin, M., Laestadius, L., Thies, C., . . . Zhuravleva, I. (2008). Mapping the World's Intact Forest Landscapes by Remote Sensing. *Ecology and Society, 13*(2).

Reichstein, M., Ciais, P., Papale, D., Valentini, R., Running, S., Viovy, N., . . . Zhao, M. (2007). Reduction of ecosystem productivity and respiration during the European summer 2003 climate anomaly: a joint flux tower, remote sensing and modelling analysis. *Global Change Biology, 13*(3), 634-651.

Ropelewski, C. F., & Halpert, M. S. (1986). North-American Precipitation and Temperature Patterns Associated with the Elnino Southern Oscillation (Enso). *Monthly Weather Review, 114*(12), 2352-2362. doi: Doi 10.1175/1520-0493(1986)114<2352:Napatp>2.0.Co;2

Running, S. W., Nemani, R. R., Heinsch, F. A., Zhao, M. S., Reeves, M., & Hashimoto, H. (2004). A continuous satellite-derived measure of global terrestrial primary production. *Bioscience, 54*(6), 547-560. doi: Doi 10.1641/0006-3568(2004)054[0547:Acsmog]2.0.Co;2

Sandquist, D. R., & Ehleringer, J. R. (2003). Population- and family-level variation of brittlebush (Encelia farinosa, Asteraceae) pubescence: Its relation to drought and implications for selection in variable environments. *American Journal of Botany, 90*(10), 1481-1486. doi: DOI 10.3732/ajb.90.10.1481

Schulze, E. D. (2013). Large-scale biogeochemical research with particular reference to forest ecosystems, an overview. *Forest Ecology and Management*(0). doi: http://dx.doi.org/10.1016/j.foreco.2013.07.054

Seager, R., Tzanova, A., & Nakamura, J. (2009). Drought in the Southeastern United States: Causes, Variability over the Last Millennium, and the Potential for Future Hydroclimate Change. *Journal of Climate, 22*(19), 5021-5045. doi: 10.1175/2009JCLI2683.1

Singh, R. P., & Sirohi, A. (1994). Spectral reflectance properties of different types of soil surfaces. *ISPRS Journal of Photogrammetry and Remote Sensing, 49*(4), 34-40. doi: http://dx.doi.org/10.1016/0924-2716(94)90045-0

Tamayo, P., Weiss, O., & Sánchez-Moreiras, A. (2003). Gas Exchange Techniques in Photosynthesis and Respiration Infrared Gas Analyser. In M. Reigosa Roger (Ed.), *Handbook of Plant Ecophysiology Techniques* (pp. 113-139): Springer Netherlands.

Tucker, C. J. (1979). Red and Photographic Infrared Linear Combinations for Monitoring Vegetation. *Remote Sensing of Environment, 8*(2), 127-150. doi: Doi 10.1016/0034-4257(79)90013-0

Turner, D. P., Ollinger, S. V., & Kimball, J. S. (2004). Integrating remote sensing and ecosystem process models for landscape- to regional-scale analysis of the carbon cycle. *Bioscience, 54*(6), 573-584. doi: Doi 10.1641/0006-3568(2004)054[0573:Irsaep]2.0.Co;2

Turner, D. P., Ritts, W. D., Cohen, W. B., Gower, S. T., Running, S. W., Zhao, M. S., . . . Ahl, D. E. (2006). Evaluation of MODIS NPP and GPP products across multiple biomes. *Remote Sensing of Environment, 102*(3-4), 282-292. doi: DOI 10.1016/j.rse.2006.02.017

Turner, D. P., Ritts, W. D., Cohen, W. B., Maeirsperger, T. K., Gower, S. T., Kirschbaum, A. A., . . . Gamon, J. A. (2005). Site-level evaluation of satellite-based global terrestrial gross

primary production and net primary production monitoring. *Global Change Biology, 11*(4), 666-684. doi: DOI 10.1111/j.1365-2486.2005.00936.x

United States National Agricultural Statistics Service. (2009). *2007 census of agriculture. Volume 1, Geographic area series*. Washington, DC: United States Dept. of Agriculture, National Agricultural Statistics Service.

Walker, S. (1991). *Great Smoky Mountains: The splendor of the southern Appalachians*: Camelback Design Group.

Wang, H., Fu, R., Kumar, A., & Li, W. H. (2010). Intensification of Summer Rainfall Variability in the Southeastern United States during Recent Decades. *Journal of Hydrometeorology, 11*(4), 1007--1018 DI 1010.1175/2010.

Woolley, J. T. (1971). Reflectance and Transmittance of Light by Leaves. *Plant Physiology, 47*(5), 656-&. doi: Doi 10.1104/Pp.47.5.656

Xiao, J. F., Zhuang, Q. L., Baldocchi, D. D., Law, B. E., Richardson, A. D., Chen, J. Q., . . . Torn, M. S. (2008). Estimation of net ecosystem carbon exchange for the conterminous United States by combining MODIS and AmeriFlux data. *Agricultural and Forest Meteorology, 148*(11), 1827-1847. doi: DOI 10.1016/j.agrformet.2008.06.015

Yang, F. H., White, M. A., Michaelis, A. R., Ichii, K., Hashimoto, H., Votava, P., . . . Nemani, R. R. (2006). Prediction of continental-scale evapotranspiration by combining MODIS and AmeriFlux data through support vector machine. *Ieee Transactions on Geoscience and Remote Sensing, 44*(11), 3452-3461. doi: Doi 10.1109/Tgrs.2006.876297

Yang, W. Z., Huang, D., Tan, B., Stroeve, J. C., Shabanov, N. V., Knyazikhin, Y., . . . Myneni, R. B. (2006). Analysis of leaf area index and fraction of PAR absorbed by vegetation products from the terra MODIS sensor: 2000-2005. *Ieee Transactions on Geoscience and Remote Sensing, 44*(7), 1829-1842. doi: Doi 10.1109/Tgrs.2006.871214

CHAPTER 3

HISTORICAL PERSPECTIVES ON THE OCCURRENCE, VARIABILITY AND TRENDS OF DRY AND WET PERIODS IN THE SOUTHEASTERN UNITED STATES, INCLUDING SEVERE AND EXTREME EVENTS[1]

[1] Bernardes, S., Shepherd, M. and Madden, M. To be submitted to the *Journal of Climate*.

Abstract

Climatic fluctuations in the Southeastern United States (SEUS) during recent decades include intensified summer droughts, persistent multi-year droughts, as well as instances of anomalous wet periods. Climate projections suggest significant changes in precipitation in the Southeast during the 21st century. Particularly in the SEUS, these impacts have affected biota, ecosystem services, critical economical activities and the lives of almost 80 million people living in one of the fastest growing regions in the United States. This investigation used a time series of drought descriptors for twelve states in the Southeast and period 1895-2012 to understand how recent climate events compare to previous events in the region's climatological record. A probabilistic drought/water balance index (Standardized Precipitation-Evapotranspiration Index-SPEI) was investigated at multiple time scales providing a characterization of climatic variability in the region, with emphasis on the spatiotemporal variation of severe and extreme dry and wet periods. Analyses involved the spatial distribution, the intensity and the duration/temporal variability of these events, including trends and spatiotemporal patterns. The work identified the spatiotemporal distribution of dry and wet events in the region for the entire 117-year time series and characterized the occurrence and frequency of dry and wet events in the Southeast, particularly those at longer time scales. The work confirms current concerns regarding patterns and trends of recent climatic variability in the SEUS, indicating a positive trend in area affected by severe and extreme dry events. Trends showing increased climatic variability in the region in the recent past were also identified.

Keywords: drought, precipitation, drought index, time series analysis, SPEI

3.1 Introduction

The Southeastern United States (SEUS) accumulates a growing record of high variability in precipitation and temperature. Regional climatic fluctuations in the SEUS during recent decades include intensified summer droughts (Wang, Fu, Kumar, & Li, 2010), persistent multi-year droughts (Seager, Tzanova, & Nakamura, 2009), as well as instances of anomalous wet periods (data from the U.S. National Climatic Data Center-NCDC). Climate projections suggest significant changes in precipitation in the Southeast during the 21st century (Sheffield & Wood, 2008). Model outputs indicate that the region will suffer reductions in rainfall during summer, winter and spring and that increases in precipitation will be observed during fall (Karl, Melillo, & Peterson, 2009). In addition, substantial warming in temperature extremes is expected during this century, suggesting increased likelihood that heat waves will become longer, more frequent and/or intense over most land areas (IPCC, 2012).

The study of climate variability and extreme climate events is of particular significance to humanity. Adverse effects of hydroclimate and temperature extremes can ripple through multiple key biotic and abiotic systems. Particularly in the SEUS, these impacts have affected biota, ecosystem services, critical economical activities and the lives of almost 80 million people living in one of the fastest growing regions in the United States (Bernardes, Box, Jordan, & Madden, in preparation; Bernardes, Donovan, & Madden, in preparation; Ding & Smith, 2008). During the extreme drought of 2007, areas used for agriculture in the Southeast (currently approximately 34% of the region's land area) were impacted by reduced rainfall, resulting in economic losses to major field crops surpassing US$1.3 billion (Ding & Smith, 2008). During the same year, low water levels recorded in reservoirs throughout the SEUS led states to adopt and enforce water use control policies and to engage into water rights disputes (Lathrop, 2009). Extremely wet periods in the SEUS have historically received less attention than droughts, but these events also have the potential to cause considerable local and regional impacts, particularly when they result in soil saturation, waterlogging, increased stream level, mass movement and floods (Andersen &

Shepherd, 2013). The 2009 floods in Atlanta alone caused damages that may have approached US$300 million (National Weather Service, 2010).

These recent severe and extreme dry and wet periods in the SEUS have raised multiple questions, including those involving how recent climate extremes compare to previous events in the region's climatological record. Of particular interest are the spatial distribution, the severity and the duration/temporal variability of these events. In addition, potential deleterious effects in the region caused by a new atmospheric greenhouse gas concentration reality have motivated investigators to identify trends and spatiotemporal patterns associated with those extremes. This study addresses some of these questions by providing a characterization of climatic variability in the SEUS, with emphasis on the spatiotemporal variation of severe and extreme dry and wet periods in the region. In this respect, the work analyzes fine-resolution departures from normal water balance conditions in the Southeast using a probabilistic drought/water balance index for the period 1896-2012.

3.2 Study area

The spatial domain of this investigation comprises twelve states in the Southeastern United States (SEUS), covering an area of approximately 1.4 million square kilometers. Understanding climatic variability and how severe and extreme events of climate affect this region is of particular relevance, considering that 42 counties located in nine states in the SEUS were ranked among the one hundred fastest growing counties in the United States during the period 2010-2012 (data from the United States Census Bureau). Multi-billion dollar economic activities in the region include agriculture and forestry, which have suffered the effects of recent droughts. In Georgia alone, agriculture contributes US$71.1 billion to the state's economy (Georgia Farm Bureau, 2013) and production losses due to severe and extreme events surpassed US$787 million during the 2007 drought (Flanders, McKissick, & Shepherd, 2007).

The natural environment in the SEUS is characterized by high landscape variability and complexity. The region has considerable topographic variation and elevation ranges from a vast low lying coastal plain to 2,037 meters in the Appalachian Mountains of North Carolina. Most of the area of study is characterized by a humid climate, with a north-south gradient of winter temperature, from cold to mild winters. A warm extreme of this gradient is represented by the tropical climate of the southern tip of the Florida peninsula. Average rainfall reaches 1,300 mm/year, being well distributed over the year for most of the region, with no marked dry season. The region's high physiographic diversity is reflected in the distribution of a variety of terrestrial ecosystems, including zonal and azonal representatives (Hudson, 2002). Most of the SEUS is covered by a mosaic of cropland/natural vegetation, with significant natural vegetation types including mixed forests, deciduous broadleaf forests, woody savannas and evergreen broadleaf forests. Although less represented in area, savannas, grasslands, evergreen needleleaf forests and permanent wetlands also occur (data source: MODIS/Terra Land Cover Type Yearly L3 Global). Further, several areas important for conservation occur in the region, including the highly diverse Southern Appalachian Mountains (Walker, 1991), as well as extensive wetland areas.

3.3 Data

The study uses non-provisional (stable) surfaces of precipitation and temperature generated by the PRISM Climate Group at Oregon State University (www.prism.oregonstate.edu, accessed on October 22, 2013). The data, described by Daly, Neilson, and Phillips (1994), were created using the Parameter-elevation Regressions on Independent Slopes Model (PRISM) climate mapping and knowledge-based system. PRISM generates continuous grids of climate fields by considering point measurements of precipitation and temperature, a digital elevation model and expert knowledge to account for climatic variation resulting from complex factors, including coastal effects and topographic variability (e.g., rain shadows). PRISM products

considered by this work were generated using the Climatologically-Aided Interpolation (CAI) method, which is robust to variations in station data density. Surface modeling incorporated only station networks having at least multiple stations with more than twenty years of data. PRISM models climate elements at 30-degree seconds spatial resolution, with output resolution for the products used at approximately 4 km. From PRISM, this work used 118-year time series of total monthly precipitation, monthly minimum temperature and monthly maximum temperature data spanning the period 1895 to 2012.

For comparison purposes, a time series for the same period above representing yearly average values of the widely used Palmer Drought Severity Index (PDSI) for 87 climatological divisions and 12 states in the SEUS were accessed through NCDC's data portal (www.ncdc.noaa.gov/cag/time-series/us, accessed on October 20, 2013). PDSI was proposed by Palmer (1965) and indicates cumulative drought or abnormally wet conditions based on water balance and departures of the expected moisture supply for a given location. The index considers water input and output by incorporating water supply (precipitation), demand (evapotranspiration) and loss (runoff) (Szep, Mika, & Dunkel, 2005). Soil moisture is incorporated into computations by explicitly considering soil water storage and the stratification of the soil volume into two layers. PDSI implementation considers that the soil bottom layer receives water after the top layer is saturated (field capacity = 25 mm). Water loss by evapotranspiration is estimated when potential evapotranspiration, calculated by the Thornthwaite method, exceeds precipitation for a given month. The PDSI classification scale suggested by Palmer (1965) is presented in Table 3.1.

Table 3.1: Categories of wetness and dryness and corresponding value ranges for the Palmer Drought Severity Index (PDSI) and for the Standardized Precipitation-Evapotranspiration Index (SPEI).

Categories	PDSI[1]	SPEI[2]
Extremely wet	≥ 4.0	≥ 2.00
Very/severely wet	3.00 to 3.99	1.50 to 1.99
Moderately wet	2.00 to 2.99	1.00 to 1.49
Slightly wet	1.00 to 1.99	-
Incipient wet spell	0.50 to 0.99	-
Near normal	0.49 to -0.49	0.99 to -0.99
Incipient drought	-0.50 to -0.99	-
Mild drought	-1.00 to -1.99	-
Moderate drought	-2.00 to -2.99	-1.00 to -1.49
Severe drought	-3.00 to -3.99	-1.50 to -1.99
Extreme drought	≤-4.00	≤-2.00

[1] source: Palmer (1965).
[2] based on categories of dryness proposed for the Standardized Precipitation Index (SPI) by McKee, Doesken, and Kleist (1993).

3.4 Methods and data analysis

Investigations have pointed out several limitations of PDSI, including its use of a single time scale (reported to be between nine and twelve months); the residual influence of conditions preceding this time scale; the challenges in comparing PDSI from multiple locations; as well as concerns associated with the development of the PDSI model by using a small set of stations located in Iowa and Kansas (Alley, 1984; Guttman, 1998). From an implementation perspective, PDSI requires soil information compatible with the spatial scale being investigated, which may not always be available.

Studies also have indicated that different components of the geobiosphere respond to reduced water availability at scales shorter than nine months (Vicente-Serrano et al., 2012; Vicente-Serrano et al., 2013). More recently, attempts to overcome PDSI limitations have produced drought indices based on water balance and incorporating precipitation and temperature at multiple time scales. These attempts include the Moisture Balance Drought Index or MBDI (Ellis, Goodrich, & Garfin, 2009) and the Standardized Precipitation-Evapotranspiration Index or SPEI (Vicente-Serrano, Beguería, & López-Moreno, 2010). SPEI is a probability index

representing departures from normal water balance, which can be estimated for multi-month time scales. The index incorporates time series of precipitation and temperature and allows for the comparison of water balance departures for different locations. SPEI does not consider soil information, but contrary to the also widely used Standardized Precipitation Index-SPI (McKee et al., 1993), it accounts for changes in temperature, an important component of terrestrial water balance. This investigation used PRISM data to calculate SPEI at multiple time scales (3, 6 and 12 months). Potential evapotranspiration (PET) used by the SPEI algorithm was computed based on considerations presented by Lu, Sun, McNulty, and Amatya (2005) and their work on comparing six PET formulations for the SEUS. The Hamon method was observed to correlate well with actual evapotranspiration and was recommended for watershed-scale applications in the Southeast. Average daylength required by the Hamon method was computed by implementing the Center for Biosystems Modelling (CBM) model proposed by Forsythe, Rykiel, Stahl, Wu, and Schoolfield (1995). SPEI calculations used water balance (precipitation minus potential evapotranspiration) and considered the probability of a given water balance value to occur at a given location. Index computation involved the fitting of a time series of monthly water balance values to a log-logistic distribution considering a 118-year calibration period and the representation of balance distribution as a cumulative probability function. The cumulative probability log-logistic function was then normalized (mean=0, standard deviation=1). SPEI represents water balance departure from the mean in units of standard deviations (Table 3.1), and can be used in comparisons over space and time.

3.5 Results and discussion

Figure 3.1 shows time series of anomalies of precipitation and temperature, as well calculated indices for the entire SEUS region and period 1896-2012. Considering that different compartments of the geobiosphere are affected by dry and wet events at different time scales,

SPEI is presented at 3-, 6- and 12-month time scales. Year-to-date averages of PDSI for December also are shown.

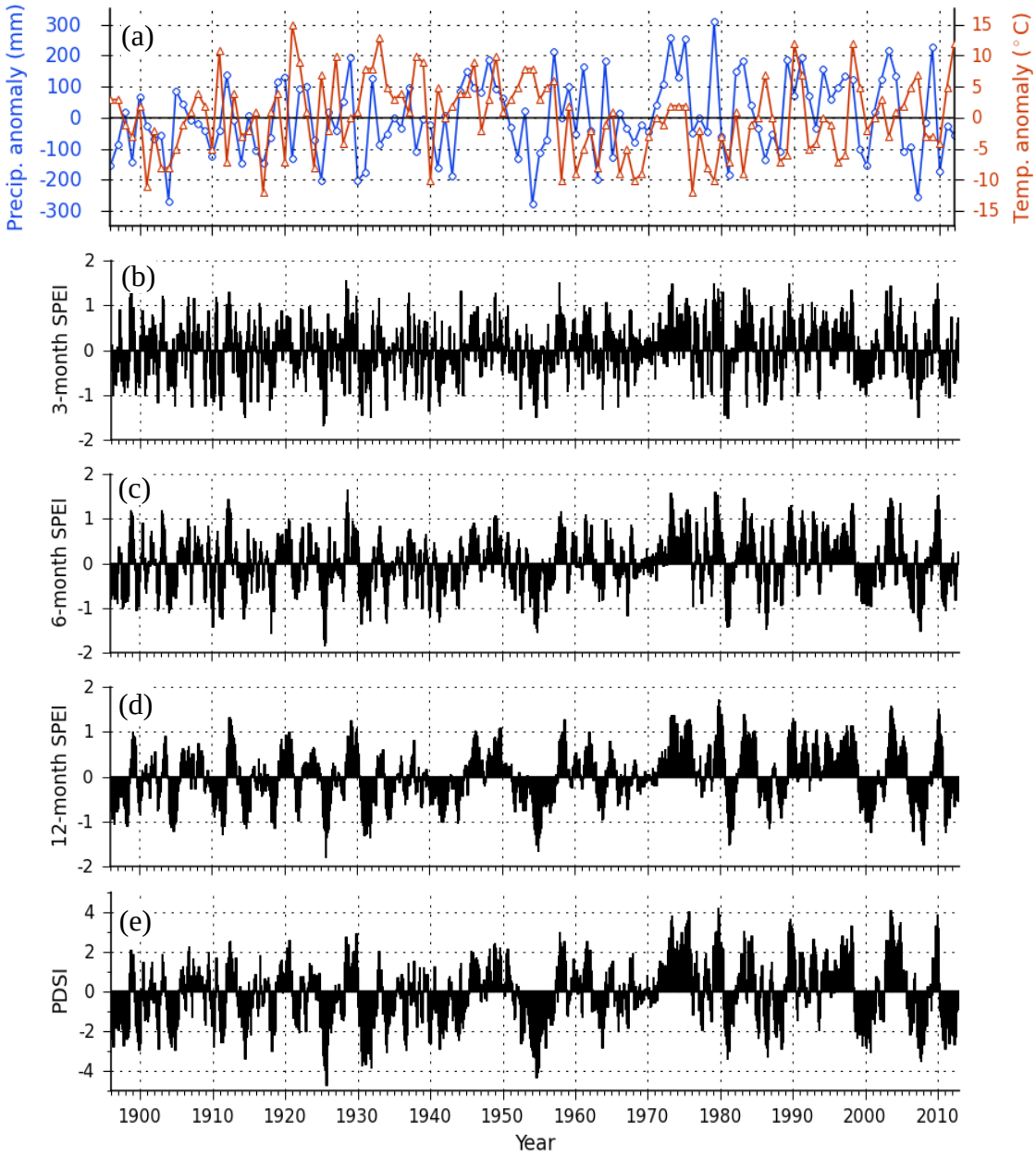

Figure 3.1: Time series of climate variables, SPEI and PDSI for the period 1896-2012, including (a) annual total precipitation anomaly (blue, circle markers) and annual average temperature anomaly (red, triangle markers); (b) 3-month SPEI; (c) 6-month SPEI; (d) 12-month SPEI and (e) year-to-date average of PDSI for December. Anomalies and indices were calculated for the entire spatial domain.

The historical record shows drops of yearly total precipitation in relation to mean values approaching 300 mm in multiple occasions in the SEUS. Often, precipitation reduction was

accompanied by positive anomalies in temperature, with few significant exceptions (e.g., 1904), when rainfall and temperature anomalies agreed in signal. Considering combined effects of precipitation and temperature, particularly significant dry events would have happened in the beginning of the 1930's, in the mid-1950's and in 2006-2007. Reported severe droughts in the SEUS during the 1980's also have a strong precipitation-temperature anomaly signal at the regional level. In the wet end of the spectrum, the 1970's experienced particularly high positive anomalies of precipitation, while temperatures stayed near or below normal levels. Also noticeable are the recent two wet periods in the SEUS (2003 and 2009), which caused significant damage due to floods in the region.

SPEI at all time scales and PDSI indicated high variability in water status for the region, which included multiple instances of dry and wet periods. The temporal distribution of these events shows considerable amplitude variation and multiple sharp transitions between consecutive months for shorter time scales of SPEI. For these short temporal scales, a dry (wet) period can end if water balance is high (low) enough for a month. Short time scales, therefore, tend to capture transient conditions, which often were observed to emerge again after a few months. Conversely, longer time scales of SPEI are less sensitive to short-term variations in water balance (i.e., short-lived dry spells or heat waves) and associated SPEI levels tend not to represent these events. Strong agreement between 12-month SPEI and PDSI confirms observations that the latter captures water availability at longer time scales. These findings also suggest that PDSI is particularly sensitive to precipitation and temperature and that, despite its non-incorporation of soil moisture, SPEI is comparable to more complex indices. Implications of the observed temporal relationships are many and include those related to water quantity and quality, as well as the effects of water balance variability on terrestrial ecosystems and crops in the region.

Dry periods are a common climatic feature in the SEUS. Considering the 3-month SPEI time scale, moderate or worse drought conditions (SPEI $\leq$ -1) occurred in all thirteen complete and incomplete decades falling inside the 1896-2012 period analyzed. Six of these decades

showed SPEI at severe drought levels. For the 12-month time scale, such low SPEI values were not observed only for the 1960's, the 1970's and the 1990's. In addition, severe or extreme droughts were observed in 1925, in 1954 and in 2007. Further, the 3-month SPEI series shows significant wet periods occurring in all decades in the SEUS. Four of these decades did not have 12-month SPEI at the moderately wet level, although this time scale captured a severely wet period in 1979, which was not identified by the 3-month SPEI. Mainly due to the wet periods in the 1970's and in the 1990's, the first half of the 117 years analyzed had more instances of shorter dry periods than the second half.

Notable periods for these series also include multi-year dry periods in the 1930's, in the 1950's and following 1998 to present. The 1920's showed extremes of both dry and wet conditions, and included the largest amplitude of 3-month and 6-month SPEI for all decades analyzed. In 1925, SPEI showed a sharp decrease to the lowest levels observed in the series. Three years later, indices indicate near normal conditions in the region. Although comparable in severity to droughts occurring in the 1950's, the 1920's drought was relatively short lived. At the 12-month time scale, significant negative anomalies in water balance are shown for 1925, 1930-1931, 1954, 1980-1981 and 2007, although amplitudes were generally smaller than those for shorter intervals. Wet analogs of the anomalies above are represented by 6-month SPEI indicating severely wet years occurring in 1911-1912, 1928 and multiple times following the 1970's. The 1980's, in particular, experienced swings of water balance anomalies that resemble recent conditions for the region, with 2-3 year wet and dry periods alternating in time. In this respect, dry and wet periods with approximately similar durations characterize the 21st century, although the SEUS has experienced more dry periods than wet periods since 2000. It is noteworthy that the choice of time scale affects the recorded duration of a given event, as well as its associated severity level.

Figure 3.2 shows the spatiotemporal variability in monthly SPEI values for the 3-month time scale and period 1896-2012. Image rows at the finest granularity (pixel level) represent 87

National Oceanic and Atmospheric Administration-NOAA's climate divisions, which are stacked by state and sorted by division identification number (a climate division map is provided in Appendix C). The distance in units of standard deviations from mean water balance values are indicated by shades of red (dry periods) and shades of blue (wet periods).

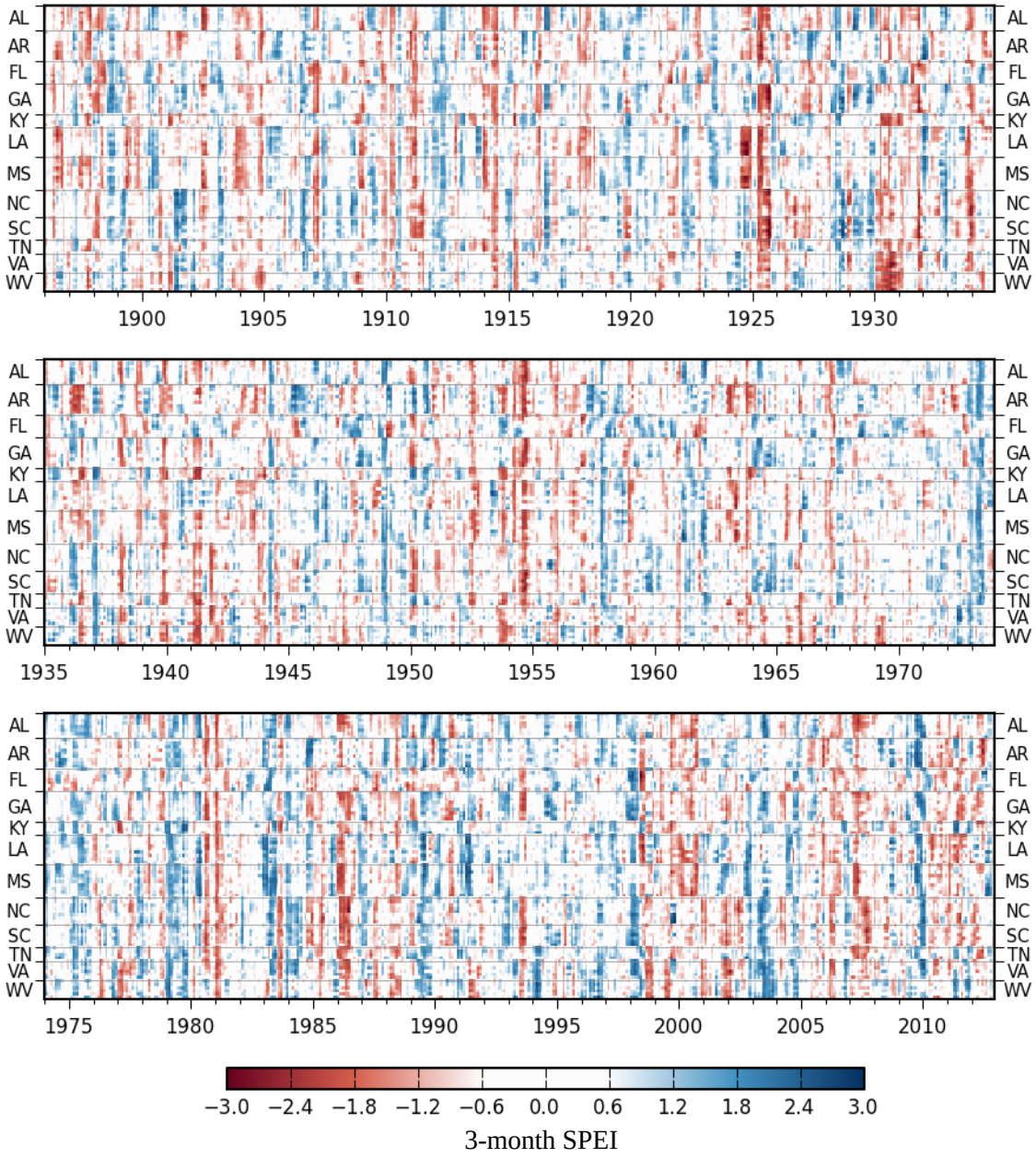

Figure 3.2: 3-month SPEI values for climate divisions and states in the SEUS and period 1896-2012. Red tones = dry conditions; blue tones = wet conditions. Tick marks represent the beginning of the year.

Dry and wet periods in the SEUS occurred locally, at the division and at the state levels (e.g., North Carolina/1973 and Florida/1982). Multiple instances of these events affecting most of the Southeast were also observed. On the dry side of the water balance gradient, droughts in 1925 were particularly severe for most of the region, with exception of Florida. During this year, water availability was particularly limited in Louisiana and Mississippi, as both states had already experienced a severe drought in 1924. Overall, dry conditions in 1925 were relatively short lived. Particularly severe dry conditions were observed also in 1930 for Virginia, West Virginia and Kentucky, with other states being comparatively less affected by reduced water balance. During the following years, several states were hit by widespread droughts multiple times, with particularly severe events occurring in 1933-1934, in 1936 and in the beginning of the 1940's. In 1953-1954, particularly severe dry conditions affected most of the Southeast and reductions in SPEI were particularly strong during mid-1954. During these events, dry conditions affected mainly the central part of the region and states located at the northern and southern limits of the SEUS were less affected. Also noticeable is a significant dry event affecting most of the region in 1986, when dry conditions were, for the most part, restricted to the first half of the year. Following 1998, multiple dry events can be observed, particularly for the period 1998-2000 and following 2006. A recurrent drought pattern for multiple states can be observed in the 2000's, although dry episodes during this decade presented reduced severity when compared to other events in the series (e.g., 1925 and 1954).

Multiple instances of wet periods were observed affecting large areas in the SEUS, particularly for the 1896-1934 and for the 1974-2012 periods. In particular, the 1970's and the 1990's are shown as considerably wet, with significant events of above normal SPEI values including large areas in 1973, 1975, 1978 and in 1998. Recent wet conditions in the region are captured by particularly elevated SPEI for 2003 and during the winter of 2009-2010. Examples of relatively normal or neutral periods ($-1 < SPEI < 1$) are equally frequent in the time series.

However, with exception of the second half of 1981 and 1982, this neutral condition was not frequent for an entire year or for multiple years, when considering the entire Southeast.

Figure 3.3 shows spatiotemporal variability for SPEI values calculated at the 12-month time scale for the period 1896-2012. The 12-month SPEI captured a larger number of multi-year dry and wet events, when compared to the shorter time-scale index. Short-lived events, such as the droughts observed for Louisiana and Mississippi in 1925 tended not to be individually represented and a longer drought was evident. At the 12-month scale, dry conditions in these states were a continuum, starting in 1924. Further, besides changes in affected area when considering the 3-month and the 12-month time scales, changes in severity also were observed. The 12-month drought occurring in 1930 in Virginia and West Virginia showed increased departures from normality, and these events were substantially more severe for larger areas. Also noticeable is the time shift between scales. Conditions of a wet January in 1930 are not considered during the computations of the 3-month indices for April the same year. However, water balance values for January will contribute to 12-month SPEI values until December the same year. These observations affect index interpretation and inferences regarding water availability to different components of the landscape. In this regard, a better understanding of these multi-scale relationships seems to be achieved when more than one time scale is incorporated into analyses.

Finally, if the 12-month SPEI time series is divided into three periods (1896-1934, 1935-1973 and 1974-2012), the SEUS was less under the effects of dry or wet conditions in the beginning of the series. Before the 1930's, long periods of near normal conditions were observed for large areas in the Southeast. However, areas under normal conditions are less significant for subsequent periods.

Figure 3.3 also suggests a comparative increase in the severity and area affected by wet episodes for 1974-2012. In this respect, patterns of wet events include the 1970's and the 1990's, while the 1980's and the years following 2000 have seen both ends of the SPEI gradient.

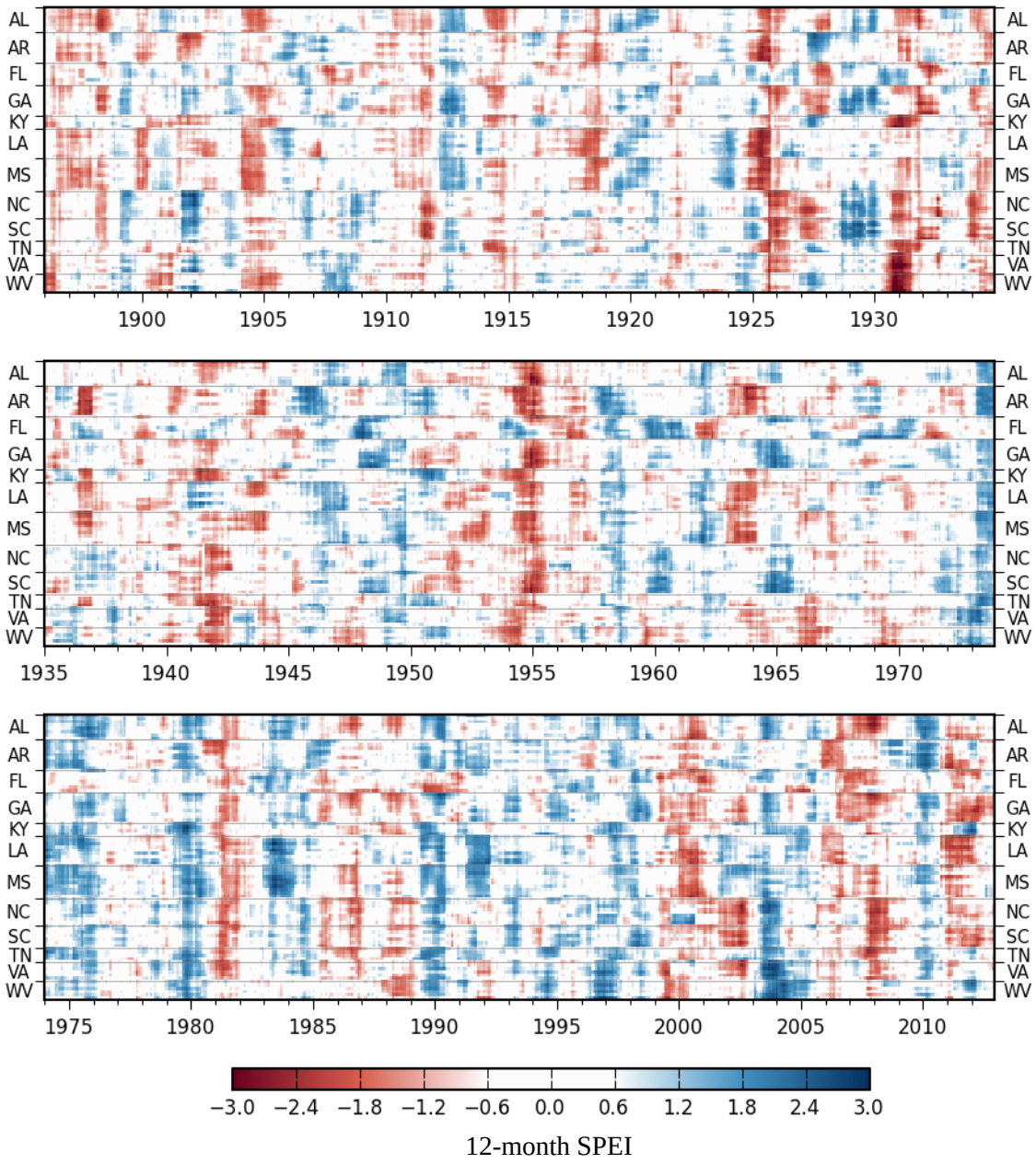

Figure 3.3: 12-month SPEI values for climate divisions and states in the SEUS and period 1896-2012. Red tones = dry conditions; blue tones = wet conditions. Tick marks represent the beginning of the year.

The frequency of dry (SPEI ≤ -1) and wet (SPEI ≥ 1) months in the SEUS was investigated further by identifying percentages of months under dry or wet conditions, as indicated by 3-month and 12-month SPEI (Figure 3.4). Considering the entire time series, dry and wet conditions affected the region at relatively similar proportions and reduced differences were

observed between time scales, although changes in spatial patterns were verified. For a large fraction of the Southeast, dry or wet conditions were observed to occur less than 18% of the months investigated. Percentages of months under wet conditions were slightly higher than those observed for dry conditions for the 3-month time scale and for some areas represented by the 12-month time scale. Higher frequency of dry conditions, as indicated by 12-month SPEI, were observed particularly for northern Florida, Georgia and South Carolina, while the lowest values were found mainly in Kentucky (3-month SPEI), Arkansas and South Carolina (12-month SPEI). Although not continuously, the region was under drought for a total period of 16.3 to 24.4 years out of the 117 years analyzed. Wet periods affected the region from 16.9 to 24.2 years.

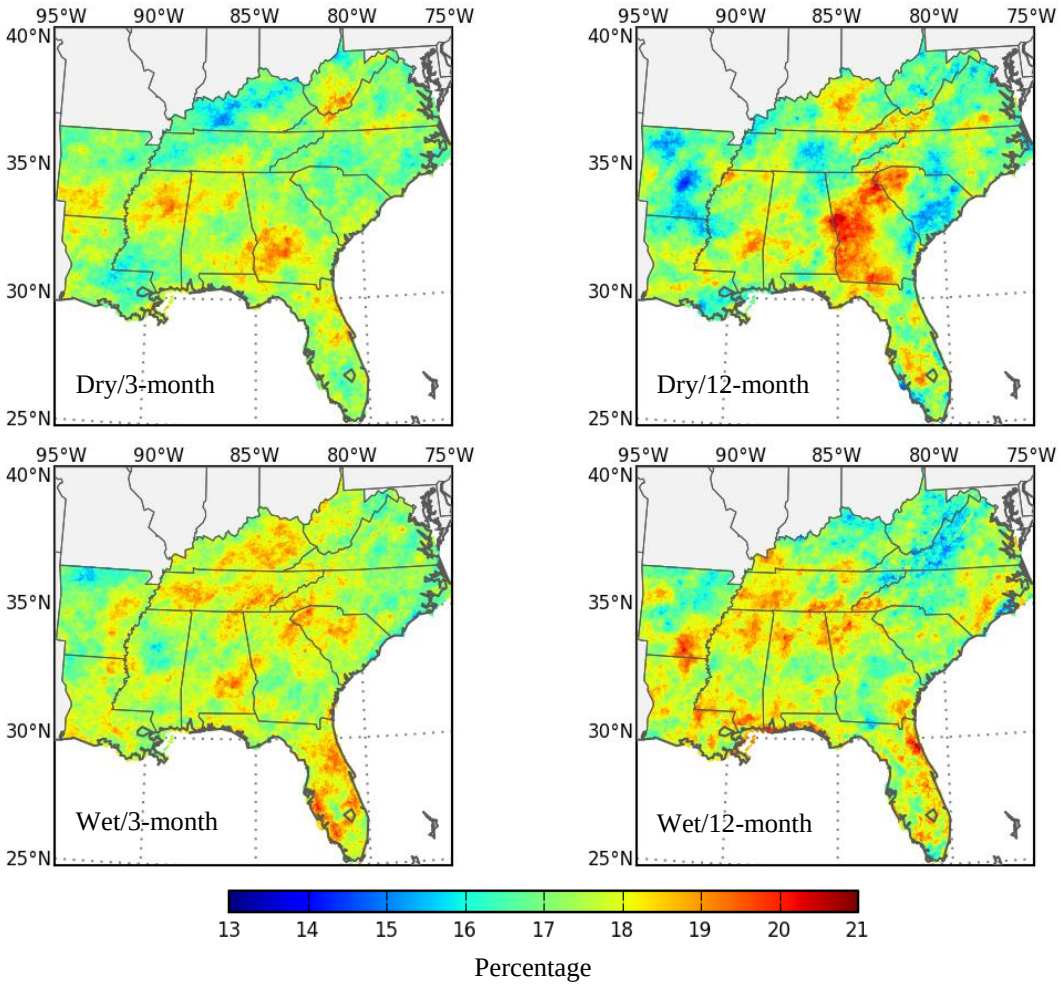

Figure 3.4: Percentage of dry (SPEI ≤ -1) and wet (SPEI ≥ 1) months for 3-month and 12-month SPEI, for the SEUS (period 1896-2012).

Considering concerns regarding the recent climatic history of the SEUS, including the frequency of dry and wet events, percentages of months under dry and wet conditions were calculated also for the period 1974-2012 (Figure 3.5). During this 39-year interval, the eastern portion of the region has experienced dry months at frequencies twice or higher than states to the west and north. Wet months were particularly common in the states in the west, as indicated by the 12-month SPEI. Percentages for the 12-month time scale of SPEI were particularly higher than those observed for the 3-month time scale, suggesting that multiple short-lived dry and wet periods were captured as a single event by SPEI.

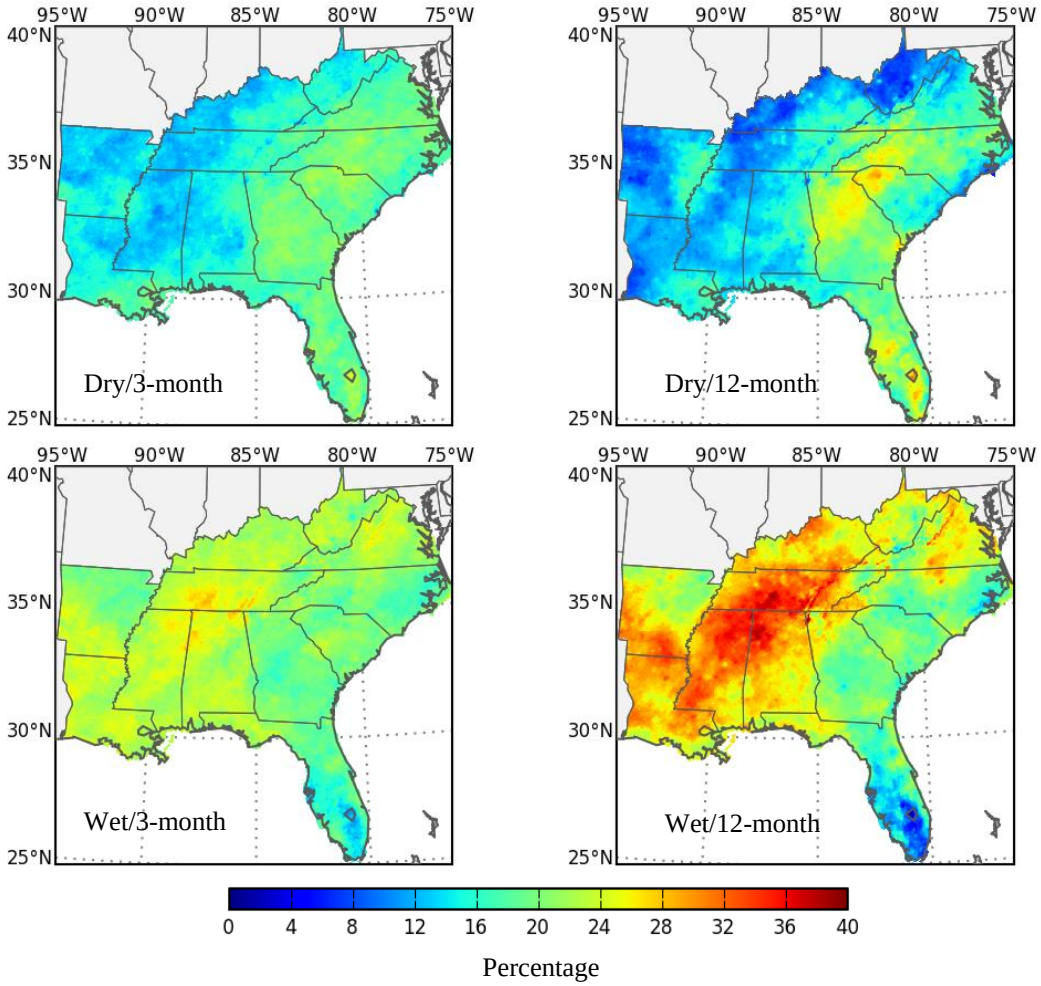

Figure 3**.5:** Percentage of dry (SPEI ≤ -1) and wet (SPEI ≥ 1) months for 3-month and 12-month SPEI, for the SEUS (period 1974-2012).

Relatively small differences exist between frequencies of severe and extreme dry and wet months when the entire time series is considered (Figure 3.6). Again, variations in spatial patterns could be verified associated with SPEI time scales and the thresholds used. SPEI values calculated for 3-month and 12-month scales show that, for most of the region, severe and extreme dry conditions (SPEI ≤ -1.5) affected less than 7.2% of the 1,404 months considered. Severe and extreme wet months (SPEI ≥ 1.5) were more frequent than severe and extreme dry months for most of the SEUS, approaching 10% of the months analyzed, particularly in Mississippi and in Arkansas.

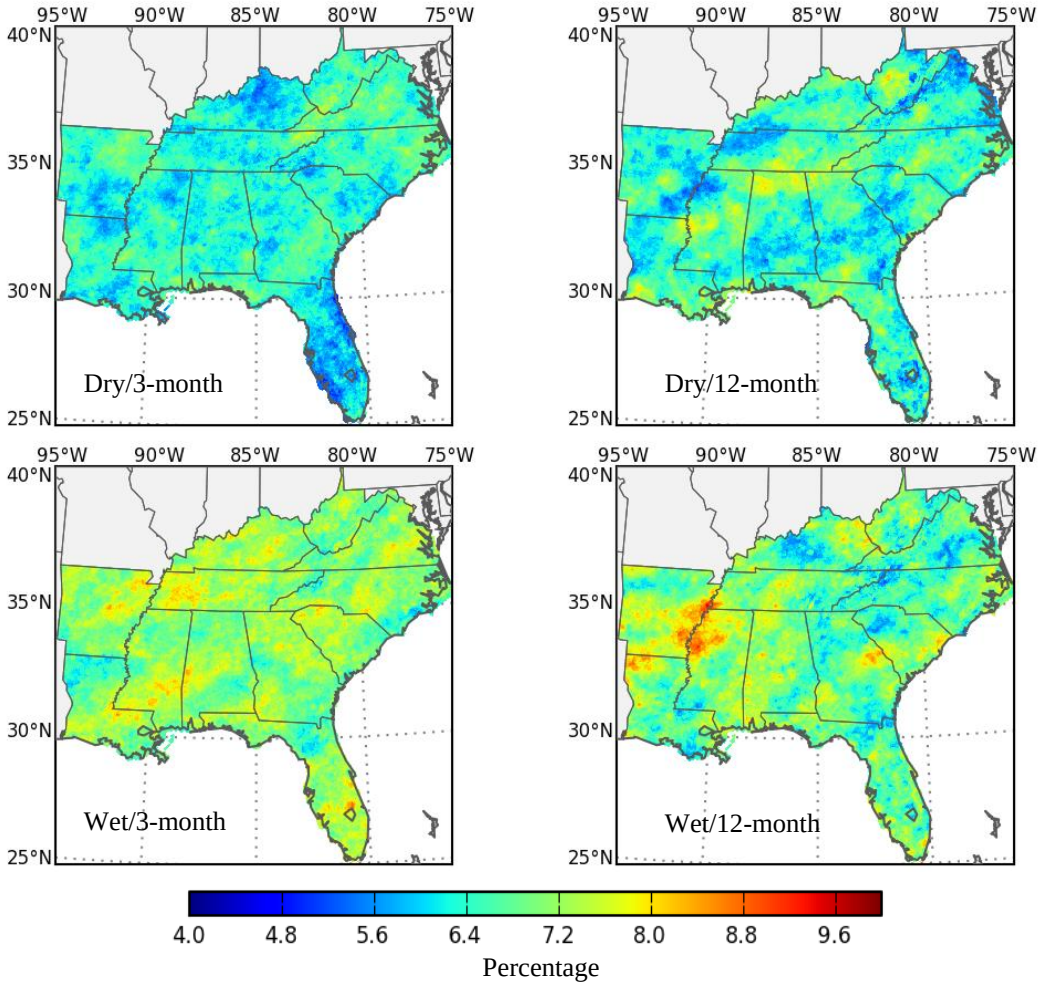

Figure 3.6: Percentage of severe and extreme dry (SPEI ≤ -1.5) and wet (SPEI ≥ 1.5) months for 3-month and 12-month SPEI, for the SEUS (period 1896-2012).

Higher frequencies of severe and extreme dry months (SPEI ≤ -1.5) and of severe and extreme wet months (SPEI ≥ 1.5) were observed when a subset of the entire time series (1974-2012) was analyzed (Figure 3.7). Overall, severe and extreme wet months were more frequent than severe and extreme dry months, considering both time scales of SPEI (exceptions included Florida and 12-month SPEI). Notable features for this 39-year interval include higher frequencies of severe and extreme dry months in the eastern portion of the SEUS, including the Carolinas, Georgia and Florida, where frequencies approached 13%. Conversely, severe and extreme wet months were more frequent in the western and northwestern portions of the region, particularly for the 12-month SPEI.

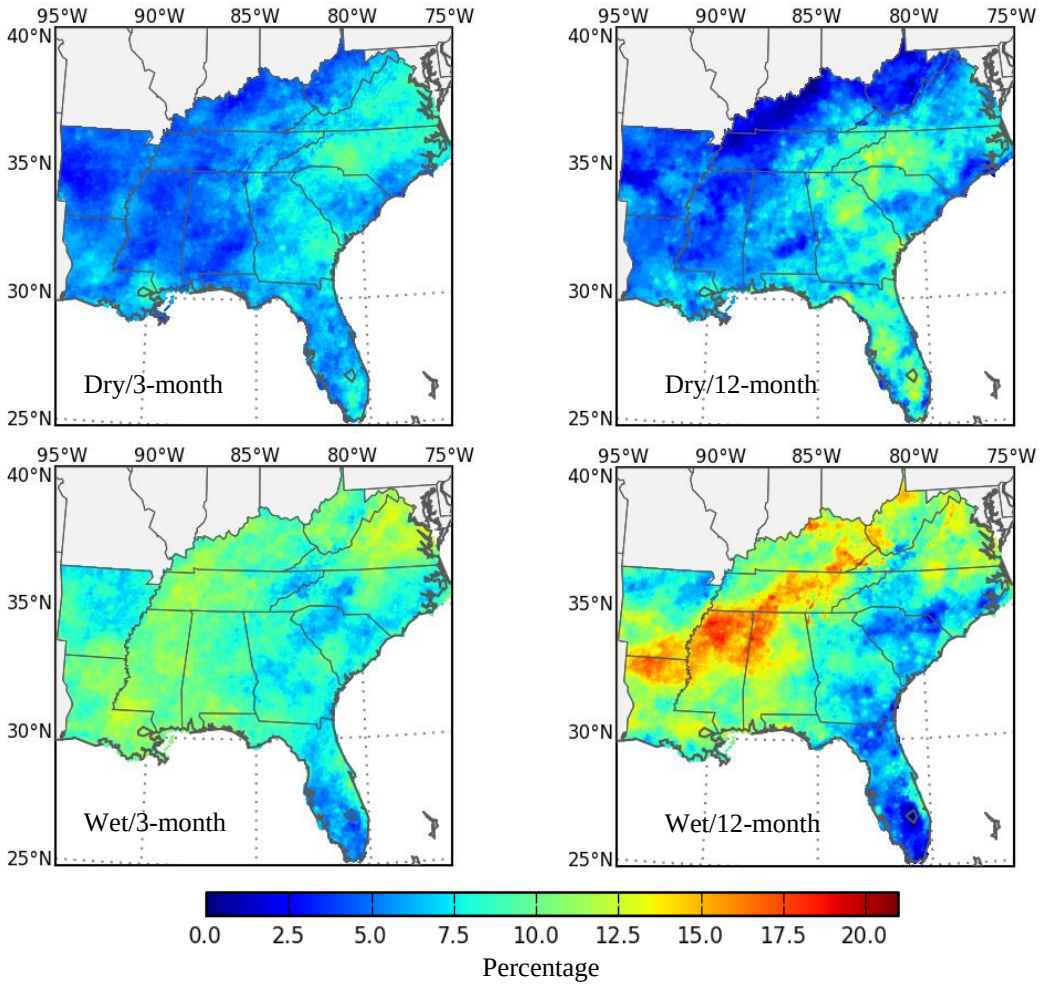

Figure 3.7: Percentage of severe and extreme dry (SPEI ≤ -1.5) and wet (SPEI ≥ 1.5) months for 3-month and 12-month SPEI, for the SEUS (period 1974-2012).

Figure 3.8 shows the area of the SEUS classified as dry (SPEI ≤ -1, red) or wet (SPEI ≥ 1, blue), for each month in the 1896-2012 series. The percentage of the region affected by these events is also presented. Considerable fluctuations in area affected by dry and wet events were observed. While several of these events had a region-wide expression, droughts and wet periods not affecting more than one third of the Southeast were frequent. Similar area totals were observed for dry and wet events when the entire series was considered for both the 3-month and for the 12-month SPEI. Area wise, SPEI values from both time scales show that the 1896-1934 year range experienced slightly more dry events than the rest of the series. This period contributed approximately 36% of the total area affected by droughts, against 31% and 32% from other periods. Larger area differences were observed for wet events, with the 12-month SPEI indicating that 45% of the area affected by wet conditions occurred between 1974 and 2012, while contributions from other periods were 30% (1935-1973) and 25% (1896-1934).

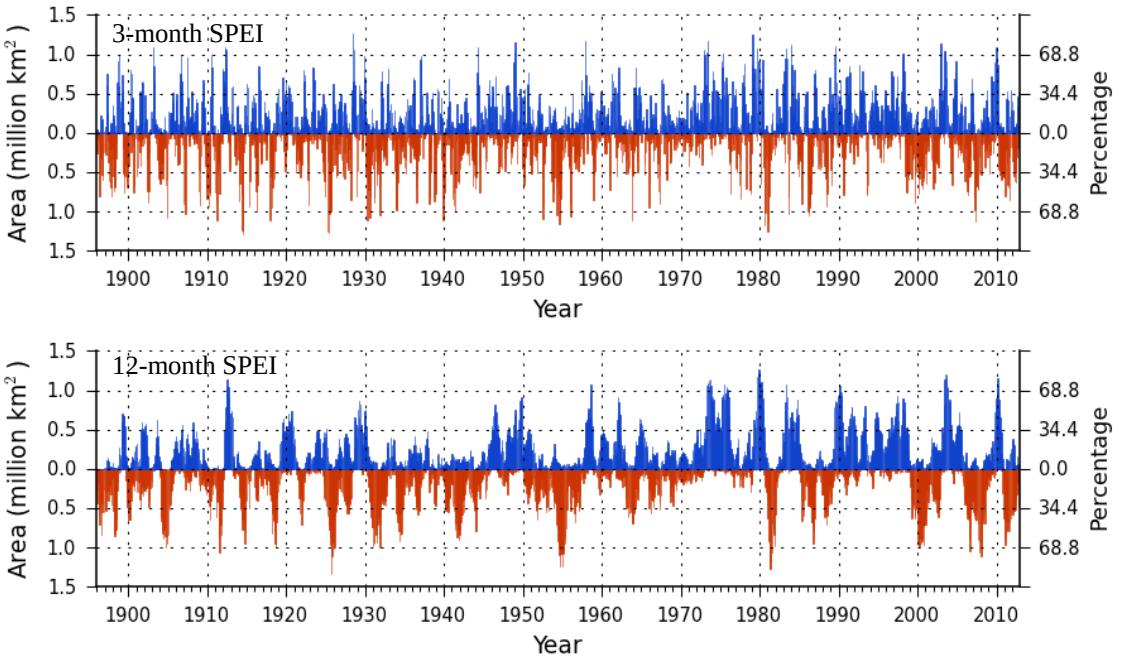

Figure 3.8: Area of the SEUS under drought (SPEI ≤ -1, in red) and wet periods (SPEI ≥ 1, blue) for 3-month and 12-month SPEI, for the period 1896-2012.

Trend analysis of the area affected by dry and wet periods using the non-parametric Mann-Kendall test showed significant trends for wet 3-month SPEI (tau = 0.086, $p < 0.0001$); for

wet 12-month SPEI (tau = 0.153; p < 0.0001) and for dry 12-month SPEI (tau = -0.056; p = 0.002). A data autocorrelation check preceding the trend analysis showed no strong seasonal signal in the dataset, and the observed autocorrelation was taken into account by using the Hamed and Rao method. Further tests were conducted to investigate trends for each of the three time periods considered and results are presented in Table 3.2.

Table 3.2: Trend analysis results for areas affected by dry and wet conditions in the SEUS for periods 1896-1934, 1935-1973 and 1974-2012.

SPEI	1896-1934		1935-1973		1974-2012	
	tau	p-value	tau	p-value	tau	p-value
Dry 3-month	0.043	0.167	-0.094	0.002*	0.149	<0.0001*
Dry 12-month	0.000	0.990	-0.114	0.000*	0.193	<0.0001*
Wet 3-month	0.047	0.129	0.055	0.077*	-0.063	0.040*
Wet 12-month	0.101	0.001*	0.112	0.000*	0.112	0.000*

* significant trend in the series

The recent climate history of the SEUS, including multiple dry and wet episodes, has raised questions regarding changes in climatic patterns and potential variability of dry and wet events in the region. Figure 3.9 shows variability of 3-month and 12-month SPEI indicators represented by standard deviation values calculated for every month of the 1896-2012 interval and for four moving window periods (5, 10, 20 and 30 years). Plotted values indicate the start date of the moving window. Results show that at the 5-year window, variability in the 21st century is smaller than the variability observed for parts of the 1970's and the 1980's, considering 3-month SPEI. SPEI values for this century are comparable in amplitude to changes in SPEI over time observed for the 1920's. Differences between the 3-month and 12-month SPEI are partly attributed to sharp drops in variability resulting from the averaging effect and reduced sensitivity to short-term episodes of longer time scales. In this respect, climatic variation over time was particularly low in the SEUS in the end of the 1960's and in the 1990's, with variability peaks occurring in the beginning of the 1980's and in the 2000's. A significant positive trend was

observed following 1990 for the 5-year window (tau = 0.572; $p < 0.0001$) and for the 10-year window (tau = 0.794; $p < 0.0001$). Trend analysis for moving window intervals show significant negative trends for three of the four time intervals considered (5, 10 and 20 years), following the end of the 1960's. A significant positive trend in variability was observed for the period when the 30-year window was considered.

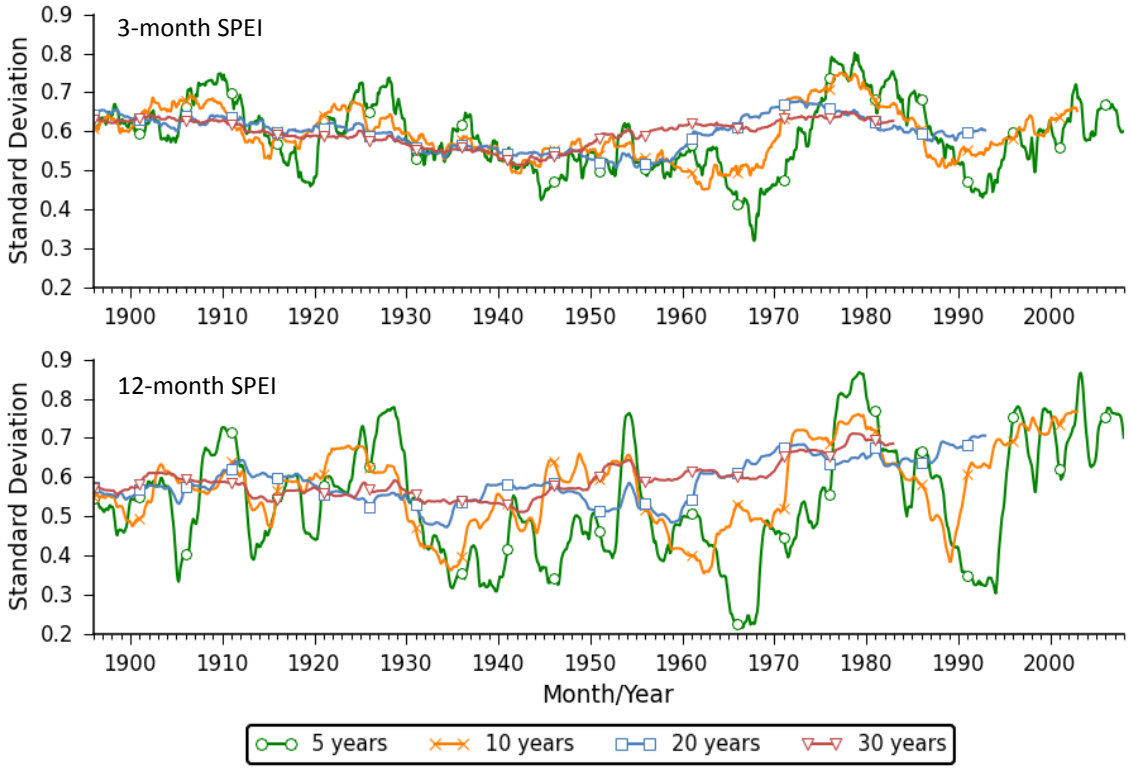

Figure 3.9: Standard deviations for 5-, 10-, 20- and 30-year windows for 3-month and 12-month SPEI and period 1896-2012. Graphed data indicate the first month of the respective moving window period.

The work analyzed dry and wet periods in the SEUS further by investigating the spatiotemporal distribution in event severity over the area. In particular, severe and extreme dry (SPEI $\leq$ -1.5) and wet (SPEI $\geq$ 1.5) events were studied, considering affected area, relationships between area and severity and location of events. Figure 3.10 details the occurrence of severe and extreme dry (red bars) and wet periods (blue bars) by representing the extent of these events in the region from 1896 to 2012. Severe and extreme dry periods affected over 35% of the region multiple times over the period analyzed and these conditions approached or surpassed 50% of the

region eight times before the 1960's. The severe and extreme droughts of 1925 and 1954 affected almost one million square kilometers in the SEUS. Severe and extreme wet conditions were also frequent in the Southeast, but these events affected a comparatively smaller area in the region. In particular, most large area severe and extreme wet events occurring in the SEUS followed the 1970's, with two events prior to 1960 covering more than 34% of the area of study. During the last 40 years, the Southeast has experienced relatively high recurrence of severe and extreme 3-month wet events affecting 10% or more of the region.

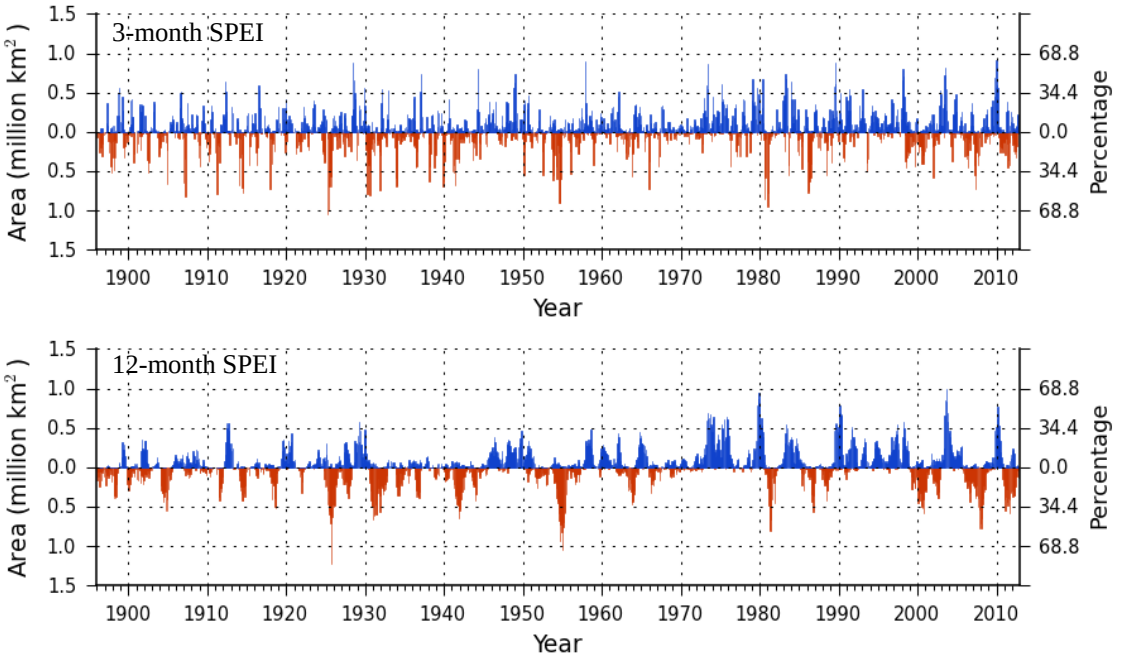

Figure 3.10: Area of the SEUS under severe and extreme dry events (SPEI ≤ -1.5, in red) and severe and extreme wet events (SPEI ≥ 1.5, in blue), for 3-month and 12-month SPEI and for the period 1896-2012

Trend analysis of the area affected by severe and extreme dry and wet conditions using Mann-Kendall as previously described showed significant trends for wet 3-month SPEI (tau = 0.117; $p < 0.0001$) and for wet 12-month SPEI (tau = 0.174; $p < 0.0001$). Further tests were conducted to check trends in area affected by severe and extreme events for three 39-year periods and results are presented in Table 3.3.

Table 3.3: Trend analysis results for areas affected by severe and extreme dry and wet conditions in the SEUS for periods 1896-1934, 1935-1973 and 1974-2012.

SPEI	1896-1934		1935-1973		1974-2012	
	tau	p-value	tau	p-value	tau	p-value
Dry 3-month	0.053	0.092	-0.070	0.024*	0.150	<0.0001*
Dry 12-month	0.018	0.557	-0.084	0.007*	0.214	<0.0001*
Wet 3-month	0.072	0.022*	0.048	0.122	-0.027	0.383
Wet 12-month	0.130	<0.0001*	0.119	0.000*	-0.057	0.067

* significant trend in the series

Four drought events were selected for further analysis, considering the occurrence of extremely dry conditions and observations above. Events occurring in 1925, 1954, 1986 and 2007 were used as input to create Severity-Area-Time Scale (SATS) curves. Curve creation is based on severity-area-duration analysis used in drought research and considered 3-month SPEI values as the duration variable. For curve construction, all dry pixels (SPEI $\leq$ -1) were identified and sorted from lowest to highest. The series of severity levels were screened and the mean severity level for incremental area categories (10,000 km^2 step) was then calculated. The methodology considers each month under dry conditions at a time and results are plotted as area distributions of severity levels. A composite curve representing the drought event is then generated by selecting the lowest values or lowest envelope (most severe) observed for each area category. Figure 3.11 shows results of the SATS analysis, indicating that during all four events large areas in the SEUS were under extremely dry conditions. Average SPEI for the 1925 drought were the lowest observed, approaching -4. In addition, this event affected the largest area from the events considered and had SPEI averages at the severe level for over 1.2 million km^2. Severity levels for the 1925 drought were highest for smaller areas, when compared to the 1954 drought, with both droughts being somewhat similar between 0.5 to almost 1.2 million km^2. Although identified as the worse drought in one hundred years, the 2007 drought presented lower severity levels when compared to the 1954 event, although the area values affected by these events are somewhat comparable.

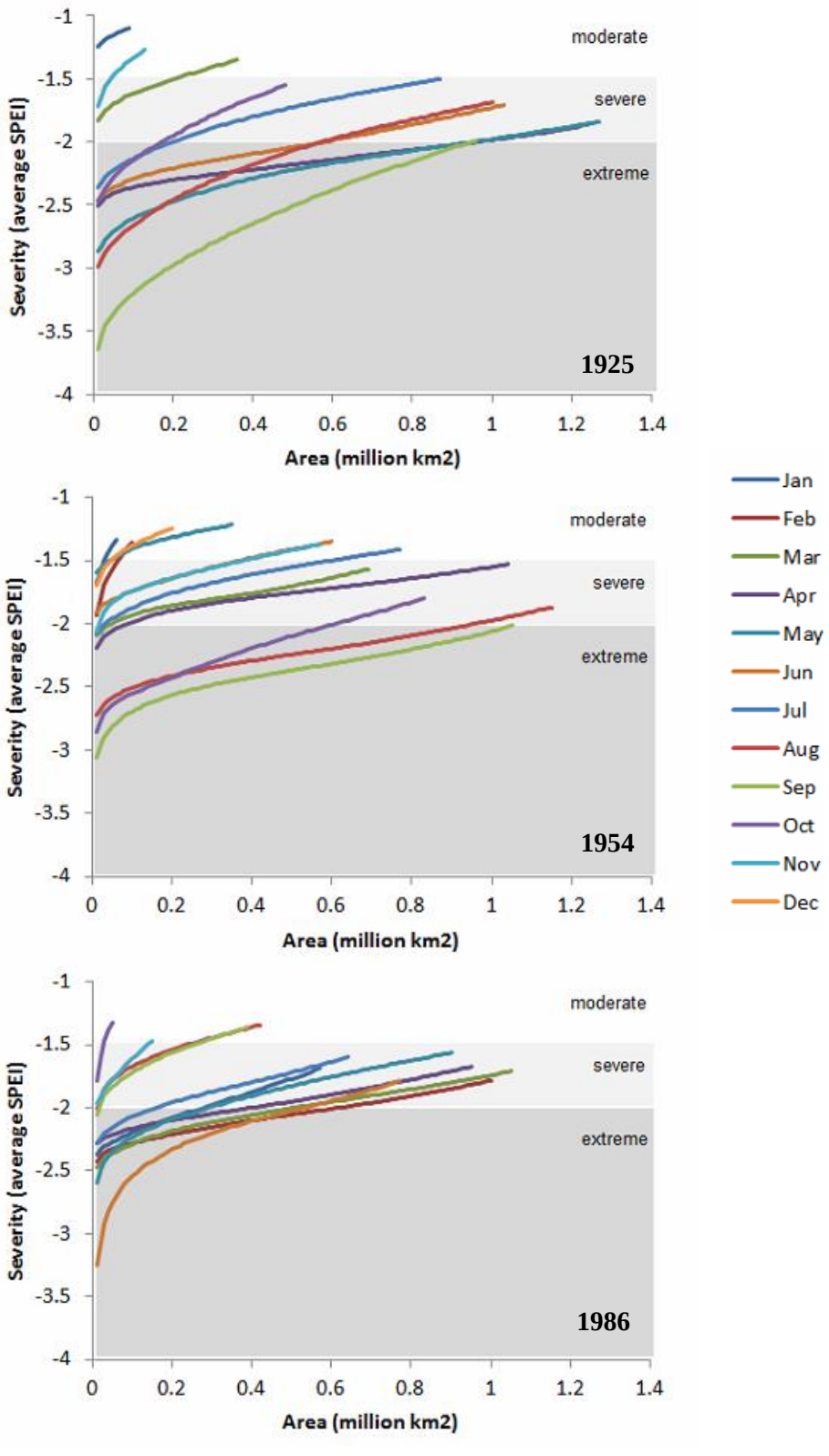
moderate
severe
extreme
1925
1954
1986
Severity (average SPEI)
Area (million km2)
-1
-1.5
-2
-2.5
-3
-3.5
-4
0
0.2
0.4
0.6
0.8
1
1.2
1.4
Jan
Feb
Mar
Apr
May
Jun
Jul
Aug
Sep
Oct
Nov
Dec

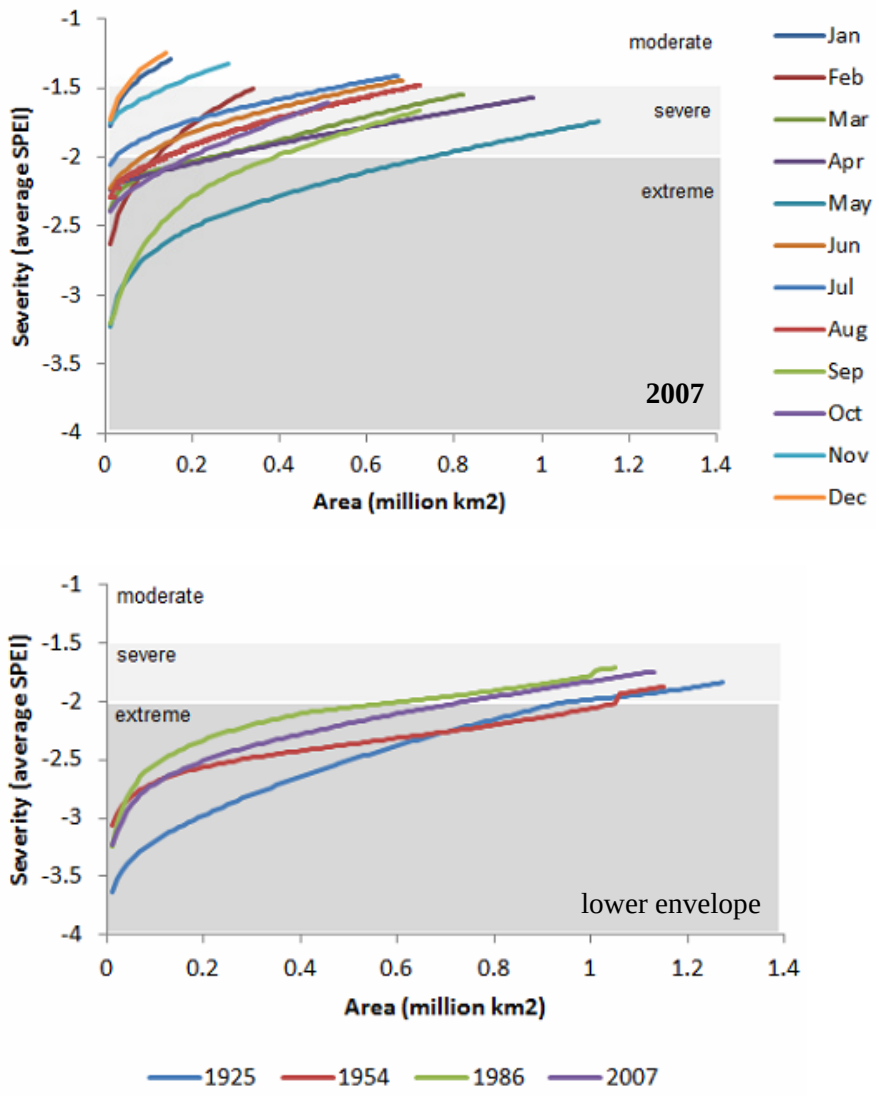

Figure 3.11: Severity-Area-Time Scale (SATS) curves for 3-month SPEI and 1925, 1954, 1986 and 2007; and corresponding lower enveloped summary curve.

Figure 3.12 to Figure 3.15 present the spatiotemporal variation in severity and area affected by these selected severe and extreme events. The time series corroborate the results from the SATS analysis and indicate that the 1925 drought was the most severe drought on record for the Southeast. A more complete presentation of these and other events, considering dry and wet periods, as well as figures for 12-month SPEI, is provided in Appendices D and E.

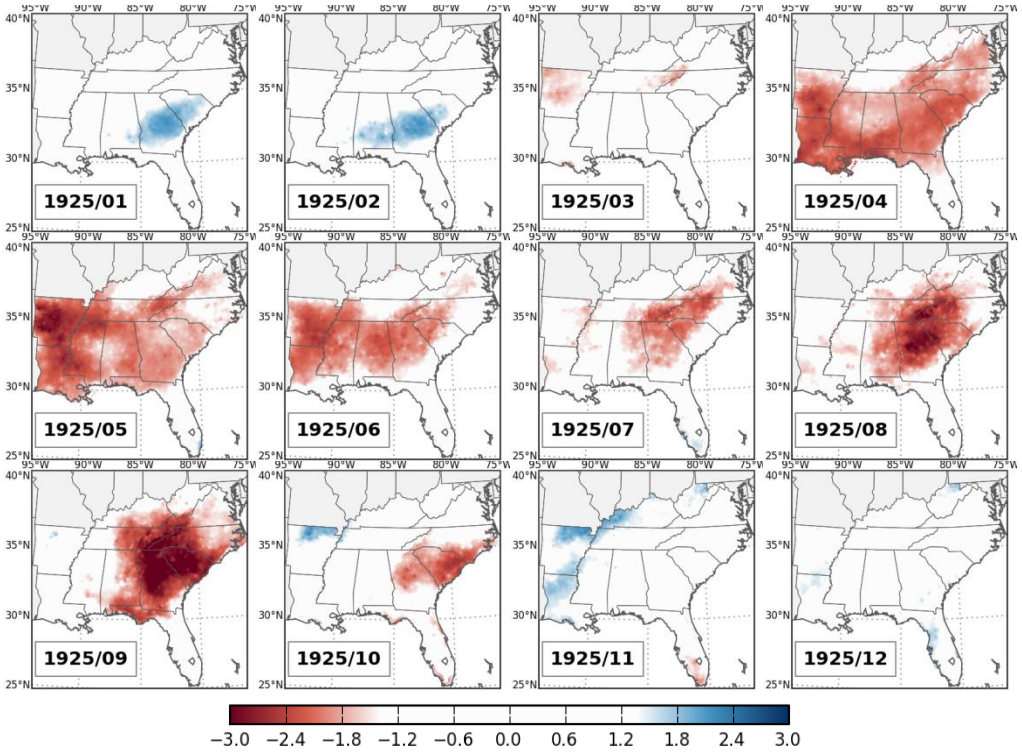

Figure 3.12: Area of the SEUS under severe and extreme dry events (SPEI ≤ -1.5, in red) and severe and extreme wet events (SPEI ≥ 1.5, in blue), for 3-month SPEI and for months of 1925.

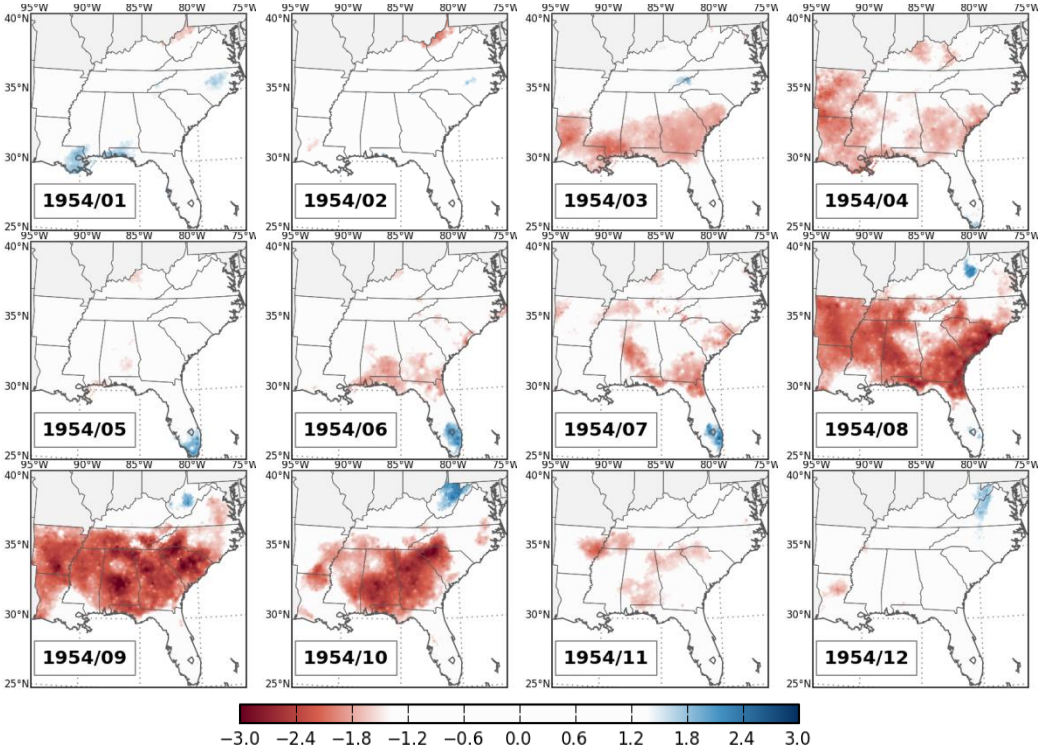

Figure 3.13: Area of the SEUS under severe and extreme dry events (SPEI ≤ -1.5, in red) and severe and extreme wet events (SPEI ≥ 1.5, in blue), for 3-month SPEI and for months of 1954.

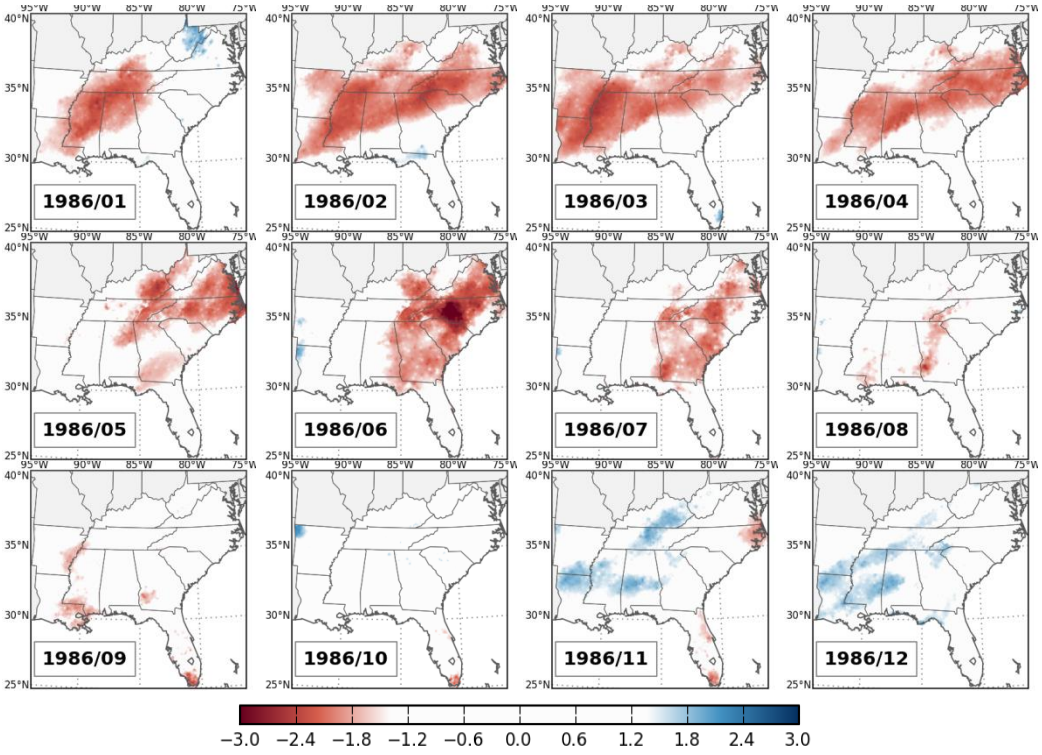

Figure 3.14: Area of the SEUS under severe and extreme dry events (SPEI ≤ -1.5, in red) and severe and extreme wet events (SPEI ≥ 1.5, in blue), for 3-month SPEI and for months of 1986.

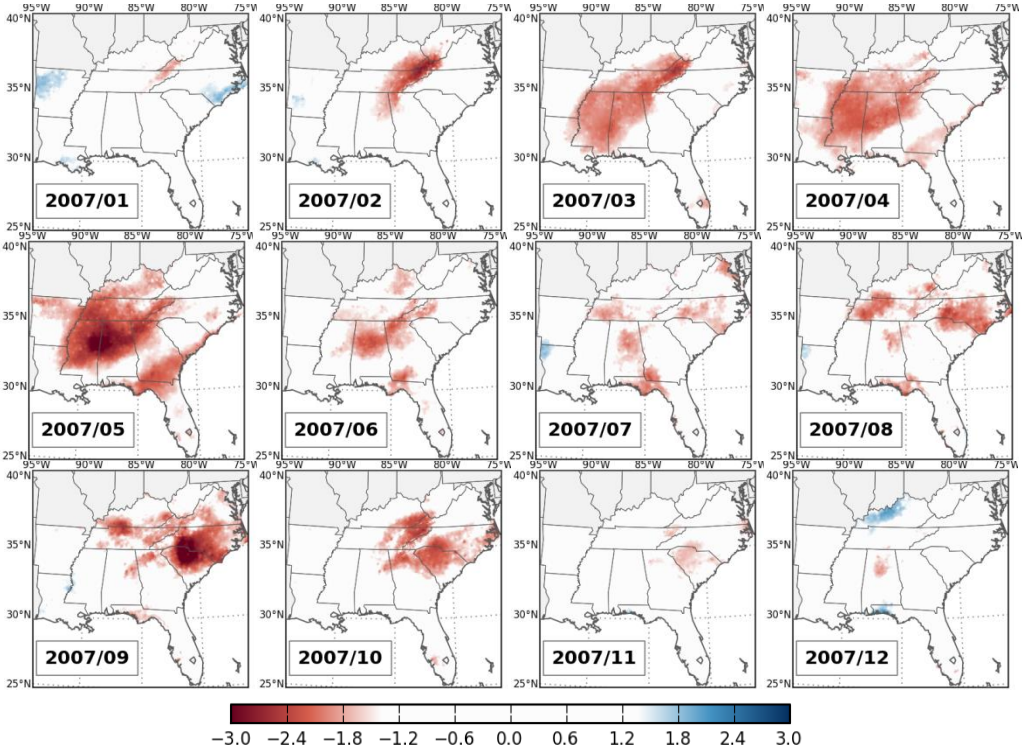

Figure 3.15: Area of the SEUS under severe and extreme dry events (SPEI ≤ -1.5, in red) and severe and extreme wet events (SPEI ≥ 1.5, in blue), for 3-month SPEI and for months of 2007.

3.6 Summary and conclusions

This investigation aimed to understand how recent climate events in the Southeastern United States, including climate extremes, compare to previous events in the region's climatological record. The work provided a characterization of climatic variability in the Southeast with emphasis being given to the spatiotemporal variation of severe and extreme dry and wet periods in the region. Analyses used a time series of climate data for twelve states and period 1895-2012 and included departures from normal water balance conditions using a probabilistic drought/water balance index (Standardized Precipitation-Evapotranspiration Index-SPEI), calculated at multiple time scales.

The analyses identified the spatiotemporal distribution of dry and wet events in the region for a 117-year time series and characterized the occurrence and frequency of dry and wet events in the Southeast, particularly those at longer time scales. The work confirms current concerns regarding patterns and trends of recent climatic variability in the SEUS, indicating a positive trend in area affected by severe and extreme dry events. Trends showing increased climatic variability in the region in the recent past were also identified.

The dataset and results can be further explored by investigating return levels and periods for severe and extreme events in the region, and finer-resolution analyses at more local level can be conducted. In this respect, analyses involving two or more time scales should be further investigated to fully identify relationships between scales and how these relationships relate to physical conditions in the field.

Acknowledgements

This research was supported by NASA Headquarters under the NASA Earth and Space Science Fellowship Program – Grant "NNX09AO18H". Support was also received from the Coweeta Long Term Ecological Research Program.

References

Alley, W. M. (1984). The Palmer Drought Severity Index - Limitations and Assumptions. *Journal of Climate and Applied Meteorology, 23*(7), 1100-1109. doi: Doi 10.1175/1520-0450(1984)023<1100:Tpdsil>2.0.Co;2

Andersen, T. K., & Shepherd, J. M. (2013). Floods in a Changing Climate. *Geography Compass, 7*(2), 95-115. doi: 10.1111/gec3.12025

Bernardes, S., Box, E., Jordan, T. R., & Madden, M. (in preparation). *Vegetation greenness and water content under high climatic variability in the Southeastern United States*. in preparation.

Bernardes, S., Donovan, L. A., & Madden, M. (in preparation). *Primary productivity of terrestrial ecosystems over the Southeastern United States: a fine-resolution analysis of spatiotemporal variation in productivity and hydroclimatic variabilityin the 21st century*. in preparation.

Daly, C., Neilson, R. P., & Phillips, D. L. (1994). A Statistical Topographic Model for Mapping Climatological Precipitation over Mountainous Terrain. *Journal of Applied Meteorology, 33*(2), 140-158. doi: Doi 10.1175/1520-0450(1994)033<0140:Astmfm>2.0.Co;2

Ding, Y., & Smith, K. H. (2008). Economic impacts of the 2007 drought. *DroughScape, the Newsletter of the National Drought Mitigation Center*, 6-9.

Ellis, A. W., Goodrich, G. B., & Garfin, G. M. (2009). A hydroclimatic index for examining patterns of drought in the Colorado River Basin. *International Journal of Climatology, 255*(February 2009), n/a-n/a. doi: 10.1002/joc.1882

Flanders, A., McKissick, J., & Shepherd, T. (2007). Georgia Economic Losses Due to 2007 Drought: Center for Agribusiness and Economic Development. University of Georgia.

Forsythe, W. C., Rykiel, E. J., Stahl, R. S., Wu, H.-i., & Schoolfield, R. M. (1995). A model comparison for daylength as a function of latitude and day of year. *Ecological Modelling, 80*(1), 87-95. doi: 10.1016/0304-3800(94)00034-F

Georgia Farm Bureau. (2013). Georgia Agriculture – The State's $71 Billion Industry. Retrieved 10/17/2013, 2013, from http://www.gfb.org/aboutus/georgia_agriculture.html

Guttman, N. B. (1998). Comparing the Palmer drought index and the standardized precipitation index. *Journal Of The American Water Resources Association, 34*(1), 113-121. doi: 10.1111/j.1752-1688.1998.tb05964.x

Hudson, J. C. (2002). *Across this land : a regional geography of the United States and Canada*. Baltimore: Johns Hopkins University Press.

IPCC. (2012). Managing the risks of extreme events and disasters to advance climate change adaptation (Vol. 1, pp. 582-582). Cambridge: Cambridge University Press.

Karl, T. R., Melillo, J. M., & Peterson, T. C. (2009). *Global climate change impacts in the United States : a state of knowledge report*. Cambridge England ; New York: Cambridge University Press.

Lathrop, A. S. (2009). A Tale of Three States: Equitable Apportionment of the Apalachicola-Chattahoochee-Flint River Basin. *Florida State University Law Review, 36*, 865.

Lu, J., Sun, G., McNulty, S. G., & Amatya, D. M. (2005). A comparison of six potential evapotranspiration methods for regional use in the southeastern United States. *Journal Of The American Water Resources Association, 41*(3), 621-633. doi: 10.1111/j.1752-1688.2005.tb03759.x

McKee, T. B., Doesken, N. J., & Kleist, J. (1993). *The relationship of drought frequency and duration to time scales.* Paper presented at the 8th Conference on Applied Climatology

National Weather Service. (2010). The Epic Floods of 2009. Retrieved 10/17/2013, 2013, from http://www.srh.noaa.gov/ffc/?n=0909epicflood

Palmer, W. C. (1965). Meteorological drought. Washington, D.C.

Seager, R., Tzanova, A., & Nakamura, J. (2009). Drought in the Southeastern United States: Causes, Variability over the Last Millennium, and the Potential for Future Hydroclimate Change. *Journal of Climate, 22*(19), 5021-5045. doi: 10.1175/2009JCLI2683.1

Sheffield, J., & Wood, E. F. (2008). Projected changes in drought occurrence under future global warming from multi-model, multi-scenario, IPCC AR4 simulations. *Climate Dynamics, 31*(1), 79-105. doi: DOI 10.1007/s00382-007-0340-z

Szep, I. J., Mika, J., & Dunkel, Z. (2005). Palmer drought severity index as soil moisture indicator: physical interpretation, statistical behaviour and relation to global climate. *Physics and Chemistry of the Earth, 30*(1-3), 231-243. doi: DOI 10.1016/j.pce.2004.08.039

Vicente-Serrano, S. M., Beguería, S., & López-Moreno, J. I. (2010). A Multiscalar Drought Index Sensitive to Global Warming: The Standardized Precipitation Evapotranspiration Index. *Journal of Climate, 23*(7), 1696-1718. doi: 10.1175/2009JCLI2909.1

Vicente-Serrano, S. M., Begueria, S., Lorenzo-Lacruz, J., Camarero, J. J., Lopez-Moreno, J. I., Azorin-Molina, C., . . . Sanchez-Lorenzo, A. (2012). Performance of Drought Indices for Ecological, Agricultural, and Hydrological Applications. *Earth Interactions, 16*. doi: Artn 10, Doi 10.1175/2012ei000434.1

Vicente-Serrano, S. M., Gouveia, C., Camarero, J. J., Begueria, S., Trigo, R., Lopez-Moreno, J. I., . . . Sanchez-Lorenzo, A. (2013). Response of vegetation to drought time-scales across global land biomes. *Proceedings of the National Academy of Sciences of the United States of America, 110*(1), 52-57. doi: DOI 10.1073/pnas.1207068110

Walker, S. (1991). *Great Smoky Mountains: The splendor of the southern Appalachians*: Camelback Design Group.

Wang, H., Fu, R., Kumar, A., & Li, W. H. (2010). Intensification of Summer Rainfall Variability in the Southeastern United States during Recent Decades. *Journal of Hydrometeorology, 11*(4), 1007--1018 DI 1010.1175/2010.

CHAPTER 4

VEGETATION GREENNESS AND WATER CONTENT UNDER HIGH CLIMATIC VARIABILITY IN THE SOUTHEASTERN UNITED STATES[2]

[2] Bernardes, S., Box, E., Jordan, T.R. and Madden, M. To be submitted to *International Journal of Remote Sensing*.

Abstract

The Southeastern United States (SEUS) has experienced increased climatic variability, including multiple extreme climatic events over the past decades. These events can potentially affect critical biogeochemical cycles, as well as plant and animal life in the region. In the first decade of the 21st century, the SEUS witnessed periods of increased wetness (e.g., 2003) and an exceptional drought following 2006, which may have affected plant leaf production, vegetation canopy properties and photosynthetic potential of important ecosystems. This work investigated the effects of changes in water availability on terrestrial ecosystems occurring in the SEUS by analyzing time-series of satellite derived indices, precipitation and temperature data for the period 2000-2013. Water availability was represented by the Standardized Precipitation-Evapotranspiration Index (SPEI), calculated at multiple time scales and using surfaces of precipitation and temperature data from the PRISM Climate Group. Vegetation conditions and responses were represented by the Enhanced Vegetation Index (EVI) and by a modified Normalized Difference Water Index (NDWIm), both calculated using images acquired by the Moderate Resolution Imaging Spectroradiometer (MODIS) sensor, onboard the Terra satellite. Anomalies of greenness were identified over multiple growing seasons, with increases in leaf mass and greenness occurring during highest water availability (2003) and reductions being particularly significant following the onset of the severe and extreme drought in 2006. Similar behavior was found for NDWIm. Spatiotemporal variability in index values was analyzed for the entire SEUS and relationships between satellite-derived and climate indices were identified.

Keywords: drought, vegetation index, precipitation, temperature, climate, MODIS, EVI, NDWI, SPEI

4.1 Introduction

During the first years of the 21st century, the Southeastern United States (SEUS) was affected by one of the most severe droughts on record for the region, with below normal precipitation being recorded for multiple consecutive years. Recent precipitation reductions observed over large areas in the SEUS were accompanied by widespread breaking of temperature records. Temperatures during the 2012 summer, for example, matched the extremes observed for 1932 and 2010, with July 2012 being one of the warmest months in the instrumental record for the region (data from the U.S. National Climatic Data Center-NCDC). During the same month, drought indicators pointed to persistent extreme and exceptional drought conditions over large areas in the SEUS (U.S. Drought Monitor, 2013). Conversely, reduced temperatures and significant increases in precipitation were also recorded for parts of the Southeast in the recent past, particularly during 2003. Increased climatic variability in the SEUS during recent decades has been reported in the literature, including intensified summer droughts and anomalous wet periods (Wang, Fu, Kumar, & Li, 2010). Future climate projections suggest that these conditions will persist during the 21st century (Sheffield & Wood, 2008), resulting in: (a) reductions in precipitation for most of the region during summer, winter and spring; and (b) increases in precipitation during fall (Karl, Melillo, & Peterson, 2009). Further, substantial warming in temperature extremes are expected during this century, being very likely that heat waves will become longer, more frequent and/or intense over most land areas (IPCC, 2012).

Extreme hydroclimatic events, such as droughts, often affect plant metabolism, negatively impacting photosynthesis, reducing primary productivity and potentially resulting in limited ecosystem functioning and services. Ecosystems affected by extreme droughts may witness catastrophic changes, with critical impacts on agriculture and loss in natural capital, including massive die-back, dominance of invasive species and extinction. The capacity to identify and characterize the biosphere's responses to climatic variability and droughts is fundamental to the understanding of impacts of these events to important ecosystems, with

consequences to future climates, food security, biodiversity and overall healthy functioning of the environment. Moreover, it is fundamental to understand vegetation responses after extreme conditions cease to exist. This investigation contributes to the understanding of relationships between vegetation status and water availability by quantifying and spatializing changes in vegetation greenness and plant liquid water content during the 21st century in the SEUS. The study specifically aimed to: (a) map and quantify the spatiotemporal variability in satellite-derived greenness and water content indices during fourteen growing seasons in the SEUS, starting in the year 2000; and to (b) investigate temporal and spatial linkages between these changes and water availability, as described by a drought index derived from weather station data. The study hypothesizes that vegetation responded to hydroclimatic and temperature variability in the SEUS during the 21st century and that responses of vegetation involved physiological and structural changes identifiable by using a series of metrics derived from spectral data acquired by an orbital remote sensor.

4.2 Study area

The spatial domain of this investigation is the Southeastern United States (SEUS, Figure 4.1), a region encompassing approximately 1.4 million square kilometers and twelve states (bounding box: 40.63^{o}N - 94.61^{o}W; 24.89^{o}N - 75.46^{o}W). The SEUS is characterized by high physiographic variability and landscape complexity, resulting from vast areas with diverse geological and geomorphological histories. Topography plays a significant role in defining environments in the region, which ranges from lower areas in a vast coastal plain, transitioning to the hilly relief of the Piedmont Plateau and to the mountains of the Appalachian Plateau. Most of the region has a humid climate, with a north-south gradient of winter temperature, from cold to mild winters. Precipitation is well distributed over the year for most of the region, with relevant regional variations including the Florida Peninsula, the Gulf Coast and areas along the Appalachian Mountains. Mean total precipitation in the SEUS averages 1,300 mm for the year,

ranging from 800 mm in the region's northern part to over 2,200 mm in Southern Appalachia (data source: PRISM Climate Group).

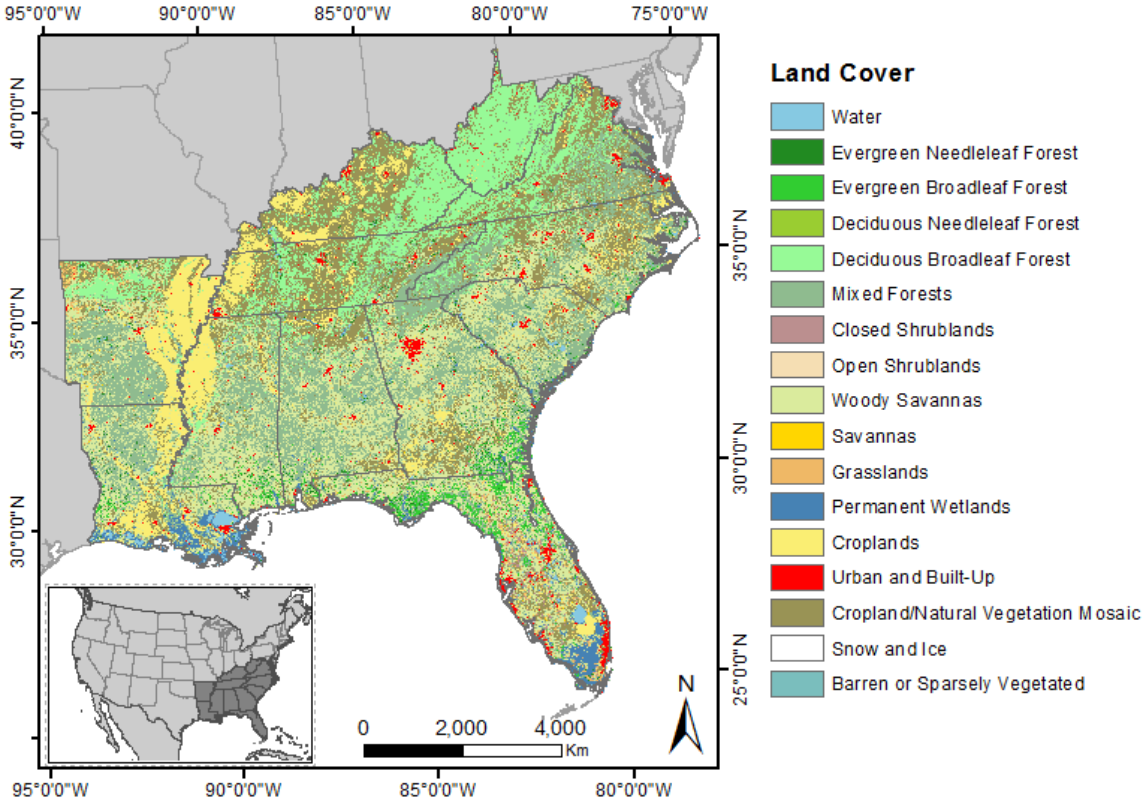

Figure 4.1: Land cover classes over the Southeastern United States, with emphasis on vegetation cover (data source: MOD12Q1, 2012, IGBP classification scheme)

The combination of climate history and landscape variability in the SEUS makes the Southeast an ideal model for investigations regarding responses of vegetation to extreme hydroclimatic events. Approximately 34% of the region's land area is used for agriculture and crops are particularly important along the Mississippi Valley and other areas in the Coastal Plain, as well as in the Piedmont Plateau. These agricultural areas have been impacted by recent extremes in hydroclimate and in 2007 alone major field crops accumulated losses of over US$1.3 billion due to widespread drought (Ding & Smith, 2008). Natural vegetation is represented by large areas of broadleaf deciduous and mixed forests (broadleaf deciduous + evergreen needleleaf) in the northern part of the SEUS. Other significant vegetation types in the region include broadleaf evergreen forests, woody savannas, grasslands and permanent wetlands.

Examples of particularly important areas in the region regarding climate impacts include the Southern Appalachian Mountains, one of the most biodiversity rich temperate regions on the planet (Walker, 1991).

4.3 Data

This work used data derived from the Moderate Resolution Imaging Spectroradiometer (MODIS) sensor, a payload component of NASA's Terra satellite. Terra is a quasi-polar satellite, with a revolution period of 16 days and revisiting time of 1-2 days, depending on the latitude. MODIS acquires 2,330 km image swaths in 36 spectral bands and three spatial resolutions, including 250 meters (two bands), 500 meters (5 bands) and one kilometer (29 bands). The spatial resolution and spectral characteristics of MODIS make this system a widely used tool for detecting and analyzing variations in vegetation responses to environmental stressors, including droughts. Sets of eight 10-degree MODIS Collection 5 tiles (total: 1,248 tiles) of the Vegetation Indices Monthly L3 Global 1km product (MOD13A3) and covering the entire SEUS were considered by this investigation. Over 13 years of MOD13A3 data were analyzed, spanning the period May 2000 to September 2013. The resulting dataset comprised a monthly archive of Enhanced Vegetation Index (EVI) and reflectance data for entire 14 growing seasons for most of the area of study. Vegetation index tiles were accessed by using the MODIS Data Pool (http://e4ftl01.cr.usgs.gov/MOLT/, access date: October 21, 2013).

The Constrained-View Maximum Value Composite (CV-MVC) algorithm involved in the generation of MOD13A3 selects the highest vegetation index value for a given pixel during a 30-day interval and incorporates a viewing angle threshold (Solano, Didan, Jacobson, & Huete, 2010). This procedure assists in reducing contamination by clouds and contributes to the generation of a composite image with the highest-quality pixels available. Despite the incorporation of this algorithm, some residual contamination may persist in the dataset. To support the identification and processing of pixels affected by reduced quality, the current work

also analyzed quality assurance (QA) layers of MOD13A3, including multiple quality flags. In addition to MOD13A3, the MODIS Land Cover Type product (MCD12Q1), produced yearly for the period 2001-2012, at the spatial resolution of 500 meters was used to identify cover classes affected by climatic variability. The International Geosphere-Biosphere Programme (IGBP) classification scheme was selected. Images acquired by Landsat 5 Thematic Mapper (TM) and by Landsat 7 Enhanced Thematic Mapper Plus (ETM+) over selected areas in the SEUS were used to further investigate anomalies in EVI and NDWI regarding potential changes in land cover over time. From Landsat, this study used bands in the visible, near infrared and mid infrared spectral regions, all at 30-m spatial resolution.

Non-provisional monthly total precipitation and monthly mean temperature data distributed by the PRISM Climate Group at Oregon State University (www.prism.oregonstate.edu, accessed on October 22, 2013) were used to characterize climatic variability in the region of study. PRISM data are outputs of the Parameter-elevation Regressions on Independent Slopes Model (PRISM) climate mapping and knowledge-based system (Daly, Neilson, & Phillips, 1994) and consist of continuous grids of multiple climate fields. Surface generation by the PRISM algorithm considers point measurements of precipitation and temperature from multiple weather stations across the Southeast, a digital elevation model and expert knowledge to incorporate complex factors driving climatic variation. In this respect, PRISM accounts for coastal effects, variability resulting from surface features, such as relief and rain shadows, and is robust to variations in density of stations. Modeling resolution is 30 degree seconds, with output spatial resolution of approximately 4 km. PRISM data spanning the period 1895-2012 were used in the generation of a time series of water balance descriptors. Due to their provisional status at the time of writing, PRISM data for the 2013 growing season were not used by this study.

4.4 Methods

Vegetation greenness over the SEUS was analyzed using a time series of Enhanced Vegetation Index (EVI) derived from images acquired by MODIS. MOD13A3 layers for 30-day composites of EVI and near infrared (NIR) and mid infrared (MIR) were mosaicked and mapped to an equal area projection using the MODIS Reprojection Tool (MRT) software. A set of 156 seamless mosaics at 1-km spatial resolution covering the entire area of study was generated for the period March 2000 to September 2013. Mosaicking and reprojection were also performed for other MOD13A3 science datasets, including the VI Quality Detailed QA, the View Zenith Angle and the Pixel Reliability Summary QA.

Vegetation indices are arguably the most widely used products derived from remotely sensed data, with innumerous applications involving the identification and characterization of the dynamics of environmental phenomena at multiple spatial and temporal scales. These indices are based on spectral bands situated in the optical part of the electromagnetic spectrum and usually involve relationships between radiance or reflectance in the red and near infrared regions of the spectrum. This work used a series of mosaics of EVI (Huete et al., 2002; Huete, Justice, & van Leeuwen, 1999), as presented below:

$$EVI = 2.5 \times \frac{(\rho NIR - \rho Red)}{\rho NIR + (6 \times \rho Red - 7.5 \times \rho Blue) + 1}$$

where ρNIR, ρRed, $\rho Blue$ are MOD13A3 monthly reflectances in the near infrared, red and blue spectral regions, respectively. The EVI improves over other vegetation indices by being less sensitive to saturation due to high biomass and high leaf area and incorporates adjustment coefficients to account for residual atmospheric contamination (aerosol resistance terms) and from canopy background (Huete et al., 2002). In addition to vegetation indices, images representing vegetation liquid water derived from satellites also have been used to investigate the effects of climatic events on vegetation, including monitoring droughts. These indices assume that factors associated with plant vigor (e.g., turgor, cell walls, water content) change under water

stress conditions and have been specifically developed to study effects of water stress on plants. In this context, a series of images representing monthly Normalized Difference Water Index (NDWI) (Gao, 1996) was also generated as part of this study. Computations involved a band substitution and used a 2090-2350 nm band to calculate a modified NDWI (NDWIm). The procedure used reflectance bands from MOD13A3 and included near-infrared (ρNIR) and mid-infrared (ρMIR, band 7) (Anderson et al., 2010; Gu et al., 2008). NDWIm was defined as:

$$NDWIm = \frac{(\rho NIR - \rho MIR)}{(\rho NIR + \rho MIR)}$$

Indices derived from orbital remote sensors operating in the optical region of the electromagnetic spectrum are sensitive to variations in image quality resulting from cloud contamination, shadows, aerosols, faulty sensors and others. Reductions in image quality can be particularly problematic, as affected images can still produce indices within valid value ranges. These indices, however, will not be representative of the target considered. To account for potential negative effects of image quality reductions on the accuracy of analyses, mosaics of quality-related variables (i.e., Detailed QA, Pixel Reliability and View Angle) were investigated. Figure 4.2 shows the spatial variability in quality of MOD13A3 monthly composites over the Southeast, represented by the percentage of image pixels that were flagged as cloudy, were contaminated by shadows or had high aerosol content. It is noteworthy that longer time composites, such as the 30-day MOD13A3, tend to result in relatively high quality pixels. Considering the low number of pixels affected by reduced quality (less than 6% of the time series for most of the region) data smoothing, including spike removal, was considered adequate for data preprocessing.

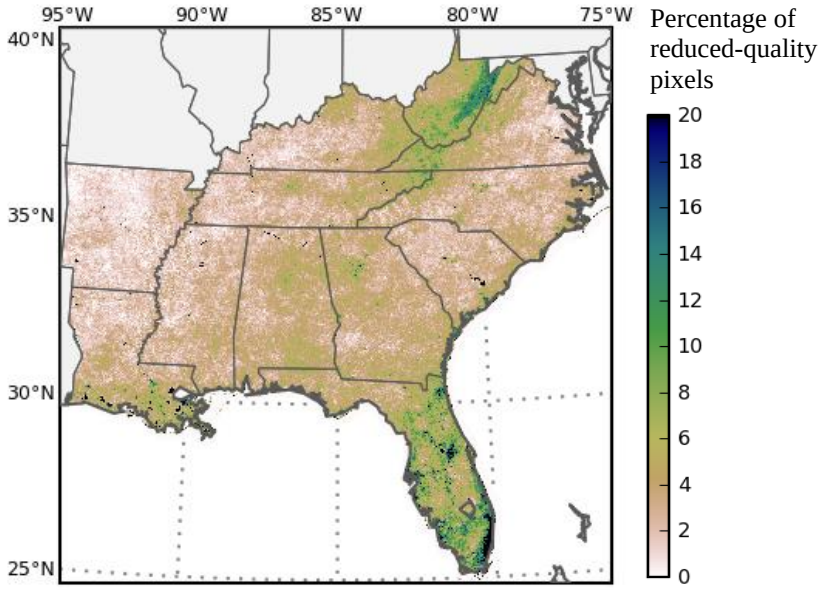

Figure 4.2: Quality analysis of MOD13A3 and time-series reconstruction procedure represented by percentages of reduced-quality pixels over the SEUS for the period February/2000-September/2013.

To process images for data quality, a rule set was developed and used with a rule-based classifier to categorize each mosaic pixel according to three classes: low, medium and high quality. Classification considered cloud contamination, aerosol quantity, shadows and snow/ice. In addition to the factors above, reflectance quality also can be impacted by large viewing angles, particularly for systems with large fields of view, such as MODIS. The identification of pixels associated with large view zenith angles followed the work of Sakamoto et al. (2005) and flagged angles larger than 32.35^{o}.

Using the procedures above, reduced-quality pixels were located in time and space and spikes for the Enhanced Vegetation Index (EVI) and the Normalized Difference Water Index (NDWIm) mosaics were then removed using the curve fitting functionality of TIMESAT (Jonsson & Eklundh, 2004). Time-series reconstruction using TIMESAT incorporated weights based on each of the three quality classes used by this work. Because curve fitting using monthly vegetation descriptors can alter original index values, parameters for the Savitzky-Golay fitting method were selected conservatively to preserve the original data while removing spikes. Spike removal used a median filter over time for each pixel of the mosaic, for the entire time series.

Other conservative fitting parameters included envelope interactions = 2, adaptation strength = 1 and window size = 1.

Monthly precipitation and temperature surfaces from PRISM were used to compute the multi-scalar Standardized Precipitation-Evapotranspiration Index (SPEI) for the region of study, following the work of Vicente-Serrano, Beguería, and López-Moreno (2010). SPEI computation included the calculation of the climatic water balance (precipitation minus potential evapotranspiration) for a long-term precipitation record (1895-2012) and the fitting and normalization of the results. SPEI represents departure from the mean of the water balance for a given location and time scale, when compared to the historical record and is given in units of standard deviation. Negative SPEI indicates water balance below normal and may signal drought conditions. Positive SPEI indicates water surplus and potentially a wet period. Table 4.1 presents a classification of SPEI based on ranges of standard deviations used in this study:

Table 4.1: Categories of wetness and dryness and corresponding value ranges for the Standardized Precipitation-Evapotranspiration Index (SPEI)

Categories	SPEI[1]
Extremely wet	≥ 2.00
Very/severely wet	1.50 to 1.99
Moderately wet	1.00 to 1.49
Near normal	0.99 to -0.99
Moderate drought	-1.00 to -1.49
Severe drought	-1.50 to -1.99
Extreme drought	≤-2.00

[1] based on categories of dryness proposed for the Standardized Precipitation Index (SPI) by McKee, Doesken, and Kleist (1993).

Because vegetation responses to water scarcity or surplus is a function of time, including the temporal interval considered, and to account for lags and system inertia this work calculated SPEI for multiple time scales (i.e., 1, 2, 3, 4, 6, 9, 12 and 18 months), To allow for data overlay and the retrieval of statistics over space and time, the images resulting from SPEI computations were spatially matched to satellite-derived indices.

4.5 Results and discussion

Figure 4.3 presents precipitation and mean-temperature anomalies (top) and 4-month SPEI values (bottom), for the SEUS and period covered by this study. Conditions before 2000 were included due to their potential contribution to vegetation conditions in the first years of the 21st century. Notable climatic features for the period include above normal precipitation in 1998, 2003 and in 2009. Positive temperature anomalies were particularly large in 1998 and in 2012, when mean temperature for the region was 10°C above the historical average.

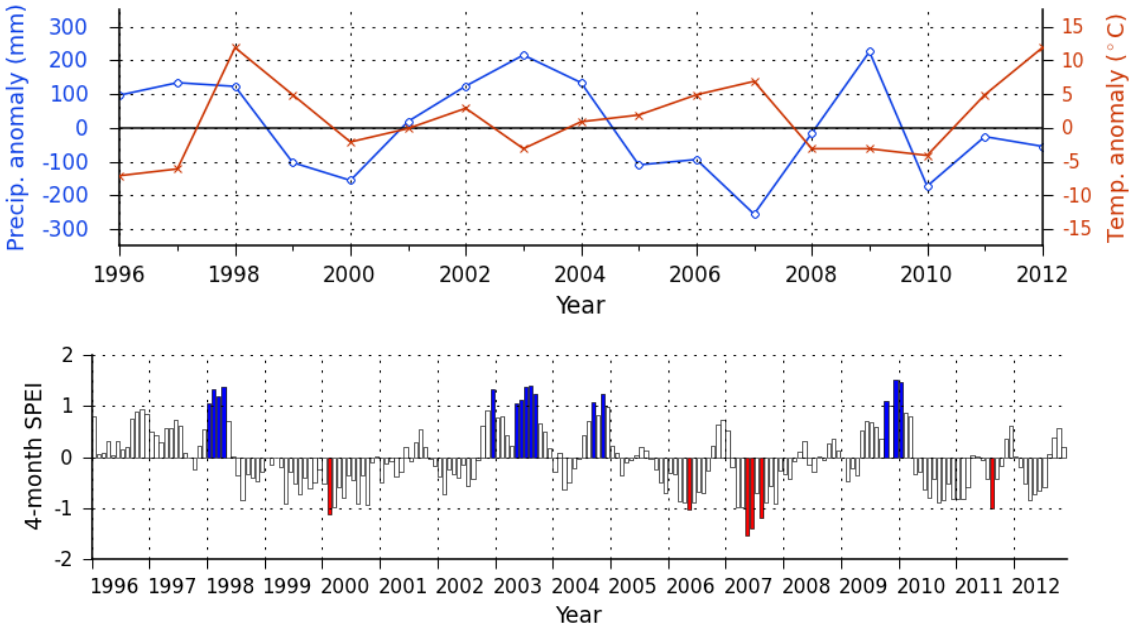

Figure 4.3: Climatic variability in the SEUS over the period 1996-2012, represented by (top) anomalies of annual precipitation (blue, circle marker) and anomalies of annual mean temperature (red, "x" marker); and (bottom) 4-month SPEI. Bar colors indicate wet (blue) or dry (red) conditions.

Reductions in precipitation from 1996 to 2012 were observed for multiple years and were significantly severe in 2007, when anomalies of precipitation for the region approached -250 mm. Positive temperature anomalies surpassing 5°C were observed for the same year, exacerbating the effects of reduced rainfall for most of the Southeast and contributing to the lowest SPEI values observed for the period of study. In 2007, severe drought affected large parts of the Southeast. It is noteworthy that the values shown represent averages for the region of study and that multiple local extreme conditions were observed during the development of this investigation.

Standardized anomalies of EVI and NDWIm were used to identify departures from normal conditions over space and time. These standardized metrics show distances from mean values in units of standard deviation and were calculated by computing the mean and standard deviation values for each time unit analyzed (i.e., each month or multi-month period) using a temporal cross section of the entire time series. The mean indices were then subtracted from the index value for the current time unit and the result was divided by the standard deviation, as follows:

$$SA_u = \frac{x_u - \overline{x_s}}{\sigma(x_s)}$$

where SA_u is the standardized anomaly for a given time unit u; x_u is the index value for the time unit; $\overline{x_s}$ is the mean index for the time unit calculated over the entire time series and $\sigma(x_s)$ is the index standard deviation for the time unit, calculated over the series.

The use of standardized anomalies brings multiple advantages to analyses, allowing for the identification of change signals over time, which are usually masked by the seasonalities of phenological cycles. These anomalies also allow for comparisons of index departures at different locations and times, and support the identification of the relative significance of these departures. In this study, values of standardized anomalies located at 0.5 standard deviations or less from the mean value for a given index were considered indicative of near normal conditions. Although somewhat arbitrary, this threshold selection is conservative and considers that under normal climate conditions interannual swings in health and vigor of natural vegetation systems are smaller than interannual variability observed for other complex systems, including the climate system, for which one standard deviation has been used to describe non-normal conditions.

A time series of standardized anomalies calculated for monthly averages of EVI for the entire SEUS and period 2000-2013 is presented in Figure 4.4. Mean greenness for the region increases in the first six years analyzed, dropping to below average values during the second half of the period of study. Exceptions include 2010 and, particularly, 2012, which showed positive

spikes in greenness. Strong positive greenness anomalies reaching two standard deviations from mean values can be observed for 2002, 2004 and 2012. Negative greenness anomalies were particularly strong following 2008, approaching negative two standard deviations in all years, with the exception of 2013.

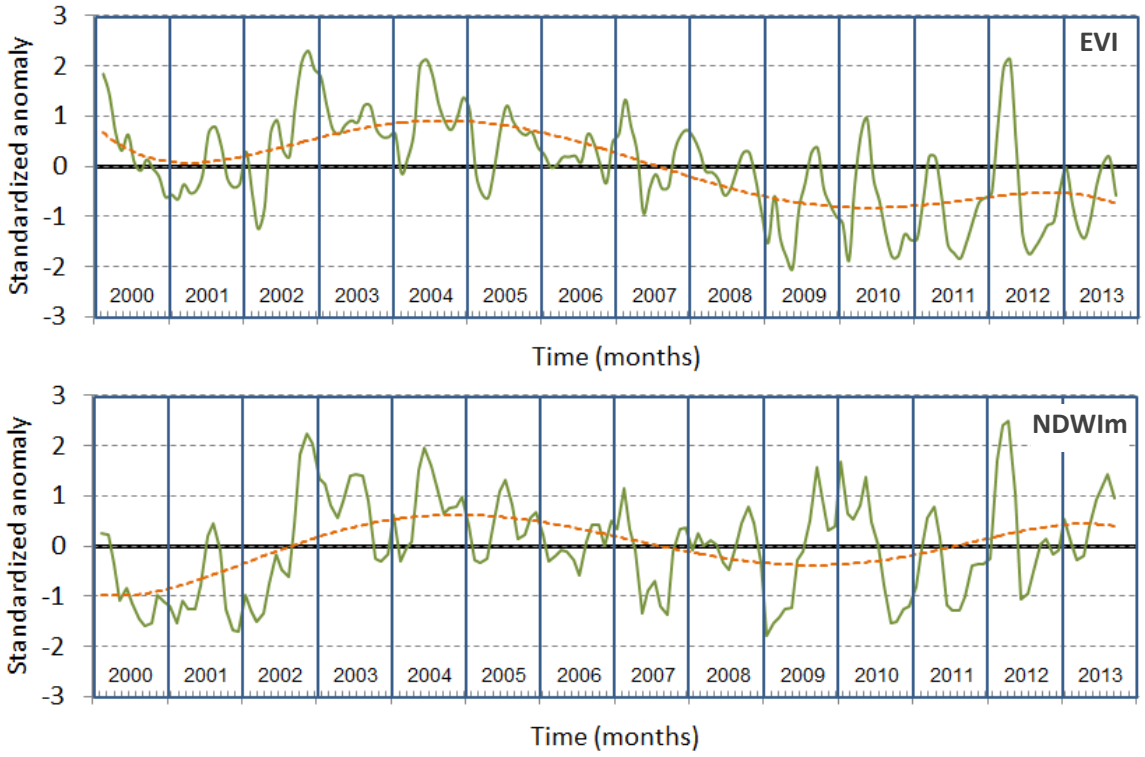

Figure 4.4: Standardized anomalies (solid lines) of EVI and NDWIm, considering all months for the period February/2000-September/2013 and entire SEUS. Trend lines (dashed) are also shown.

General agreement can be observed between greenness anomalies; climate anomalies and SPEI (see Figure 4.3 for climate data). In particular, peaks in greenness in 2001 and in 2002 may have been associated with timely positive water balance in the Southeast and above normal greenness observed for 2005 may have resulted from wet conditions during the second half of 2004. Fall and winter are periods of reduced evapotranspiration in the SEUS, and precipitation during this period is critical for replenishing soil water storage. Positive 4-month SPEI values for the period Nov/2006-Jan/2007 may have contributed to the peak in greenness observed during the beginning of 2007. Strong reductions in water balance observed for most of 2007 are likely to have impacted plant foliage during the growing season that year. However, in spite of the reduced

water availability, an increase in greenness can be observed for the end of 2007, possibly associated with non-homogeneous distribution of water balance anomalies over the region for the year. Monthly SPEI for 2007 indicate conditions ameliorating at the western side of the Southeast as the year progressed. Although the 4-month SPEI indicates near normal conditions for 2008 and for the beginning of 2009, greenness reached its global minimum for the region in the first half of 2009.

Similar general agreement between climate descriptors and NDWIm was observed for the 2000-2013 period (Figure 4.4). In addition, NDWIm and EVI presented comparable amplitudes, although significant dissimilarities between the series can be observed. Differences are particularly evident associated with negative water balance in 2000 and with positive water balance in 2009-2010. Values of 4-month SPEI reached negative one standard deviation in the beginning of 2000, and below normal water balance prevailed for most of that year (Figure 4.3). Negative standardized anomalies of NDWIm observed for 2000- 2001 indicate reductions in plant liquid water, although EVI values showed no significant change in photosynthetic potential for the period. Significant disagreements between EVI and NDWIm included also the winter of 2009-2010, when anomalies for both indices were particularly strong, but showed opposite signs (EVI = -1.87; NDWIm = +1.68). During the end of 2009 and the beginning of 2010, SPEI values were more than one standard deviation above normal, but no increase in photosynthetic potential was observed during the period. Results point to an increase in explanatory power of changes in vegetation status associated with climatic variability when EVI and NDWIm series are analyzed together. This work agrees with Gao (1996) that these indices have a complementary nature. Overall, the results above indicate critical times for water availability, and suggest lags in vegetation response to changes in water balance status. The observed patterns stress the importance of incorporating into analyses time of precipitation and temperature events at fine enough spatial and temporal scales to capture the temporal variability of the observed phenomenon.

In addition to monthly analyses, EVI and NDWIm were evaluated for a five-month window (from May to September - MJJAS), aiming to capture vegetation and water content status during the peak of the growing season for most of the SEUS. Although the length of this season may be significantly longer in some areas of the Southeast, the use of a five-month window was considered to adequately capture attributes during a key period for vegetation in the region. The use of a shorter time window, as opposed to analyzing the entire year, also allowed for the extension of the time series to years when MODIS datasets are incomplete (i.e., 2000 and 2013). Vegetation status for the MJJAS period used integrated EVI and NDWIm (iEVI and iNDWIm, respectively), which were calculated by temporally adding monthly index values for each pixel and month from May to September. Integrated indices were then used to compute standardized anomalies using the MJJAS period as unit of time. Standardized anomalies of integrated indices were spatially represented and compared for multiple years.

Figure 4.5 shows standardized anomalies of iEVI for the MJJAS period from 2000 to 2013. The series of maps depicts considerable variability in greenness for the region during the first years of the 21st century, as both positive and negative anomalies are well represented in space and time. These results extend the work of Peters, Ji, and Walter-Shea (2003), who found similar relationships for the period 1989-1999, while investigating the effects of ENSO in the SEUS. Positive anomalies were particularly strong for most of the region during the MJJAS period of 2004. States less affected by these conditions included West Virginia (with exception of its northern part), parts of Florida, Arkansas and Louisiana, the latter presenting areas with negative anomalies. As previously mentioned, SPEI indicates a very wet fall 2003, and increased precipitation may have replenished soil moisture in the region and contributed to the observed elevation in greenness.

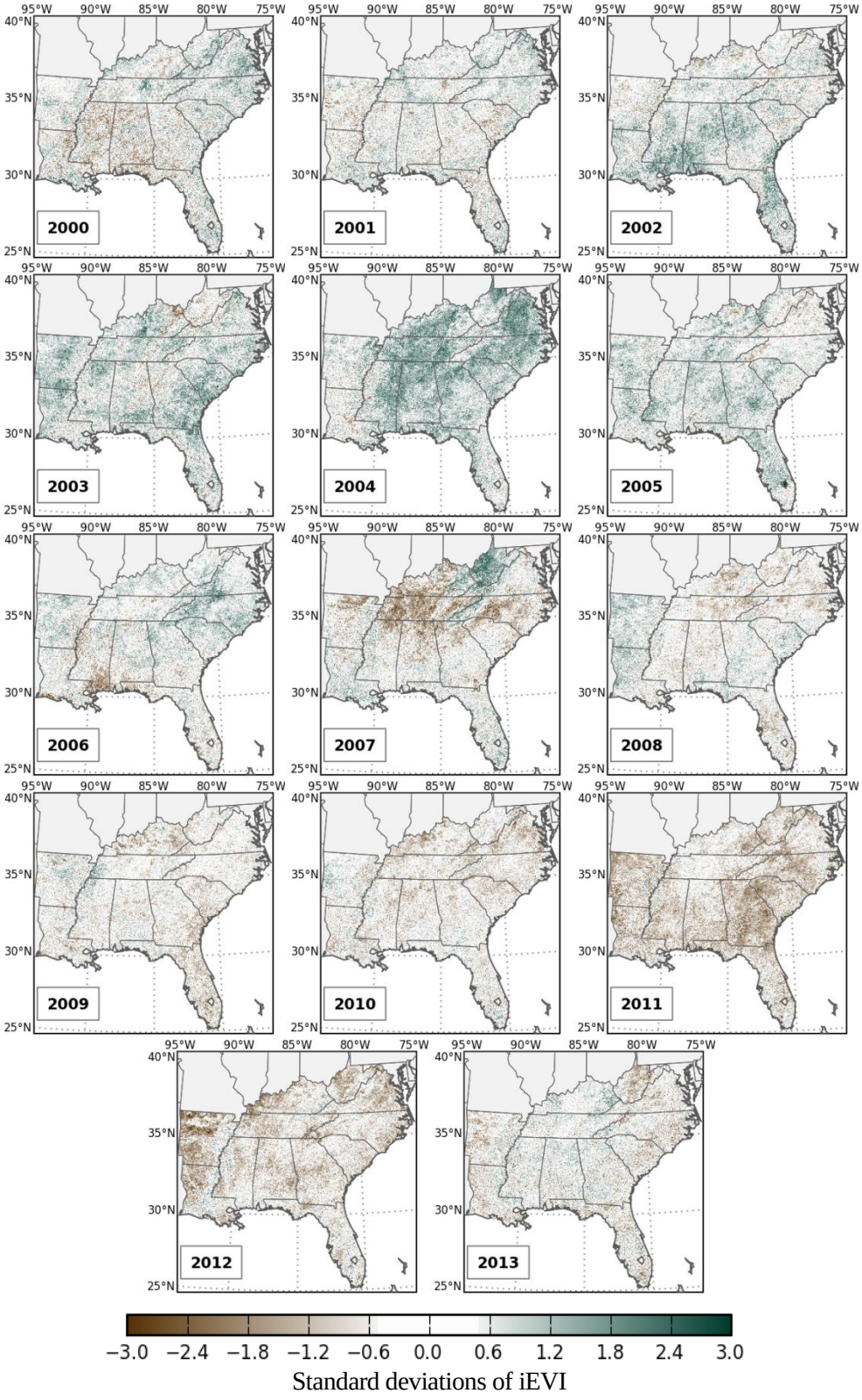

Figure 4.5: Standardized anomalies of iEVI over the MJJAS period and years 2000-2013 for the SEUS.

In 2006, a particularly strong reduction in greenness was observed for eastern and southern Mississippi. However, although negative iEVI anomalies were observed for the region preceding 2007, the last seven years of the period analyzed were characterized by large areas of negative greenness anomalies. In particular, the period March-September of 2007 experienced very strong negative greenness anomalies, which reached three standard deviations below mean iEVI. These reductions in photosynthetic potential were particularly severe in multiple states across the SEUS, especially impacting Tennessee and Kentucky. A decline in greenness for 2008 and 2009 was also observed for the whole region, although less strongly than the 2007 episode.

Greenness reductions were observed also for 2012, particularly in Arkansas. Although precipitation for the period was not particularly low in the region, these results can be explained by the strong heat wave that affected the SEUS in 2012, which significantly increased evapotranspiration and atmospheric water demand. Finally, it is noteworthy that although considerable browning affected almost the entire SEUS in 2011, the impacted areas differed from those affected by a similar event in 2007. Observations of this nature are particularly important, contributing to the establishment of an episode recurrence baseline and contributing to transitioning from single event to multi-event analyses. These analyses support the understanding of compound impacts of reduced water availability to ecosystems in the region. Growing time series of remotely sensed data should allow for a better consideration of these recurrence intervals and severity levels, incorporating the monitoring of vegetation status and how vegetation responds to successive stress episodes.

Spatial variability in vegetation liquid water content over the SEUS for the MJJAS period is represented by standardized anomalies of iNDWIm (Figure 4.6). Negative anomalies of water content were observed for 2000 and were particularly strong in the southwestern part of the area of study, including most of Mississippi and Alabama. Greenness anomalies for the same region and period were not as significant, suggesting that reductions in water balance and water availability were not immediately translated into reductions in leaf area and/or vegetation vigor.

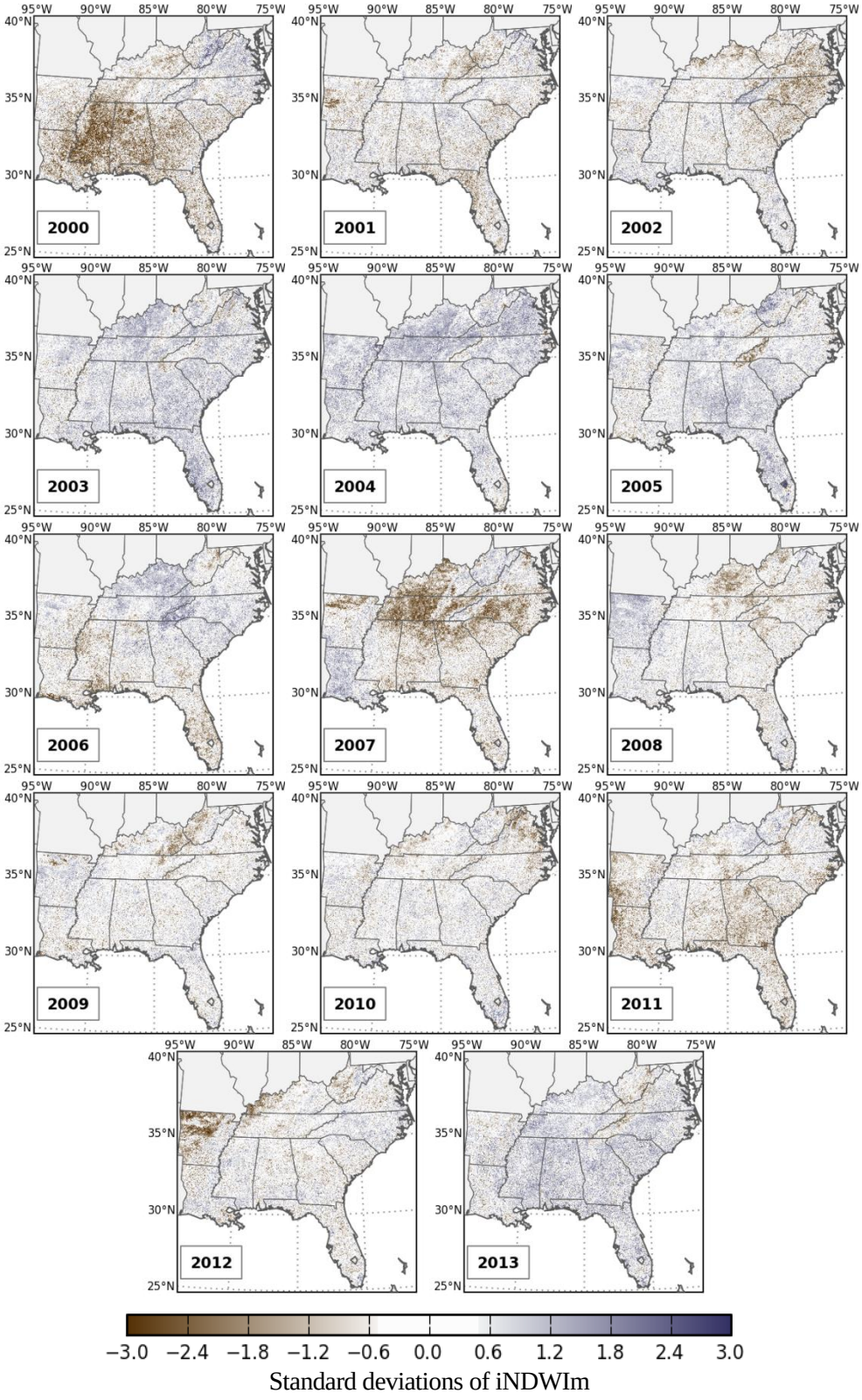

Figure 4.6: Standardized anomalies of iNDWIm over the MJJAS period and years 2000-2013 for the SEUS.

Other occurrences of similar relationships include the growing season of 2002 over the region's eastern coast. Increased plant liquid water content can be observed for multiple years and were particularly widespread in 2003, 2004 and 2013. Similar to the values observed for iEVI, strong negative anomalies of iNDWIm were verified for MJJAS 2007, particularly in western Tennessee and Kentucky. These responses coincided with sharp decreases in water balance, particularly during the first semester of 2007 and affected other areas in the Southeast as well. It is noteworthy that the magnitude of iNDWIm anomalies for 2007 was larger than corresponding values observed for iEVI for the same period.

Areas affected by widespread browning observed for 2012 showed a relatively less strong iNDWIm signature, with exception of Arkansas and Kentucky. Values of iNDWIm for MJJAS 2012 showed positive and negative anomalies for the index for most of the region, with very strong negative values at its western fringe. These results suggest that plant water content was not particularly low in many parts of the Southeast, but significant temperature increases observed during 2012 may have contributed to reductions in plant photosynthetic potential.

Variability in water content reflected the physiographic diversity of the Southeast, resulting in particularly evident regional footprints. In this respect, the Blue Ridge Province (land cover: deciduous broadleaf and mixed forests) in Southern Appalachia had distinct iNDWIm signatures in 2006 (relatively wet) and in 2007 (relatively neutral) when compared to the Piedmont and other surrounding regions with predominance of cropland/natural vegetation mosaics and including mixed forests. Similar relationships can be observed for the Interior Low Plateaus and its cropland and natural vegetation areas, as well as for the deciduous broadleaf forests of the Appalachian Plateaus in 2007.

A large percentage of the SEUS is covered by a mosaic of croplands and natural vegetation at finer spatial scale than the pixel size of the MODIS bands used by this study. As a result, these different land cover types cannot be resolved by the MODIS sensor and were considered as a single cover class by this study. In this respect, changes in iEVI and iNDWIm

reported by this investigation and occurring over areas used by agriculture (particularly the Coastal Plain, Piedmont and Interior Low Plateaus) may have been associated with agriculture, including widespread crop failure in the region during extreme droughts (e.g., during the growing season of 2007). In addition, comparatively smaller variability in integrated indices was observed for the Mississippi Valley, although this region was affected by reductions in precipitation during the 2000-2013 period. Reductions in iEVI and iNDWIm were more common around the valley, where areas not heavily used for agriculture occur. These results suggest that water availability, more than temperature, is defining greening/browning status in the region and that irrigation practices are supplying water to crops during periods of reduced precipitation.

To investigate relationships between vegetation status and water balance, including the effects of extended below normal water balance on greenness, this work investigated anomalies of EVI and SPEI at multiple time scales for the each month of the MJJAS period. Identifying these relationships has multiple ecological implications and may be used in predictive models of vegetation responses to climate scenarios in the region. Figure 4.7 shows a series of regression models considering monthly standardized anomalies of EVI and SPEI at 1, 2 , 3, 4, 6, 9, 12 and 18 months. Considering that non-provisional precipitation and temperature data from PRISM were not available for the 2013 growing season during the time of writing, regression models considered variables only for the period 2000-2012. Model development used standardized anomaly of EVI and SPEI for the same month of index computation and included above and below normal water balance values.

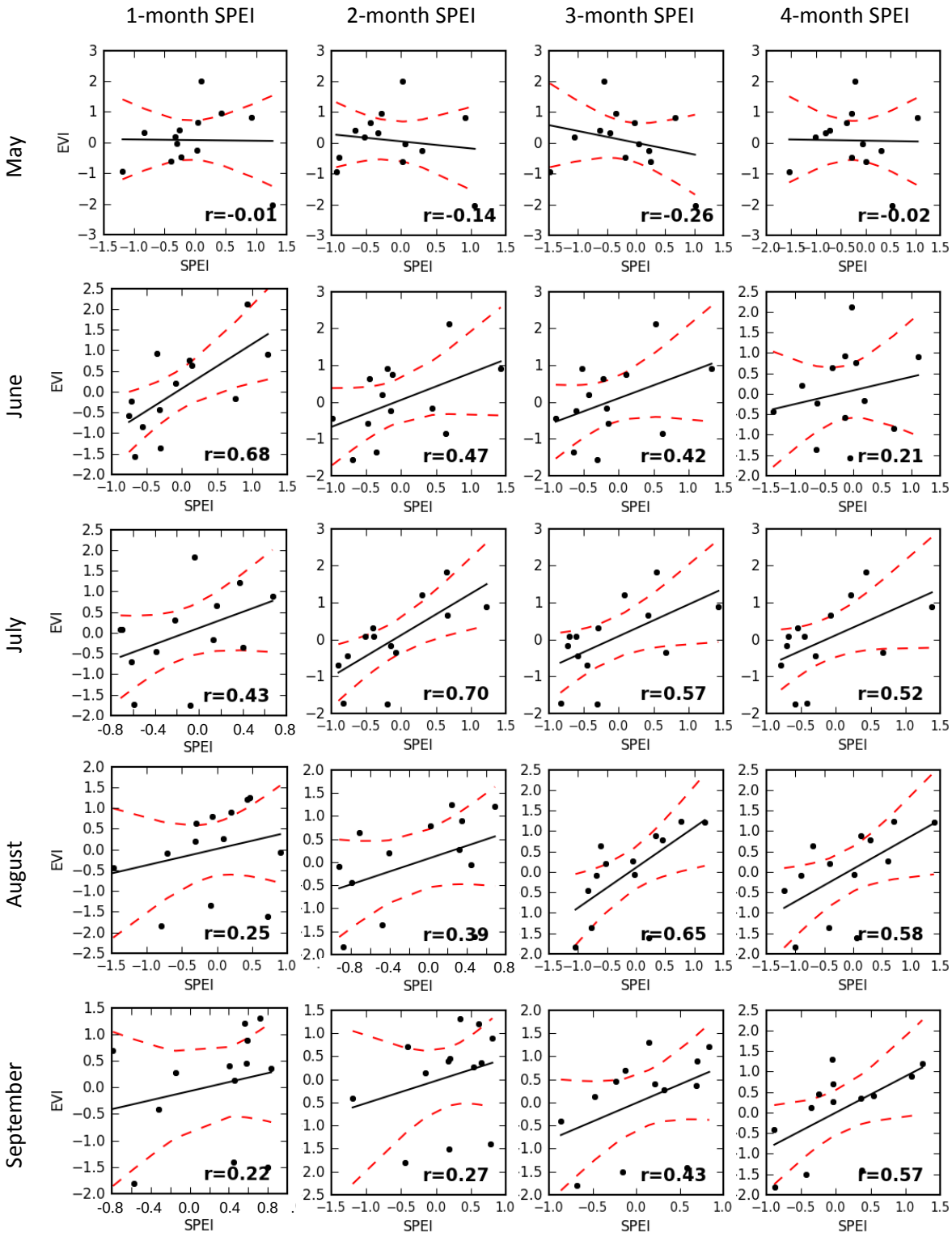
1-month SPEI
2-month SPEI
3-month SPEI
4-month SPEI
May
June
July
August
September
EVI
SPEI
r=-0.01
r=-0.14
r=-0.26
r=-0.02
r=0.68
r=0.47
r=0.42
r=0.21
r=0.43
r=0.70
r=0.57
r=0.52
r=0.25
r=0.39
r=0.65
r=0.58
r=0.22
r=0.27
r=0.43
r=0.57

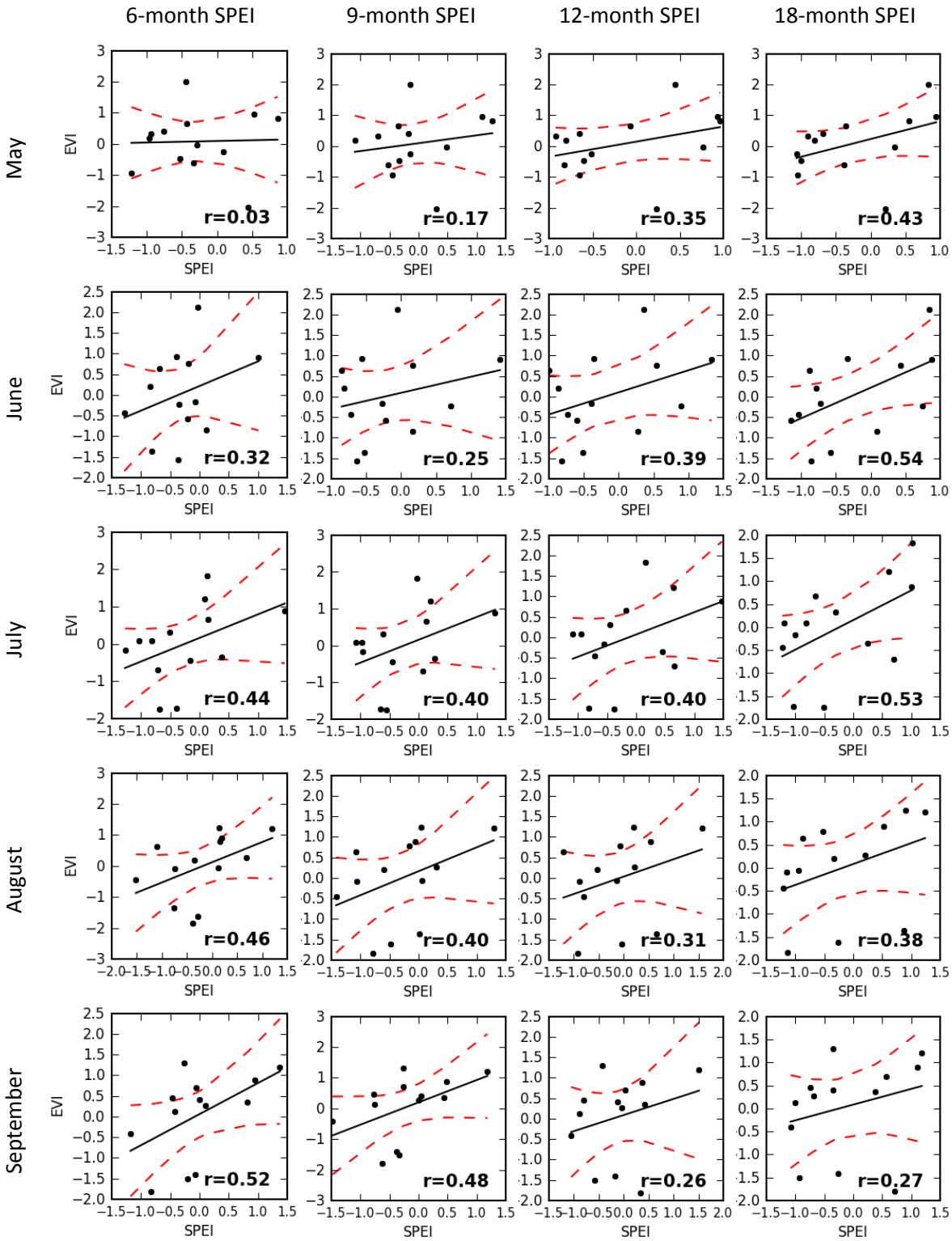

Figure 4.7: Linear regression lines (solid line) for SPEI (time-scales: 1, 2, 3, 4, 6, 9, 12 and 18 months) and EVI for the period MJJAS and years 2000-2012. Coefficients of correlation and 95% confidence bands (dashed lines) are indicated.

Relationships between SPEI and greenness were particularly weak for the month of May across most of the time scales considered. In one instance (3-month SPEI), negative correlation was observed between standardized anomalies of EVI and departures from normal water balance. Stronger correlations for May were found for longer SPEI time scales, peaking at the 18-month period. Relatively shorter wet and dry periods occurring in the SEUS would have little effect on greenness during May, as shown by regression results. Closer relationships were found for subsequent months and SPEI, particularly for June (1-month, r=0.68), July (2-month, r=0.70), August (3-month, r=0.65) and September (4-month, r=0.57). These observations corroborate the results by Vicente-Serrano et al. (2013), who found strong relationships between SPEI and vegetation in the SEUS for time scales below nine months for most of the region.

Stronger correlations for the 1-month SPEI were observed as the growing season progressed, with largest coefficients for this time scale associated with the month of June. Correlation strength then decreased towards the end of the growing season. The results suggest that same-month below-normal precipitation or water surplus has less negative or positive influence on greenness in September than in June. This observation may be associated with crops maturing in the region and may include critical times for water availability associated with natural vegetation phenology. Also noticeable is a shift in relationship strength as a function of SPEI time scale, particularly for time scales ranging from 1-month to 4-month. For longer time scales, the month when the strongest relationships were observed moved from June to August-September. Capturing this variability at relatively shorter time scales stresses the importance of using drought descriptors representing fine temporal resolution for these analyses, as opposed to using indices associated with fixed and coarser scales (e.g., PDSI). Further, periods of below or above normal water balance extending over one year and occurring at the 18-month time scale have been recorded in the SEUS. The results presented indicate the importance of considering shorter time scales, but also suggest that relationships between water balance and greenness at longer scales in the region should not be ignored.

Regression models were developed also considering NDWIm and SPEI at multiple time scales (Figure 4.8). Considerations regarding time scales, data availability and methods, presented when describing model development for standardized anomalies of EVI are also valid here. Regression models used standardized anomalies of NDWIm and SPEI for the same month of index computation. Relationships between anomalies of NDWIm and SPEI were stronger than those observed for EVI for all months. These results suggest that plant water content in the SEUS is responding to changes in precipitation and temperature over the region and that NDWIm is capturing the variability of liquid water content in plants. Further, results indicate that water content is more sensitive to shorter time scales of water balance than the relationships previously seen for EVI, as water transport and leaf flushing, senescence and abscission may operate at different temporal scales. Regression models also indicate an increase of on average one time step in sensitivity for NDWIm, when compared to EVI. As a result, stronger short time scale (one to six months) correlations between anomalies of NDWIm and SPEI were observed for June (2-month, r=0.67), July (3-month, r=0.79), August (4-month, r=0.90) and September (3-month, r=0.85). Also noteworthy is that water content for the first three months of the MJJAS period showed strongest relationships when considering longer time periods of SPEI (12-month and 18-month time scales). The results above suggest strong contributions of water balance conditions following the month of May to the definition of plant water content during the MJJAS period. These observations, together with those results presented for EVI, emphasize the importance of water balance conditions in the region starting in May and June and their strong contribution to photosynthetic potential and plant water content during the growing season for most of the SEUS.

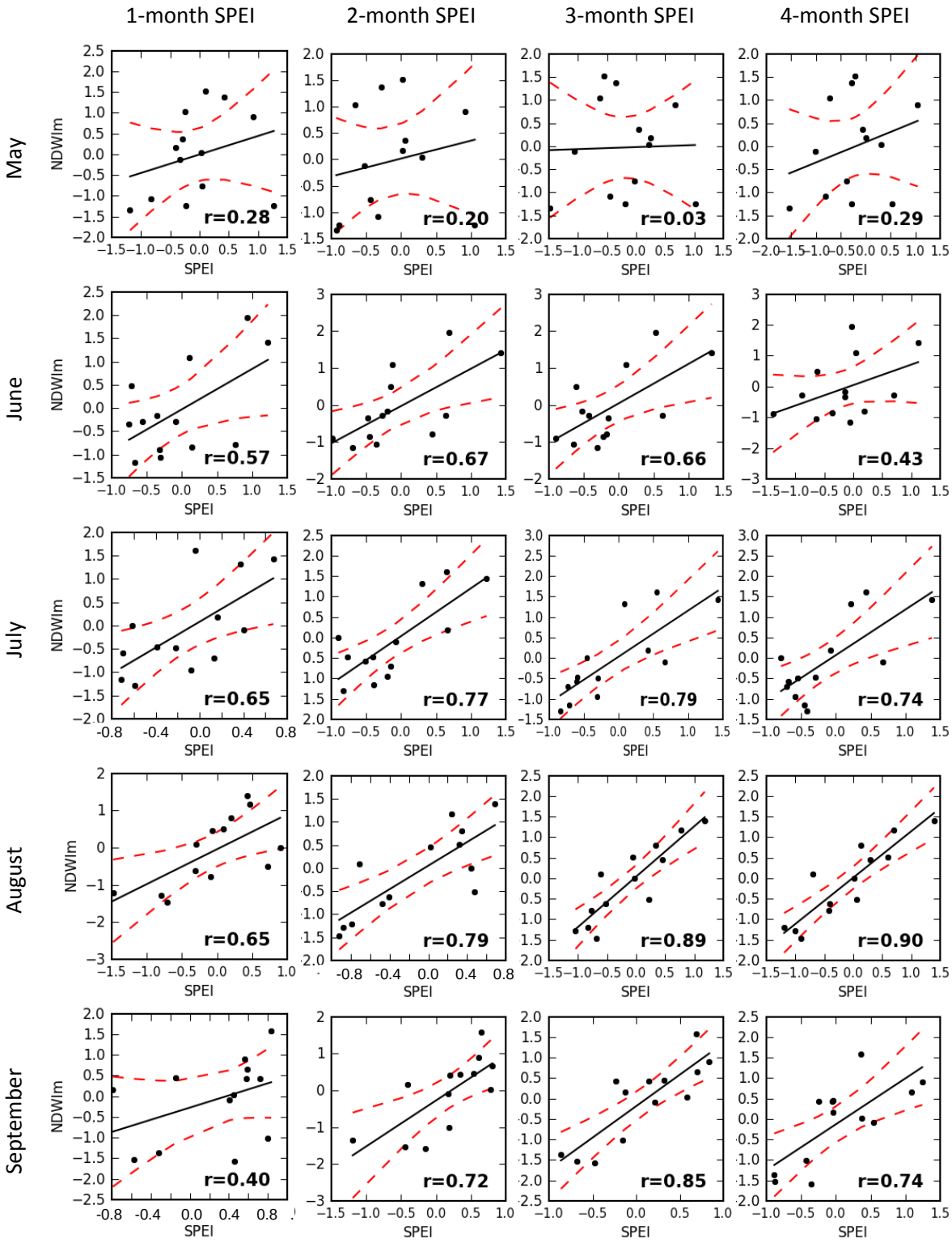
1-month SPEI
2-month SPEI
3-month SPEI
4-month SPEI
May
June
July
August
September
NDWIm
SPEI
r=0.28
r=0.20
r=0.03
r=0.29
r=0.57
r=0.67
r=0.66
r=0.43
r=0.65
r=0.77
r=0.79
r=0.74
r=0.65
r=0.79
r=0.89
r=0.90
r=0.40
r=0.72
r=0.85
r=0.74

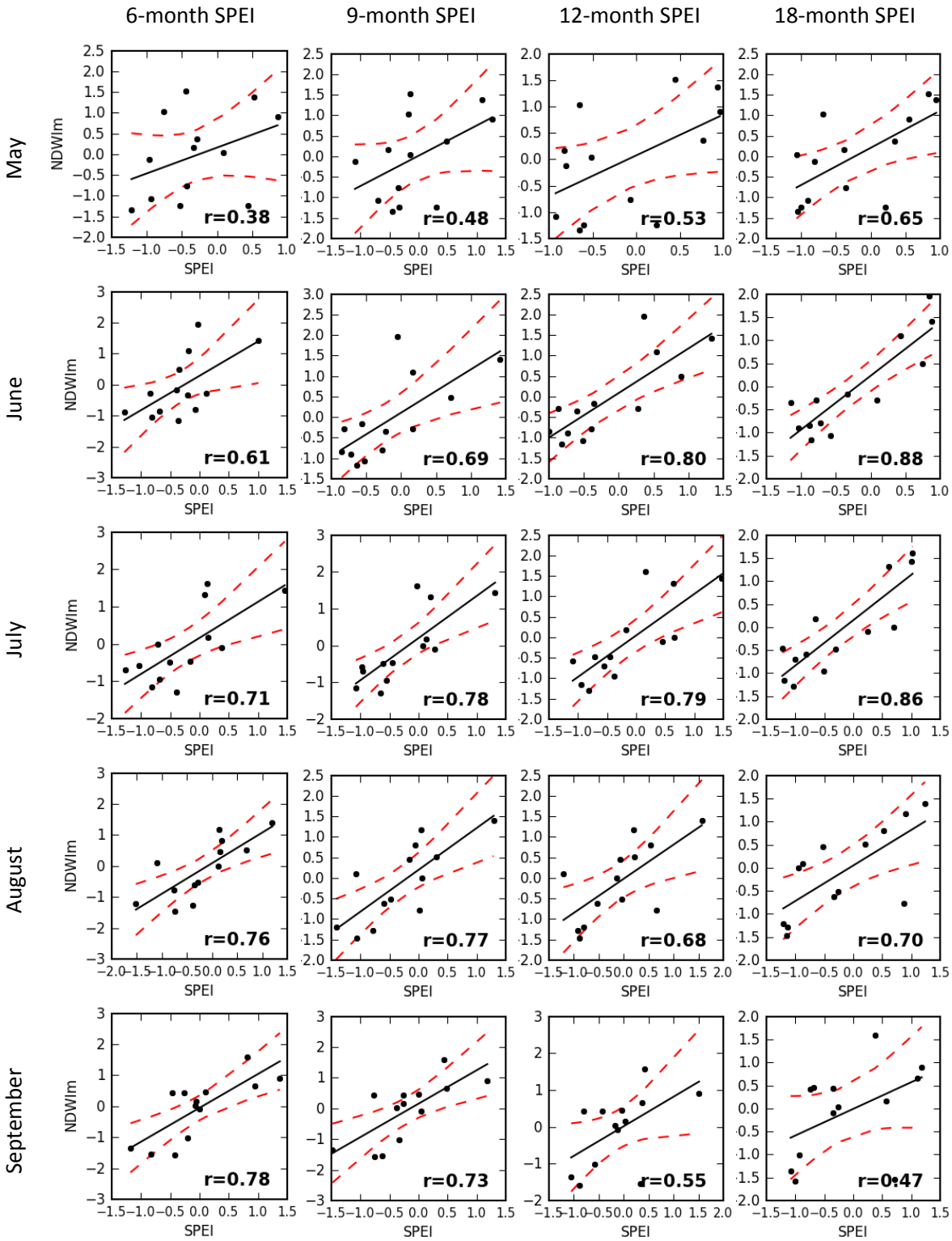

Figure 4.8: Linear regression lines (solid line) for SPEI (time-scales: 1, 2, 3, 4, 6, 9, 12 and 18 months) and NDWIm for the period MJJAS and years 2000-2012. Coefficients of correlation and 95% confidence bands (dashed lines) are indicated.

The reported relationships are a function of the amount and the characteristics of green leaf material available during the MJJAS period, but other factors affecting greenness and water content estimates from orbital systems may be involved. In particular, variations in phenology, including the timing of leaf flushing and the start of senescence and abscission may play a significant role in how these indices are measured, thus affecting their interpretation. Further, results suggest that the particularly strong anomalies of greenness and water content observed during this investigation affected vegetation also beyond the MJJAS time interval and, perhaps, beyond the years analyzed. In this respect, it is conceivable that associated reductions in leaf material and in photosynthetic activity affected the length, the start and/or the end of growing seasons in the SEUS during the 21st century. Although identifying these specific changes in growing seasons and phenology is beyond the scope of this study, the importance of these changes should be stressed. If impacts to growing seasons are verified, changes in the exchange of energy and matter over the region may have fluctuated considerably during the period, with critical local and regional ecological implications.

4.6 Summary and conclusions

Plant productivity in the Southeastern United States is limited by temperature, water availability and radiation, with local variations in the relative importance of each of these factors (Nemani et al., 2003; Running et al., 2004). Changes in the amount or quality of these variables over the next century have the potential to affect local economy and critical ecosystems in the Southeast. It is therefore critical to expand our knowledge of how natural and man-made systems will respond to future environmental changes.

Vegetation health and vigor also are a function of multiple other factors, including competition, herbivory and management/practices. Some of these factors act at relatively local scales. Climate related events, however, often affect vegetation at regional level and may result in stronger footprints in the vegetation signal. As demonstrated by this investigation, these signals

can be captured by metrics derived from remote sensors, although limits of detectability of a variety of vegetation related phenomena are still an area of research. In this context, this work identified vegetation responses to climatic variability by using remotely-sensed data to investigate changes in vegetation greenness and water content over the Southeastern United States for the period 2000-2013. Analyses incorporated descriptors of water balance, represented by the Standardized Precipitation-Evapotranspiration Index (SPEI). Results indicated multiple instances of strong relationships between water balance and vegetation in the Southeast, including decrease in plant photosynthetic potential following periods of reduced water availability and/or above normal temperatures (i.e., negative water balance). Conversely, increases in greenness also were observed associated with above normal water balance, particularly for the first half of the period analyzed.

Acknowlegments

This research was supported by NASA Headquarters under the NASA Earth and Space Science Fellowship Program – Grant "NNX09AO18H". Support was also received from the Coweeta Long Term Ecological Research Program.

References

Anderson, L. O., Malhi, Y., Aragao, L. E. O. C., Ladle, R., Arai, E., Barbier, N., & Phillips, O. (2010). Remote sensing detection of droughts in Amazonian forest canopies. *New Phytologist, 187*(3), 733-750. doi: DOI 10.1111/j.1469-8137.2010.03355.x

Daly, C., Neilson, R. P., & Phillips, D. L. (1994). A Statistical Topographic Model for Mapping Climatological Precipitation over Mountainous Terrain. *Journal of Applied Meteorology, 33*(2), 140-158. doi: Doi 10.1175/1520-0450(1994)033<0140:Astmfm>2.0.Co;2

Ding, Y., & Smith, K. H. (2008). Economic impacts of the 2007 drought. *DroughScape, the Newsletter of the National Drought Mitigation Center*, 6-9.

Gao, B. C. (1996). NDWI - A normalized difference water index for remote sensing of vegetation liquid water from space. *Remote Sensing of Environment, 58*(3), 257-266. doi: Doi 10.1016/S0034-4257(96)00067-3

Gu, Y. X., Hunt, E., Wardlow, B., Basara, J. B., Brown, J. F., & Verdin, J. P. (2008). Evaluation of MODIS NDVI and NDWI for vegetation drought monitoring using Oklahoma Mesonet soil moisture data. *Geophysical Research Letters, 35*(22). doi: Artn L22401, Doi 10.1029/2008gl035772

Huete, A. R., Didan, K., Miura, T., Rodriguez, E. P., Gao, X., & Ferreira, L. G. (2002). Overview of the radiometric and biophysical performance of the MODIS vegetation indices. *Remote Sensing of Environment, 83*(1-2), 195-213. doi: Pii S0034-4257(02)00096-2, Doi 10.1016/S0034-4257(02)00096-2

Huete, A. R., Justice, C. O., & van Leeuwen, W. (1999). MODIS vegetation index (MOD 13) algorithm theoretical basis document, version 3: USGS Land Process Distributed Active Archive Center.

IPCC. (2012). Managing the risks of extreme events and disasters to advance climate change adaptation (Vol. 1, pp. 582-582). Cambridge: Cambridge University Press.

Jonsson, P., & Eklundh, L. (2004). TIMESAT - a program for analyzing time-series of satellite sensor data. *Computers & Geosciences, 30*(8), 833-845. doi: DOI 10.1016/j.cageo.2004.05.006

Karl, T. R., Melillo, J. M., & Peterson, T. C. (2009). *Global climate change impacts in the United States : a state of knowledge report*. Cambridge England ; New York: Cambridge University Press.

McKee, T. B., Doesken, N. J., & Kleist, J. (1993). *The relationship of drought frequency and duration to time scales.* Paper presented at the 8th Conference on Applied Climatology

Nemani, R. R., Keeling, C. D., Hashimoto, H., Jolly, W. M., Piper, S. C., Tucker, C. J., . . . Running, S. W. (2003). Climate-driven increases in global terrestrial net primary production from 1982 to 1999. *Science, 300*(5625), 1560-1563. doi: DOI 10.1126/science.1082750

Peters, A. J., Ji, L., & Walter-Shea, E. (2003). Southeastern US vegetation response to ENSO events (1989-1999). *Climatic Change, 60*(1-2), 175-188. doi: Doi 10.1023/A:1026081615868

Running, S. W., Nemani, R. R., Heinsch, F. A., Zhao, M. S., Reeves, M., & Hashimoto, H. (2004). A continuous satellite-derived measure of global terrestrial primary production. *Bioscience, 54*(6), 547-560. doi: Doi 10.1641/0006-3568(2004)054[0547:Acsmog]2.0.Co;2

Sakamoto, T., Yokozawa, M., Toritani, H., Shibayama, M., Ishitsuka, N., & Ohno, H. (2005). A crop phenology detection method using time-series MODIS data. *Remote Sensing of Environment, 96*(3-4), 366-374. doi: DOI 10.1016/j.rse.2005.03.008

Sheffield, J., & Wood, E. F. (2008). Projected changes in drought occurrence under future global warming from multi-model, multi-scenario, IPCC AR4 simulations. *Climate Dynamics, 31*(1), 79-105. doi: DOI 10.1007/s00382-007-0340-z

Solano, R., Didan, K., Jacobson, A., & Huete, A. (2010). MODIS Vegetation Index (MOD13) C5 User's Guide. Version 2.0: The University of Arizona.

U.S. Drought Monitor. (2013). University of Nebraska-Lincoln, National Drought Mitigation Center. from http://droughtmonitor.unl.edu/archive.html

Vicente-Serrano, S. M., Beguería, S., & López-Moreno, J. I. (2010). A Multiscalar Drought Index Sensitive to Global Warming: The Standardized Precipitation Evapotranspiration Index. *Journal of Climate, 23*(7), 1696-1718. doi: 10.1175/2009JCLI2909.1

Vicente-Serrano, S. M., Gouveia, C., Camarero, J. J., Begueria, S., Trigo, R., Lopez-Moreno, J. I., . . . Sanchez-Lorenzo, A. (2013). Response of vegetation to drought time-scales across global land biomes. *Proceedings of the National Academy of Sciences of the United States of America, 110*(1), 52-57. doi: DOI 10.1073/pnas.1207068110

Wang, H., Fu, R., Kumar, A., & Li, W. H. (2010). Intensification of Summer Rainfall Variability in the Southeastern United States during Recent Decades. *Journal of Hydrometeorology, 11*(4), 1007--1018 DI 1010.1175/2010.

CHAPTER 5

PRIMARY PRODUCTIVITY OF TERRESTRIAL ECOSYSTEMS OVER THE SOUTHEASTERN UNITED STATES: A FINE-RESOLUTION SPATIOTEMPORAL ANALYSIS OF PRODUCTIVITY AND CLIMATIC VARIABILITY IN THE 21ST CENTURY[3]

[3] Bernardes, S., Donovan, L.A. and Madden, M. To be submitted to *Remote Sensing of Environment*.

Abstract

Droughts may affect plant metabolism negatively, reduce primary productivity and impact services of entire ecosystems. Droughts occurring in the 21st century in the Southeastern United States (SEUS) have left unknown consequences to the biological system. This work attempts to understand some of these consequences by investigating spatial and temporal variations in carbon uptake and respiration and by quantifying changes in primary productivity of ecosystems occurring in the SEUS following 1999. Products from the Moderate Resolution Imaging Spectroradiometer (MODIS) sensor, onboard the Terra satellite, were mosaicked and smoothed/gap filled based on their quality. Climate surfaces from Daymet were used as input to a semi-empirical model based on radiation use efficiency to calculate gross and net primary productivity. Comparisons were made with productivity estimates derived from flux towers. Positive anomalies of net primary production or NPP (ΔNPP = +0.20 Pg C) were observed for the SEUS in 2003, when values of the Standardized Precipitation-Evapotranspiration Index (SPEI) reached severely wet values for multiple areas in the region. Conversely, significant reductions in NPP were observed for 2006 (ΔNPP = -0.11 Pg C) and for 2007 (ΔNPP = -0.06 Pg C), when values of the 3-month scale SPEI were lowest. Productivity anomaly analysis for the entire region showed that the SEUS sequestered less carbon during the 2000-2012 period (ΔNPP = -2.56 Pg C) than its potential for carbon uptake when optimal conditions for plant production occur. The period following the onset of the 2006-2009 drought was observed to be the main contributor to the reduction in biomass accumulation, with a net carbon balance of -1.50 Pg C. Relationships between dry conditions, as indicated by SPEI, and changes in primary productivity suggest that water limited plant vigor and impacted plant growth in the SEUS, following the onset of an extreme drought in the region in 2006.

Keywords: drought, precipitation, GPP, NPP, time series analysis

5.1 Introduction

Water is recognized as a primary limiting factor for plant growth. Because of the many essential functions water plays in the plant system (e.g., electron donor in the photosynthesis process; nutrient and hormone transport; cell growth), water stress may directly and critically limit multiple key physiological processes in plants (Lambers et al., 2008). Under reduced water availability, gross and net plant production may be reduced, affecting the availability and allocation of photoassimilates. These conditions affect growth, reproduction, survival and ecosystem function. Indirect effects of water scarcity on plants often occur. Resulting from their need to keep their water status and cope with significant differences in water potential between the plant and its surrounding environment, most plants evolved to respond actively to water-potential differences (e.g., by regulating stomatal conductance), which may affect photosynthesis indirectly. Reductions in precipitation are often spatially and temporally linked to increases in temperature and plant respiration, further affecting carbon storage (Bernardes, Shepherd, & Madden, in preparation; Lambers et al., 2008). As a result, reductions in precipitation, which are expected to occur under future climates (Karl, Melillo, & Peterson, 2009), have the potential to negatively affect plant metabolism, reduce primary productivity/carbon uptake and limit energy/matter exchange and services of entire ecosystems (Flatley, Lafon, & Grissino-Mayer, 2011; Pederson, Gray, Fagre, & Graumlich, 2006; Zhao & Running, 2010).

The Southeastern United States (SEUS) has experienced high hydroclimatic variability during the first thirteen years of the 21st century, which included periods of increased precipitation (2003) and one of the most severe droughts in the instrumental record for the region. Notably, following 2006 large areas in the SEUS have received below normal precipitation during multiple consecutive years (Bernardes et al., in preparation). Increased temperature was also recorded in the region during this period. Such extreme hydroclimatic events have the potential to bring deleterious consequences to biological systems in the SEUS and to impact the survivability of important ecosystems in the region. We know little about the effects of extreme

climatic events on vegetation in the SEUS and have no knowledge of how complex climatic scenarios affect the region, including those effects resulting from short recurrence intervals of extreme hydroclimatic events. Given future climate projections of climatic variability, including droughts for the SEUS (Sheffield & Wood, 2008), it is essential that we increase our ability to monitor and predict vegetation responses to changes in water availability and climate variation, particularly those responses affecting primary productivity.

Remote sensing has been used to investigate changes in primary productivity over large areas affected by extreme climatic events (Heinsch et al., 2006; Nemani et al., 2003; Reichstein et al., 2007; Xiao et al., 2010; Zhao & Running, 2010). Several of these efforts use a growing time series of modeled productivity data derived from the Moderate Resolution Imaging Spectroradiometer (MODIS) sensor, onboard the Terra and Aqua satellites. However, because MODIS primary productivity is calculated for the entire globe, relatively coarse climate data is used to constrain the productivity model. As pointed out by Zhao, Running, and Nemani (2006) the main source of inaccuracy associated with the modeled MODIS productivity results from the use of those coarse climatological gridded surfaces. In particular, it is expected that the impacts of coarse resolution climate data over the accuracy of productivity estimates should increase over complex terrain, such as those occurring in Southern Appalachia and other parts of the SEUS. Enhancements to the MODIS primary productivity workflow incorporate non-linear interpolation of climate fields, aiming to reduce the footprint of climate data on the final productivity layer. Although efficient in smoothing the climate grid, this interpolation does not account for topographic variability or breaklines. As a result, this approach may contribute to inaccuracies and artifacts when applied to rugged terrain.

The overall objective of this work was to assess the spatiotemporal variability in primary productivity of multiple terrestrial ecosystems over the Southeastearn United States during the first thirteen years of the 21st century. In particular, the study aimed to investigate potential relationships between water availability and productivity in the region under high hydroclimatic

variability and extreme climatic events. This investigation hypothesizes that: (a) the magnitude of the extreme climatic events occurring in the SEUS during the first thirteen years of the 21st century resulted in changes to terrestrial ecosystems in the SEUS, including changes in primary productivity; and (b) vegetation responses, represented by changes in primary productivity, can be verified and quantified by using remote sensing and a modeling approach. As a secondary goal, this investigation aimed to refine the currently available time series of productivity estimates for the SEUS by implementing, evaluating and applying a climate-constrained primary productivity model based on light-use efficiency and physiographically-adjusted fine-resolution climate surfaces.

5.2 Study area

The study investigates changes in primary productivity over the Southeastern United States (SEUS, Figure 5.1), an area of approximately 1.4 million square kilometers. The region includes twelve states and is characterized by high landscape variability and complexity. Topography plays a significant role in this variability, ranging from a vast coastal plain to multiple plateaus and the high energy topography of the Southern Appalachian Mountains. Climate is predominantly humid, with the region receiving an average of 1,300 mm of precipitation per year, although significant spatial variation in rainfall occurs. For most of the region, rainfall is well distributed over the year, with no marked dry season. Physiographic variability also is reflected in the distribution of land cover in the region. Natural vegetation in the SEUS includes forest formations, mainly deciduous broadleaf and mixed forests, with occurrence of broadleaf evergreen and needleleaf forests. Other well represented vegetation types include woody savannas and, to a lesser extent, permanent wetlands. Significant areas of croplands can be found in the northwest of the region, in the Mississippi Valley and along the Coastal Plain and the Piedmont. The region harbors important areas for conservation, including the Southern

Appalachian Mountains, one of the most biodiversity-rich temperate regions on the planet (Walker, 1991).

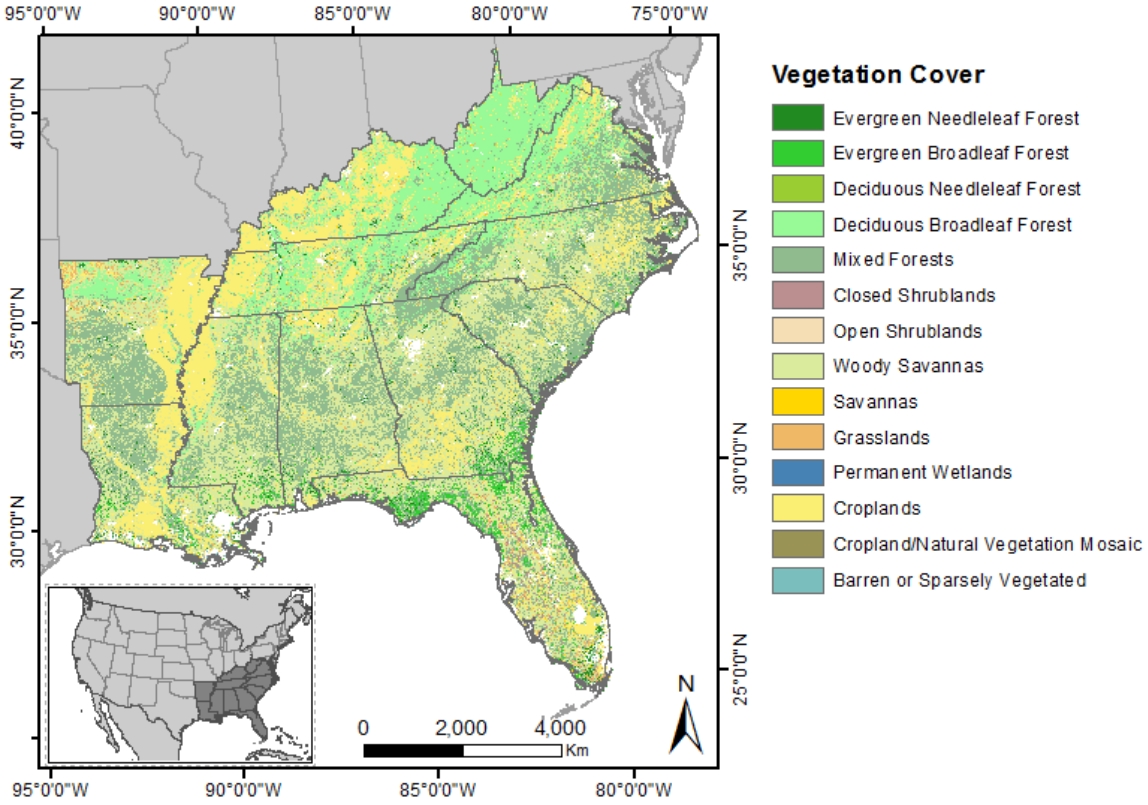

Figure 5.1: Area of study and the spatial distribution of vegetation types considered by this investigation (source: Land Cover product from the Moderate Resolution Imaging Spectroradiometer-MODIS, MOD12Q1. 2012, University of Maryland classification scheme).

5.3 Data

Daymet daily climatological data (Thornton et al., 2012) were used to constrain a semi-empirical light-use efficiency primary productivity model. Daymet outputs consist of daily 1 km-by1 km spatial-resolution gridded estimates of climatological fields, resulting from weighted interpolations and extrapolations of meteorological observations. Daymet resolution is comparable to the resolution of the satellite-derived products used by this investigation. Dataset selection also considered that Daymet's data processing workflow accounts for variations in topography, as well as heterogeneous distribution of weather stations. From Daymet, this work used daily gridded estimates of maximum temperature, minimum temperature, vapor pressure,

day length and shortwave radiation for the entire SEUS and period 2000-2012. Daymet data were also used for selected flux tower locations distributed over the conterminous United States, for the period of tower operation and flux data collection. Carbon fluxes measured by these towers were used for productivity model evaluation.

The spatial resolution of the climate layers constraining the productivity model affect model outcome, especially when the variability of a given climate field is particularly high (e.g., the altitudinal gradient in the temperature field over high energy relief). The use of climate surfaces with resolution coarser than the 1-km MODIS images leaves characteristic footprints on the final estimates of productivity. Downscaling climate data through non-linear interpolation has been proposed by Zhao, Heinsch, Nemani, and Running (2005) and is currently part of the workflow for the generation of MODIS productivity tiles. Although this solution may help reduce data footprints and support the creation of a consistent product for the entire globe, it is expected that productivity estimates would benefit from high resolution data available for specific regions. The finer spatial resolution of Daymet in comparison to global climate surfaces generated by NASA's Global Modeling Assimilation Office (GMAO) (Figure 5.2) is expected to improve model results, particularly over high energy topography.

Surfaces representing leaf area index (LAI) and the fraction of photosynthetically active radiation absorbed by vegetation during photosynthesis (FPAR) (Myneni et al., 2002), were used as input to the light-use efficiency primary productivity model. These biophysical descriptors, at 1-km spatial resolution, derive from images acquired from 2000 to 2012 by the Moderate Resolution Imaging Spectroradiometer (MODIS) sensor onboard the Terra satellite and one of two algorithms (radiative transfer model or empirical relationships). The MODIS FPAR/LAI product (MOD15A2) results from a compositing approach, representing the highest-quality estimates of these variables for 8-day time intervals. Additional MOD15A2 layers describing the quality of FPAR/LAI values were also used by this work, including the General and the Extra Quality Check datasets. FPAR/LAI is a MODIS Collection 005 product, accessed from the

MODIS Data Pool (date of access: October 22, 2013). Additional time series of FPAR/LAI values and accompanying quality data for non SEUS locations were obtained for Ameriflux flux tower sites. The period of FPAR/LAI data acquisition was a function of flux data collection by individual towers. From MODIS, this work also used the University of Maryland classification scheme of the 1-km resolution MODIS annual land cover product (MOD12Q1). Land cover was used to identify the location and spatial distribution of vegetation cover classes and to drive the productivity model.

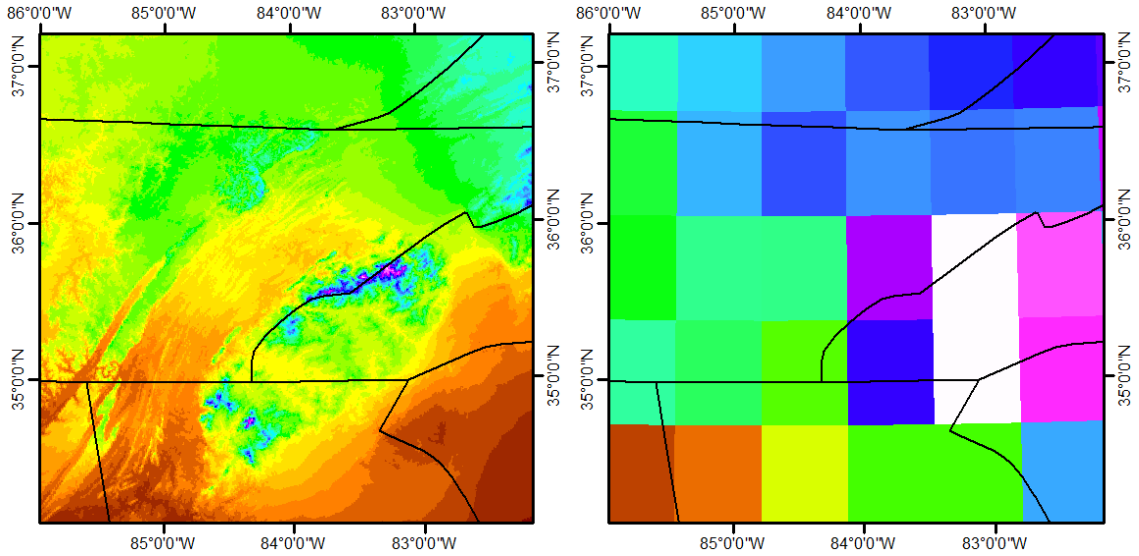

Figure 5.2: Maximum temperature surfaces over rugged terrain (Southern Appalachia) generated by (a) Daymet and (b) GMAO. Area in blue and purple shown by the Daymet dataset represents mountains in the Great Smoky Mountains National Park. Black lines are state boundaries.

Productivity-model evaluation used carbon flux estimates from flux towers and eddy covariance techniques. Daily representations of gross primary productivity (GPP) derived from eight flux towers (Arm SGP Main, Audubon, Bartlett Experimental Forest, Morgan Monroe, North Carolina Loblolly Pine, Santa Rita Savanna, Sylvania Wilderness, Kennedy Space Center) were accessed through the Ameriflux website (http://ameriflux.ornl.gov/). From Ameriflux, this investigation used Level 4 data, which is distributed gap-filled, partitioned and flagged regarding quality. The dataset results from Level 3 data being ustar-filtered and gap-filled using the Marginal Distribution Sampling (MDS) and Artificial Neural Network (ANN) methods. The

resulting data are partitioned into GPP, NEE and ecosystem respiration components. Flux data represented occurrences of multiple vegetation cover classes occurring in the SEUS, including croplands, grasslands, deciduous broadleaf forest, evergreen needleleaf forest, woody savanna, mixed forest, and closed shrublands. Flux-tower data collection temporally overlapped MODIS image acquisition and, for the majority of towers, was conducted during 2005-2006.

Productivity analysis and comparisons of results considered also Collection 5.5 of the GPP and NPP products generated by the Numerical Terradynamic Simulation Group (NTSG), at the University of Montana, and currently distributed by the Land Processes-Distributed Active Archive Center (LPDAAC). The approach used by the current investigation addresses improvements to the MOD17 products proposed by NTSG (Zhao et al., 2005), including: (a) data quality analysis and gap filling of MODIS FPAR being conducted at early stages in the productivity computation workflow; and (b) the reduction of climate data footprint on productivity layers, resulting from the coarse resolution of the climate data generated by GMAO. The productivity estimates from NTSG incorporate a non-linear interpolation of the GMAO dataset to reduce climate data footprint, but do not take into consideration topographic variability during interpolations. From NTSG this work also incorporated the biome properties look-up table (BPLUT) used in the generation of primary productivity. The BPLUT consists of biome specific parameters associated with productivity estimation, including maximum light conversion efficiency, limits for climate control of productivity and allometric relationships involving leaf and root mass and respiration.

Surfaces of non-provisional precipitation and temperature data generated by the PRISM Climate Group at Oregon State University (www.prism.oregonstate.edu, accessed on October 22, 2013) were used to characterize climatic variability in the SEUS. PRISM outputs result from modeling point data from multiple weather stations by considering topography and complex factors, including coastal effects and rain shadows (Daly, Neilson, & Phillips, 1994). This work

used monthly precipitation and temperature data from PRISM at 4-km spatial resolution and for the period 1895-2012.

5.4 Methodology

The investigation involved the spatialization, quantification and analysis of changes in primary productivity in the SEUS during the first years of the 21st century. The work included: (a) the pre-processing of MODIS FPAR/LAI data for quality assurance; (b) the preprocessing of Daymet climate data to spatially match the remote sensing derived dataset; (c) the evaluation of the productivity model using Daymet climate data and data derived from flux towers and eddy covariance techniques; (d) the modeling of primary productivity using a semi-empirical light-use efficiency model; and (e) the computation of water balance for the SEUS and period analyzed.

5.4.1 Data preparation

Individual 10 degrees by 10 degrees tiles of the MOD15A2 FPAR/LAI covering the area of study for the period 2000-2012 were used to generate a time series of seamless mosaics (46 mosaics per variable per complete year). The mosaicking included also the accompanying General and Extra Quality Check scientific datasets, which were later used for data quality analysis. Although MOD15A2 derives from atmospherically corrected reflectance data and a composite algorithm, the estimation of vegetation biophysical properties by this product can still be negatively affected by multiple factors, including instrumentation, viewing geometry and residual atmospheric noise. As a result, FPAR and LAI values may vary due to reasons extraneous to vegetation status and may present abrupt artificial changes in amplitude over space and time. As pointed out by Zhao et al. (2006), if procedures to compensate for variations in data quality are conducted after productivity computations, inconsistencies in time scales between the 8-day FPAR/LAI input data and the daily nature of productivity estimations may result in the generation of productivity artifacts. This work addressed reduced-quality data before productivity estimation using series of composite FPAR and LAI values from MODIS.

Spatiotemporal variations in MOD15A2 quality were addressed by using MODIS quality flags associated with each pixel during a spike removal and gap filling procedure. This work did not remove reduced-quality pixels from the time-series, avoiding the decrease in the temporal density of points used in the adopted curve fitting procedure for time-series reconstruction. A reduced number of FPAR/LAI points may negatively affect the success of the curve fitting (Jonsson & Eklundh, 2004). Instead, the complete FPAR and LAI data series were used and a quality-based weighting system for each pixel was developed using the General and Extra QC Scientific Datasets from MOD15A2. Using this system, reduced-quality pixels would be associated with lower weights and would have less influence over the results of the curve fitting procedures. To define weights, a rule-based classifier was implemented to categorize (rank) FPAR and LAI pixels into three quality categories (low, medium and high) according to the status of multiple quality flags, including: the success in using the product's main algorithm, the presence of a dead detector, the occurrence of clouds, cloud shadows, snow/ice or aerosol. Pixel ranking used conservative criteria and the lowest quality rank was assigned to a pixel when more than one quality flag was verified.

TIMESAT (Jonsson & Eklundh, 2004) was used for spike removal and curve fitting of the FPAR and LAI time series using the weights derived from the rule-based classifier. The performance of three curve fitting methods (Asymmetric Gaussian, Double Logistic and Savitzky-Golay) was analyzed regarding how these different approaches capture trends in the descriptor; the efficiency of the spike removal process; as well as the smoothing of the time series. A visual assessment of the results at multiple locations and time periods indicated that the double logistic fitting method (adaptation strength = 2, number of envelope interactions = 2) adequately meets the requirements of this investigation. During the double logistic fitting, the three rank categories resulting from the MODIS quality-flags analysis were assigned individual weight values (low = 0.3, medium = 0.65 and high = 1.0).

Daymet data were mosaicked and reprojected (nearest-neighbor interpolation), in order to match the MODIS FPAR/LAI mosaics spatially. Reprojected surface climate data were then used in the generation of derived climate products, including average temperature and vapor pressure deficit (VPD), following the work of Bolton (1980). Precipitation and temperature surfaces from PRISM were used in the computation of a time series of monthly images and regional values representing the Standardized Precipitation-Evapotranspiration Index (SPEI) (Vicente-Serrano, Beguería, and López-Moreno (2010). Monthly surfaces of SPEI calculated for a 3-month time scale were generated for the period 2000-2012 (calibration period: 1895-2012) and involved the fitting of water balance (precipitation minus evapotranspiration) to a log-logistic distribution, followed by the normalization of the fitted data. PET computation used the Hamon method, following recommendations by Lu, Sun, McNulty, and Amatya (2005). Departures from the historical record for the time scale analyzed are described as standard deviations, indicating positive (normal or wet periods) or negative departures (normal or dry periods). Table 5.1 presents ranges of SPEI values and associated dry/wet conditions used by this investigation.

Table 5.1: Categories of wetness and dryness and corresponding value ranges for the Standardized Precipitation-Evapotranspiration Index (SPEI)

Categories	SPEI[1]
Extremely wet	≥ 2.00
Very/severely wet	1.50 to 1.99
Moderately wet	1.00 to 1.49
Near normal	0.99 to -0.99
Moderate drought	-1.00 to -1.49
Severe drought	-1.50 to -1.99
Extreme drought	≤-2.00

[1] based on categories of dryness proposed for the Standardized Precipitation Index (SPI) by McKee, Doesken, and Kleist (1993).

5.4.2 Primary productivity model

This study implemented a light-use efficiency, primary productivity model based on concepts proposed by Monteith (1972) and following the work of Running et al. (2004) and Zhao et al. (2006). The model estimates daily GPP at per-pixel level by using a biome-based light

conversion coefficient, adjusted for climatic conditions (temperature and VPD, from Daymet) and absorbed photosynthetically active radiation (APAR), calculated using Daymet-based downwelling shortwave radiation data and quality-analyzed MODIS FPAR.

GPP is given by the relationship:

$$GPP = \varepsilon \times PAR \times FPAR$$

where ε is the maximum light-use efficiency for the biome considered, adjusted for climate constraints, and PAR is the incident photosynthetically active radiation. Values of ε derive from biome-specific maximum light-use efficiency (ε_{max}), defined as the vegetation light-conversion efficiency when optimal climatological conditions occur. The conversion from optimal to observed climatological conditions involves the adjustment of ε_{max} using Daymet-derived minimum temperature and VPD scalars, as follows:

$$\varepsilon = \varepsilon_{\max} \times T_{min}scalar \times VPDscalar$$

PAR is defined as 45% of the daily downwelling shortwave radiation, calculated using radiation flux and daylength from Daymet. NPP is computed by subtracting carbon used in the maintenance of leaves, roots and live wood from daily GPP values, considering also that growth respiration represents approximately 25% of NPP (equation below). Respiration calculations follow Q_{10} rules using coefficients from the BPLUT.

$$NPP = \sum_{i=1}^{365} \left(GPP - MR_{leaf} - MR_{froot} - MR_{wood}\right) - R_{growth}$$

where MR_{leaf}, MR_{froot} and MR_{wood} are leaf, fine root and live wood maintenance respiration, respecitively, and R_{growth} is the annual growth respiration. Maintenance respiration used Q_{10} rules, leaf mass (LAI/Specific Leaf Area) and a series of biome-specific allometric relationships between leaf mass and the mass of fine roots and live wood. Following this methodology, continuous fields of GPP and NPP were calculated for the entire SEUS. Outputs of the productivity model were then integrated into monthly and annual productivity values. To allow for model adjustment and evaluation, similar productivity computations were conducted for the

locations of eight Ameriflux flux towers across the conterminous U.S. The evaluation of computations and comparisons with flux tower productivity estimates used MODIS pixels and associated quality data for tower locations provided by Ameriflux. FPAR data for tower locations were quality analyzed and used in the computation of productivity (Chen et al., 2009; Heinsch et al., 2006; Turner et al., 2006).

5.5 Results and discussion

The analysis of the time-series of MOD15A2 quality flags included all FPAR pixels from MODIS Terra for the area of study and period 2000-2012. The area of study presents considerable spatiotemporal variation in pixel quality, which was affected mainly due to cloud cover. Areas of characteristically reduced quality include the southern tip of the Florida peninsula, sections of the Appalachian Mountains, and multiple small areas over a long stretch in the Mississippi valley, from Kentucky to Louisiana. Reductions in quality were particularly noticeable in the mountains of West Virginia. Conversely, areas less affected by quality reduction include the coastal plain and parts of the Piedmont, where good quality was observed over a wide swath from eastern Georgia to Virginia. Following quality analysis, TIMESAT was used to remove data spikes and for curve fitting. Figure 5.3 presents examples of the original FPAR values (open circles) and the results of the Double Logistic fitting (solid circles), showing three years of FPAR values for selected pixels in the area of study. Pixels were selected to represent occurring land cover classes in the area of study and were collected over a mixed forest and an evergreen needleleaf forest. The fitting procedure eliminated large and abrupt variations in FPAR amplitude, also reducing smaller data variability. In particular, results show that the fitting captured the temporal variation (including seasonality) associated with leaf status.

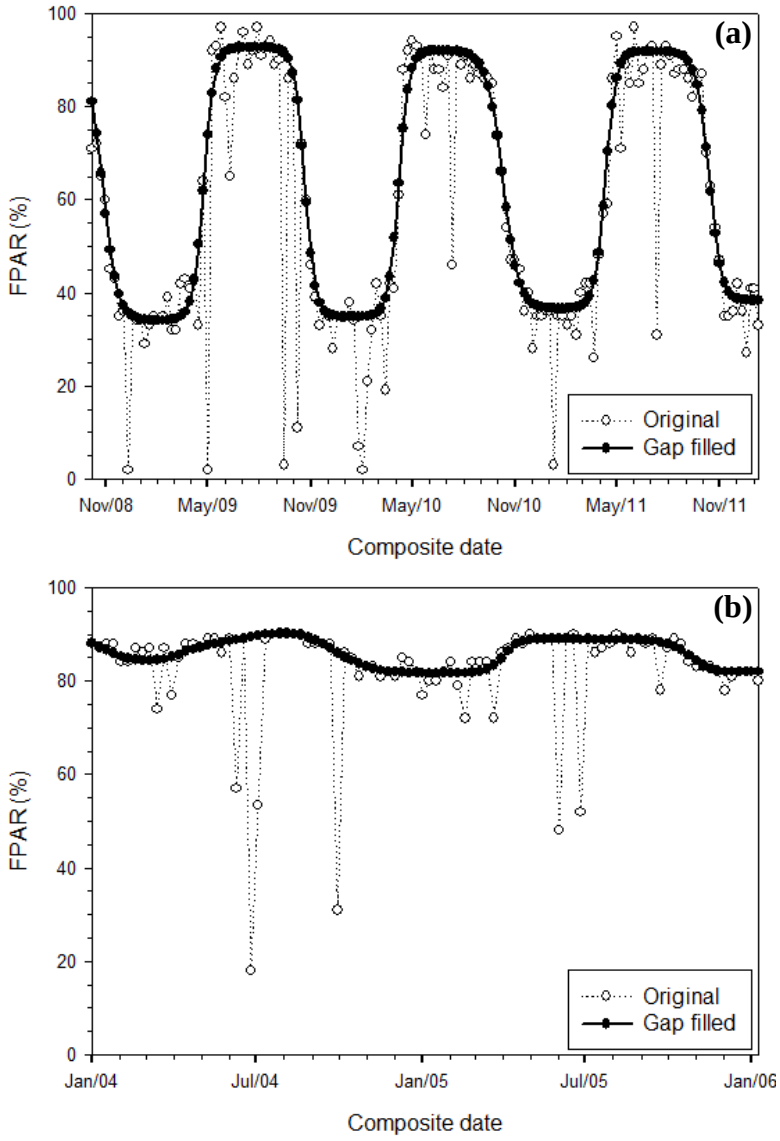

Figure 5.3: Sample spike removal and gap filling results for FPAR, considering (a) mixed forest and (b) needleleaf evergreen forest.

Results from the evaluation of the productivity model using flux tower data, MODIS FPAR and Daymet data are presented in Figure 5.4. Good agreement was observed between the model output using Daymet and productivity estimated by eddy covariance. Observed differences included modeled values in the upper envelope of flux tower results, particularly for those values in the center of the time series. Conversely, MODIS productivity estimates based on GMAO stayed below flux tower values during the same period.

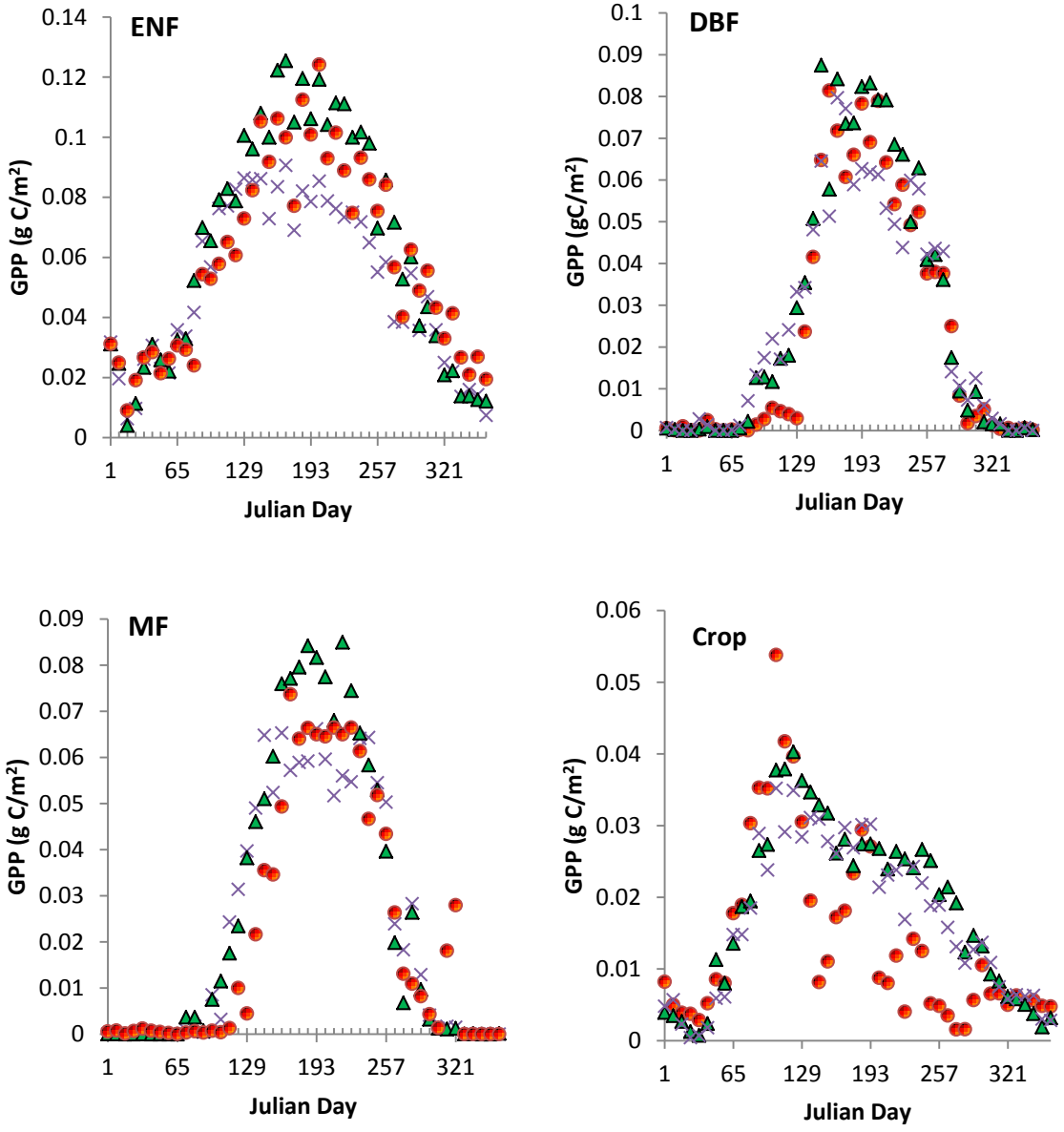

Figure 5.4: 8-day flux tower GPP (orange circles) and GPP modeled using Daymet (green triangles) and MODIS17A2 (purple "x"). Results are presented for evergreen needleleaf forest (ENF); deciduous broadleaf forest (DBF); mixed forest (MF); and cropland (Crop).

To compare model results further, productivity estimates using GMAO and Daymet were regressed against flux tower estimates. Figure 5.5 shows regression models resulting from these comparisons indicating that relationships between Daymet-derived GPP and GPP from flux towers were stronger than those obtained by using GPP derived from GMAO. The quality of the productivity results generated by this investigation should then be similar or better than the

quality of the datasets currently being generated as part of the MODIS workflow. Considering these results, it is expected that the finer resolution of the climate data used by this investigation will contribute to enhancing the quality of productivity estimates for areas of high energy topography.

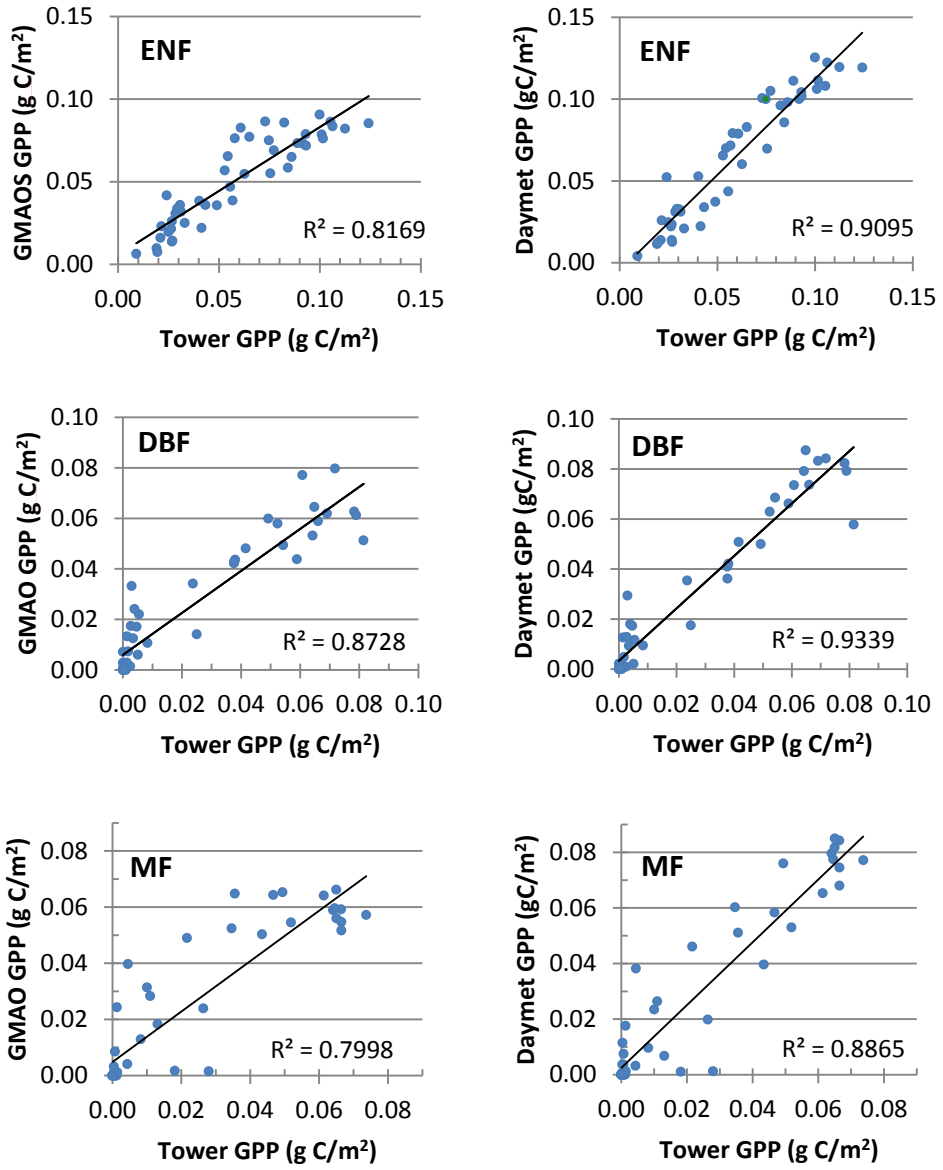

Figure 5.5: Regression lines for 8-day flux tower GPP and GPP modeled using Daymet and GMAO data. Results are presented for evergreen needleleaf forest (ENF); deciduous broadleaf forest (DBF); and mixed forest (MF).

Data analyses used standardized anomalies (*z* scores) of primary productivity, indicating distances from normal (mean) productivity values in units of standard deviations. Standardized anomalies remove seasonal signals and vegetation phenology from time series and assist in providing a common standard for spatiotemporal comparisons. Standardized anomalies for each month were computed by calculating mean and standard deviation using a temporal cross section of the 2000-2012 series. Computations considered a single month at a time for all years (e.g., Feb/2000, Feb/2001, … Feb/2012). Anomalies calculated for each year considered the entire NPP series to estimate mean and standard deviation. Standardized anomalies were calculated as follows:

$$SA_u = \frac{x_u - \overline{x_s}}{\sigma(x_s)}$$

where SA_u is the standardized anomaly for a given time unit u; x_u is the productivity value for the time unit; $\overline{x_s}$ is the mean productivity for the time unit calculated over the entire time series and $\sigma(x_s)$ is the standard deviation of productivity for the time unit, calculated over the series.

Figure 5.6 presents standardized anomalies calculated for monthly GPP for the entire SEUS and period 2000-2012. Values of 3-month SPEI are also presented and indicate significant climatic variability and fluctuations in water balance for the same time interval. Wet periods and periods of considerable dryness occurred multiple times and reached severe levels (see Table 5.1) on more than one occasion. Large departures from normal water balance included a wet year in 2003 (SPEI = 1.32), when periods of increased rainfall coincided with the growing season for most of the region of study. High SPEI also was observed for the second semesters of 2002 and 2004, both El Niño Southern Oscillation-ENSO years. Following a year with total rainfall and water balance approaching the historical average (2008), the strong 2009 El Niño brought increased precipitation to the Southeast. SPEI values for December 2009 reached the highest values observed for the period analyzed (SPEI = 1.47), approaching severely wet conditions.

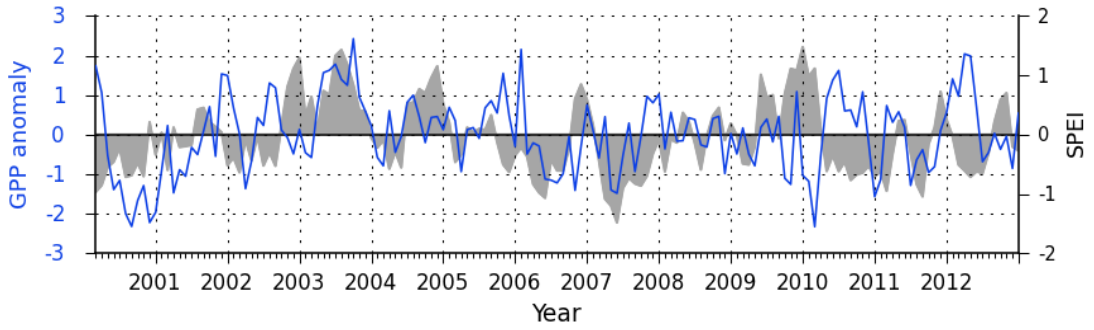

Figure 5.6: Monthly **s**tandardized anomaly of GPP (solid line, blue), and monthly 3-month SPEI (gray areas), considering all months for the period Jan/2001-Dec/2012 and entire SEUS. Year numbers indicate January for the year.

Reductions in SPEI were observed in the beginning of the series and were frequent following 2005. Decreases in SPEI were particularly strong during the 2006 and 2007 growing seasons. In 2007, 3-month SPEI reached the lowest values for the period analyzed during the month of May (SPEI = -1.48), approaching severely dry conditions. The three last years investigated show SPEI levels associated with dry conditions for the SEUS. Monthly gross primary productivity presented strong fluctuations over the period analyzed and varied with water balance in multiple instances. Increases in productivity and positive plant response were observed for periods when water was not limited during a growing season (2003) or for critical periods preceding the season (2010). This observation includes the largest positive anomalies of GPP for the period (1.78), observed in 2003. The lowest monthly GPP anomalies, -2.321 and -2.329, were observed in 2000 and in 2010, respectively. Negative anomalies of GPP followed or coincided with dry periods multiple times, with significant episodes including 2000, 2006, 2007 and 2011. Interestingly the sharp drops in productivity in 2009 and during the first semester of 2010 followed very positive SPEI values.

Values of NPP also showed considerable variability during the thirteen years investigated. Figure 5.7 shows anomalies of NPP in units of standard deviations and total carbon uptake anomaly for the SEUS, in petagrams (Pg) of carbon. Carbon uptake anomaly for the year

was calculated considering year uptake minus the average uptake for the period. Values of 3-month SPEI (right axis) are also presented.

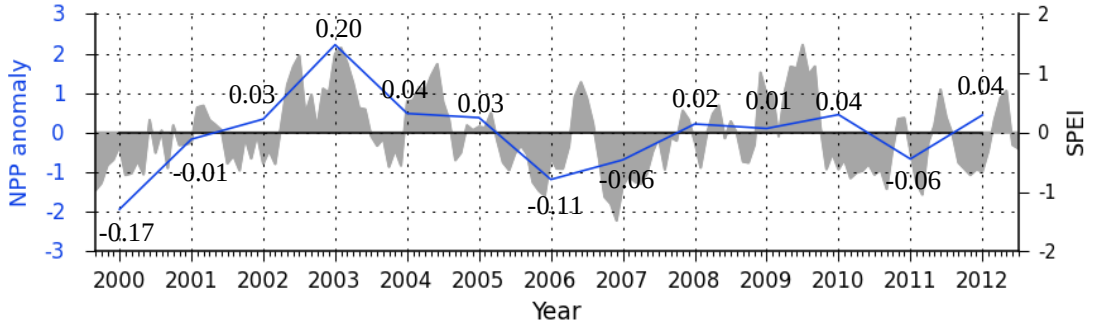

Figure 5.7: Annual **s**tandardized anomaly of NPP (blue line) for the period 2000-2012 and entire SEUS. 3-month SPEI is presented in gray. Values of NPP anomalies (Pg C/SEUS) are also shown. Year values indicate center of the year.

Deviations from normal carbon uptake indicated positive anomalies of net productivity (ΔNPP = +0.20 Pg C) for the SEUS in 2003, suggesting that productivity responded to positive water balance observed during 2002 and 2003. The 3-month SPEI for 2003 showed near normal conditions (SPEI = 0.06) preceding the growing season, and wet conditions (SPEI > 1.0) from June to August. Similarly high 3-month SPEI was verified for 2002, but associated only with the October to December period, while the preceding months showed negative SPEI values at near normal levels. Results suggest that the timing of positive water balance conditions in 2002 was associated with the relatively lower productivity observed for that year. Significant reductions in NPP were observed for 2000 (ΔNPP = -0.17 Pg C); for 2006 (ΔNPP = -0.11 Pg C) and for 2007 (ΔNPP = -0.06 Pg C), when values of the 3-month scale SPEI were lowest. During these years, SPEI reached -4 standard deviations in some areas of the SEUS (not shown), signaling extreme water deficit conditions. Reduction in productivity at a similar level was observed also for 2001 (ΔNPP = -0.06 Pg C), following a period of negative SPEI values within the near normal range. Productivity analysis for the entire region showed that vegetation in the SEUS sequestered 13.1 Pg C during the 2000-2012 period. Above average carbon sequestration was observed for the period 2000-2005, when NPP anomalies added to +0.12 Pg C. This six-year period witnessed the two extremes in carbon uptake in the series (2000 and 2003). Following 2006, anomalies of NPP

added to -0.12 Pg C. The observed relationships between GPP, NPP and SPEI stress the importance of considering the timing of water availability associated with critical stages of vegetation, including the need for using water balance and drought descriptors at a temporal scale compatible with the analysis.

During productivity anomaly analyses, a scenario considering the year of maximum carbon sequestration was investigated for anomaly computations. For this purpose, NPP for 2003 was considered as reference and the resulting anomalies showed that the SEUS sequestered considerably less carbon during the 2000-2012 period than its potential for sequestration (ΔNPP = -2.56 Pg C). In particular, the period following the onset of the 2006-2009 drought would be the main contributor to the reduction in biomass accumulation, with a net balance of -1.50 Pg C.

Figure 5.8 presents the spatiotemporal variation in anomalies of NPP for each year in the period 2000-2012. Particularly strong negative anomalies of NPP were widespread in 2000, affecting most of the region. Exceptions were the Carolinas, part of Florida and Louisiana, where increases in net productivity approaching one standard deviation occurred. Conversely, NPP was high almost for the entire region in 2003, and significant positive anomalies were recorded for Kentucky, West Virginia and Southern Appalachia, in the western part of North Carolina. Negative anomalies of NPP in west (2006) and central (2007) parts of the SEUS coincide with precipitation reductions in 2006 and 2007, suggesting that these conditions contributed to affect carbon uptake by vegetation. Near normal carbon sequestration levels were observed for the entire region from 2008 to 2010. Despite precipitation increases at the end of 2009 and at the beginning of 2010, changes in net productivity for the region were relatively small in 2010, including positive anomalies of NPP in the southwest of the region and reductions of NPP in the northeast. This spatial variation in positive and negative anomalies contributed to the reduced overall net productivity value for 2010 presented in Figure 5.7. Net productivity values for 2011 and for 2012 show increases in NPP for the entire region. In this respect, the 2011 negative NPP

anomalies in Mississippi, Louisiana and Arkansas transitioned to normal carbon uptake levels in 2012. Further, increase in carbon uptake also included a large portion of the eastern side of the SEUS, which showed positive anomalies of NPP in 2012.

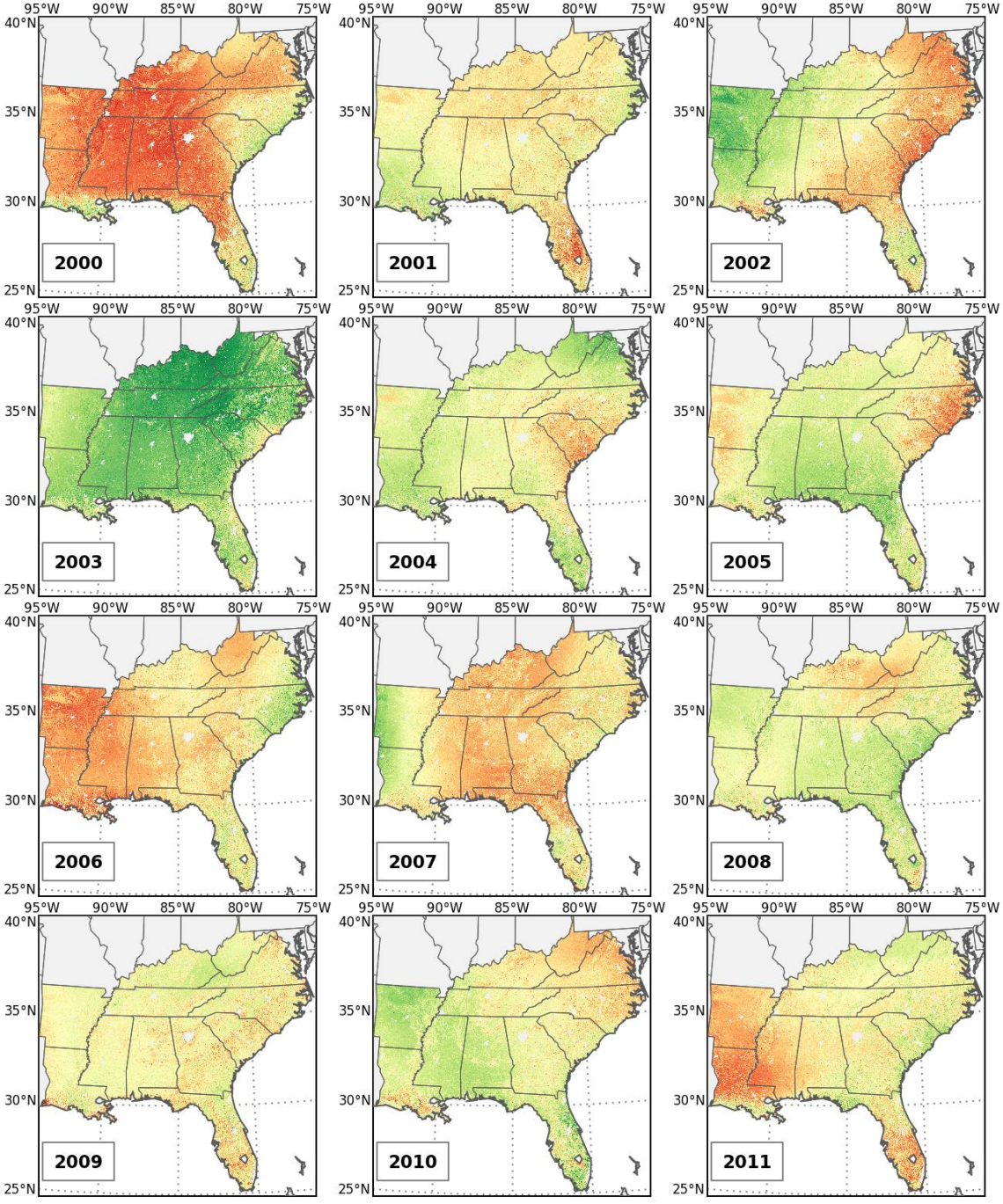

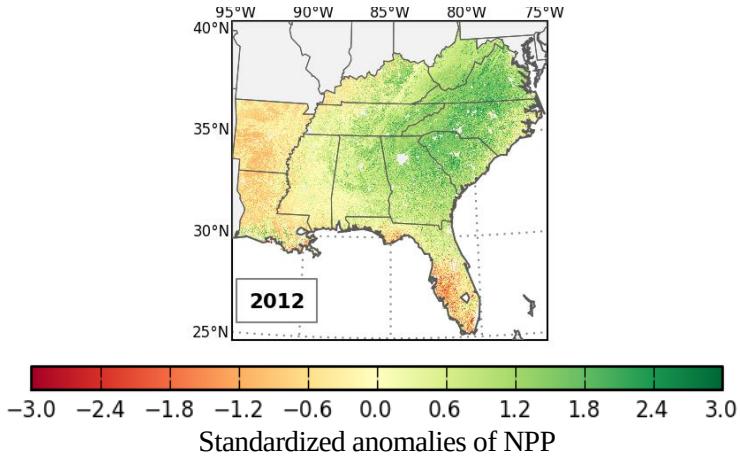

Figure 5.8: Standardized anomalies of NPP for the SEUS and period 2000-2012.

5.5.1 The 2007 extreme drought in the SEUS and spatiotemporal variation in primary productivity

In 2007, an extreme drought affected most of the SEUS, particularly during the region's growing season. This section investigates monthly changes in gross primary production in the region for each month in 2007. The analysis considers changes in water balance in the region during the same period, represented by 3-month SPEI. Figure 5.9 shows the spatiotemporal distribution of SPEI at the 3-month time scale for twelve months in 2007. Reduced SPEI was observed for January 2007 along the western fringe of the Appalachian Mountains, from West Virginia to Alabama. SPEI values reached -1.94 in the region, resulting from dry conditions during the end of 2006. Near normal SPEI values can be found for most of the region in January and particularly wet conditions can be observed in the east and in the west parts of the SEUS. SPEI reductions were significant during following months, reaching -3.6 in May in western Alabama. Negative SPEI values can be found for most of the region from March to June 2007, with exception of Virginia, the southeastern part of West Virginia and the southern tip of Florida. Conditions ameliorated in the western side of the region following May, including positive SPEI values observed for Louisiana, Arkansas and Mississippi. Drought severity increased considerably in eastern SEUS during following months, peaking in the Carolinas in September (minimum SPEI = -3.6). Precipitation in the end of 2007 contributed to positive water balances in

the region (maximum SPEI = 2.26), affecting states in the north (West Virginia, Kentucky and Tennessee), as well as those states along the Gulf Coast (Alabama, Mississippi and Florida).

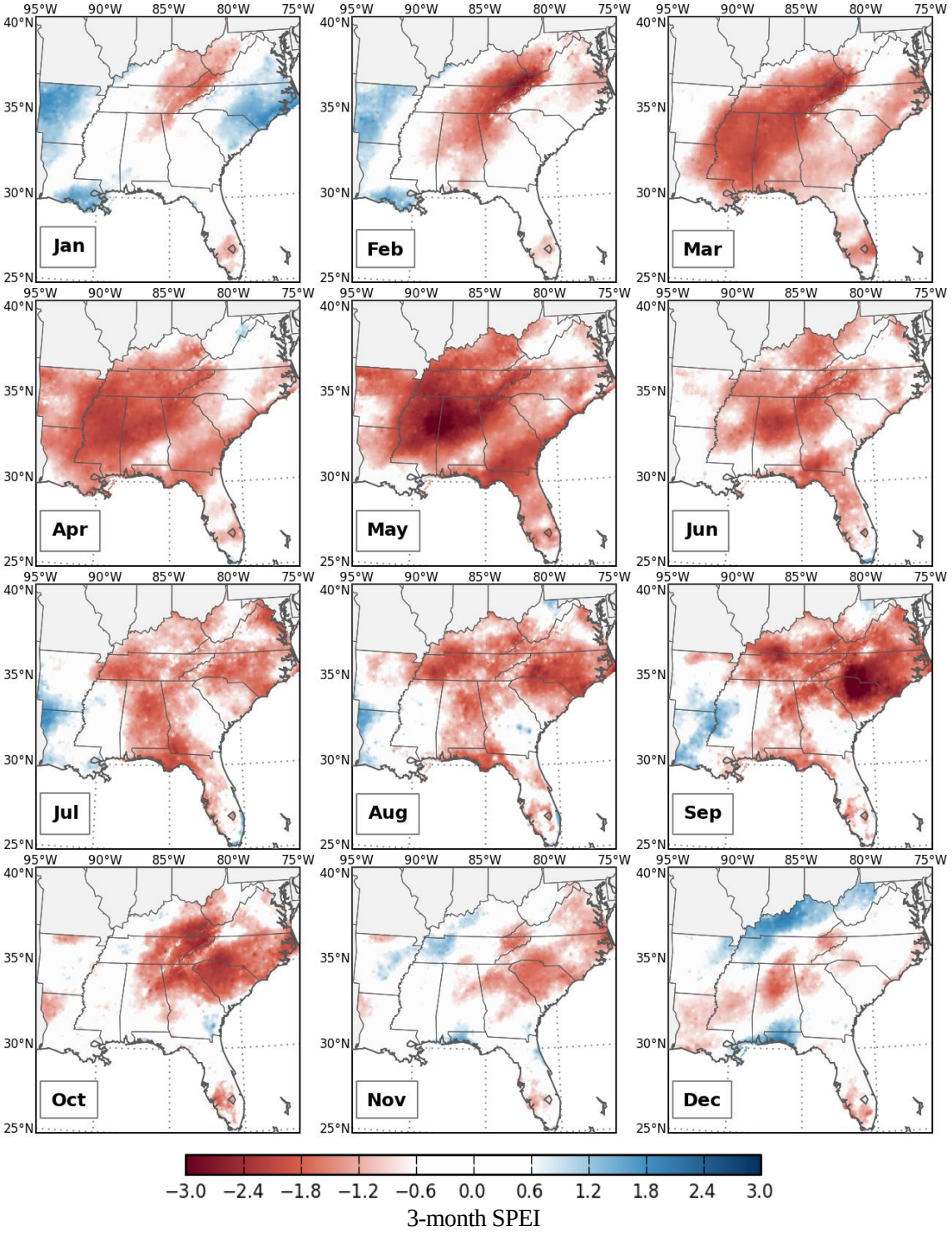

Figure 5.9: Spatial distribution of the 3-month SPEI for each month in 2007.

During January 2007, significant negative anomalies of GPP were observed along the Gulf Coast, and in the Atlantic side of the Florida Peninsula, while most of the SEUS presented near normal or slightly above normal productivity. An increase in GPP was observed for February for the northern part of the region of study. Absolute productivity values for these months should be particularly low, considering region-wide reduced temperatures, physiological limits to productivity and associated productivity model constrains. Under these circumstances, episodes of small absolute variations in productivity may result in large anomalies being recorded.

Reductions in GPP in the region were particularly noticeable in April. Standardized anomalies for this month were negative for most of the SEUS, with exceptions including parts of south Florida and the Mississippi Valley. The lowest GPP anomaly values observed for this month were recorded in southern Mississippi, where anomalies reached -3.23 standard deviations below normal conditions for the month. Decreases in GPP also were particularly significant in May, affecting multiple states in central SEUS. Affected areas involved croplands and natural vegetation, including large areas of mixed and broadleaf deciduous forests. No significant change in area showing GPP anomalies was observed for June and departures from normal conditions were less significant this month. In July, closer to normal gross primary productivity conditions were observed for the SEUS. Considering the extremely low SPEI values observed during April and May, it is particularly striking that no significant region-wide anomaly event was observed. However, anomalies of GPP observed in August in western Tennessee, Kentucky, and northern Mississippi and Alabama may have been associated with those departures of water balance earlier in the season. In this regard, signs of this reduction were still noticeable in September. Possibly due to the timing of events, including extreme conditions in the Carolinas late in the growing season (September), no substantial change in productivity was observed for these states, with the exception of relatively small areas in North Carolina. Although the Florida Peninsula and southeastern Georgia were affected by precipitation reductions in 2007, particularly strong

reductions in GPP were observed for the region only in October. These reductions were short-lived and positive anomalies of GPP were recorded for November and December 2007.

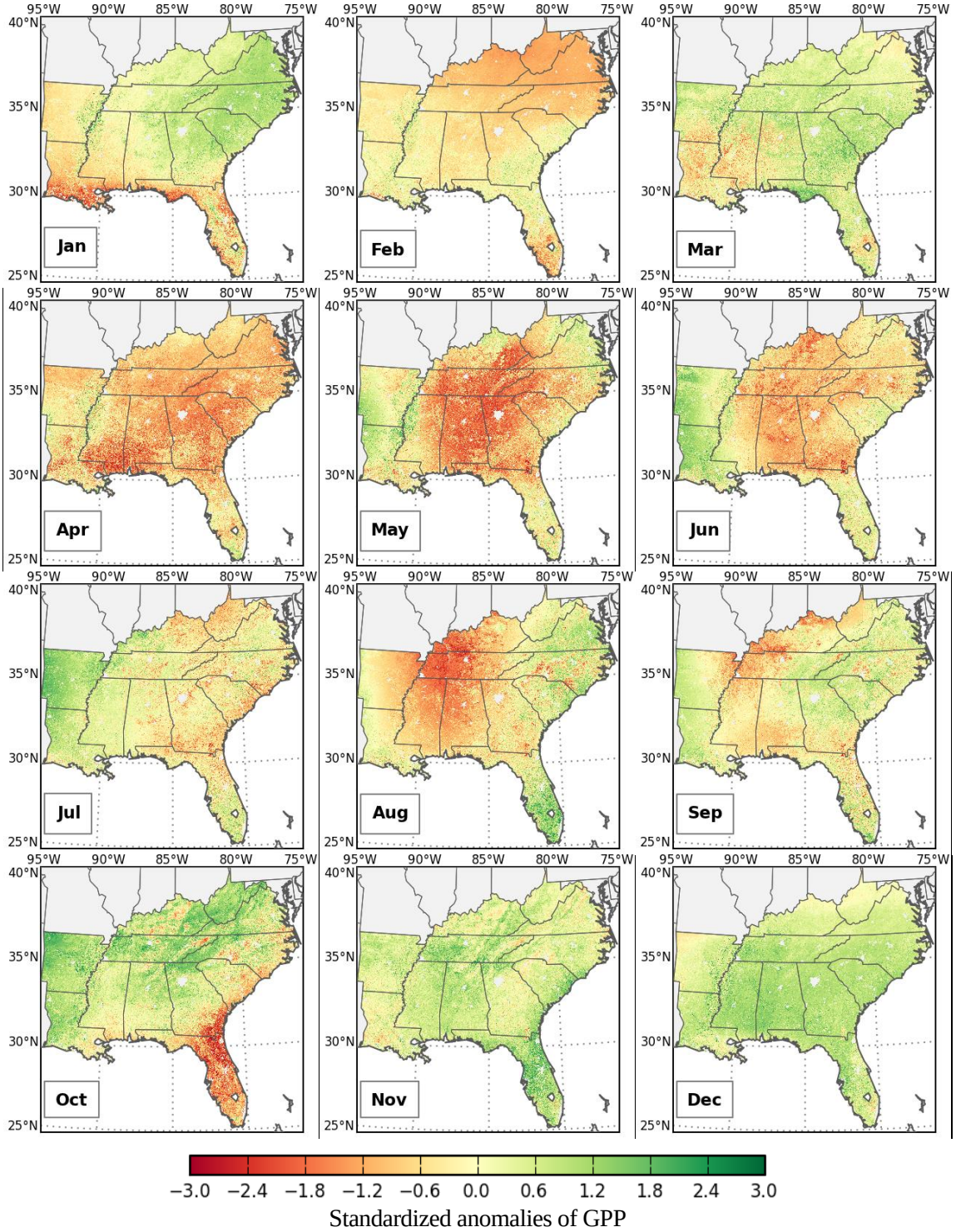

Figure 5.10: Standardized anomalies of GPP for each month in 2007

5.6 Summary and conclusions

This work investigated relationships between hydroclimate and temperature variability and vegetation conditions in the Southeastern United States during the first years of the 21st century. The Standardized Precipitation-Evapotranspiration Index (SPEI) was used to indicate water balance departures from the historical record and to characterize dry and wet periods in the Southeast. Results showed that the region witnessed high climatic variability in the period 2000-2012, as well as significant severe and extreme events.

The study also implemented and tested a semi-empirical primary productivity model for the Southeastern United States, based on light-use efficiency concepts and using fine-resolution climatological surfaces and MODIS remotely-sensed data. Comparisons between model outputs showed agreement with productivity estimates derived from flux towers over the conterminous United States. Products of the current implementation are expected to be superior to MODIS products currently distributed to the scientific community, particularly when considering high energy terrains, such as those occurring in the SEUS.

The observed spatiotemporal relationships between SPEI and primary productivity suggest that climatic events in the SEUS and associated changes in water availability to plants affected plant physiology and structure. These relationships included increases in productivity during or following wet periods and decreases when SPEI values showed water scarcity. Results show that primary productivity and carbon uptake in the region were below their potential for the region during the period analyzed, and suggest connections with suboptimal climate conditions.

High SPEI also was observed for the second semesters of 2002 and 2004, both El Niño Southern Oscillation-ENSO years. Following a year with total rainfall and water balance approaching the historical average (2008), the strong 2009 El Niño brought increased precipitation to the Southeast. SPEI values for December 2009 reached the highest values observed for the period analyzed (SPEI = 1.47), approaching severely wet conditions.

Acknowledgements

This research was supported by NASA Headquarters under the NASA Earth and Space Science Fellowship Program – Grant "NNX09AO18H". Support was also received from the Coweeta Long Term Ecological Research Program. The author thanks Maosheng Zhao from the Numerical Terradynamic Simulation Group at the University of Montana for providing key information regarding the latest developments in the MODIS primary productivity algorithm.

References

Bernardes, S., Shepherd, M., & Madden, M. (in preparation). *Historical perspectives on the occurrence, return levels and trends of severe and extreme dry and wet periods in the Southeastern United States*. in preparation.

Bolton, D. (1980). The Computation of Equivalent Potential Temperature. *Monthly Weather Review, 108*(7), 1046-1053. doi: Doi 10.1175/1520-0493(1980)108<1046:Tcoept>2.0.Co;2

Chen, B. Z., Black, T. A., Coops, N. C., Hilker, T., Trofymow, J. A., & Morgenstern, K. (2009). Assessing Tower Flux Footprint Climatology and Scaling Between Remotely Sensed and Eddy Covariance Measurements. *Boundary-Layer Meteorology, 130*(2), 137-167. doi: DOI 10.1007/s10546-008-9339-1

Daly, C., Neilson, R. P., & Phillips, D. L. (1994). A Statistical Topographic Model for Mapping Climatological Precipitation over Mountainous Terrain. *Journal of Applied Meteorology, 33*(2), 140-158. doi: Doi 10.1175/1520-0450(1994)033<0140:Astmfm>2.0.Co;2

Flatley, W. T., Lafon, C. W., & Grissino-Mayer, H. D. (2011). Climatic and topographic controls on patterns of fire in the southern and central Appalachian Mountains, USA. *Landscape Ecology, 26*(2), 195-209. doi: DOI 10.1007/s10980-010-9553-3

Heinsch, F. A., Zhao, M. S., Running, S. W., Kimball, J. S., Nemani, R. R., Davis, K. J., . . . Flanagan, L. B. (2006). Evaluation of remote sensing based terrestrial productivity from MODIS using regional tower eddy flux network observations. *Ieee Transactions on Geoscience and Remote Sensing, 44*(7), 1908-1925. doi: Doi 10.1109/Tgrs.2005.853936

Jonsson, P., & Eklundh, L. (2004). TIMESAT - a program for analyzing time-series of satellite sensor data. *Computers & Geosciences, 30*(8), 833-845. doi: DOI 10.1016/j.cageo.2004.05.006

Karl, T. R., Melillo, J. M., & Peterson, T. C. (2009). *Global climate change impacts in the United States : a state of knowledge report*. Cambridge England ; New York: Cambridge University Press.

Lambers, H., Chapin, F. S., & Pons, T. L. (2008). *Plant physiological ecology* (2nd ed.). New York: Springer.

Lu, J., Sun, G., McNulty, S. G., & Amatya, D. M. (2005). A comparison of six potential evapotranspiration methods for regional use in the southeastern United States. *Journal Of The American Water Resources Association, 41*(3), 621-633. doi: 10.1111/j.1752-1688.2005.tb03759.x

McKee, T. B., Doesken, N. J., & Kleist, J. (1993). *The relationship of drought frequency and duration to time scales.* Paper presented at the 8th Conference on Applied Climatology

Monteith, J. L. (1972). Solar-Radiation and Productivity in Tropical Ecosystems. *Journal of Applied Ecology, 9*(3), 747-766. doi: Doi 10.2307/2401901

Myneni, R. B., Hoffman, S., Knyazikhin, Y., Privette, J. L., Glassy, J., Tian, Y., . . . Running, S. W. (2002). Global products of vegetation leaf area and fraction absorbed PAR from year one of MODIS data. *Remote Sensing of Environment, 83*(1-2), 214-231. doi: Pii S0034-4257(02)00074-3, Doi 10.1016/S0034-4257(02)00074-3

Nemani, R. R., Keeling, C. D., Hashimoto, H., Jolly, W. M., Piper, S. C., Tucker, C. J., . . . Running, S. W. (2003). Climate-driven increases in global terrestrial net primary production from 1982 to 1999. *Science, 300*(5625), 1560-1563. doi: DOI 10.1126/science.1082750

Pederson, G. T., Gray, S. T., Fagre, D. B., & Graumlich, L. J. (2006). Long-duration drought variability and impacts on ecosystem services: A case study from Glacier National Park, Montana. *Earth Interactions, 10*.

Reichstein, M., Ciais, P., Papale, D., Valentini, R., Running, S., Viovy, N., . . . Zhao, M. (2007). Reduction of ecosystem productivity and respiration during the European summer 2003 climate anomaly: a joint flux tower, remote sensing and modelling analysis. *Global Change Biology, 13*(3), 634-651.

Running, S. W., Nemani, R. R., Heinsch, F. A., Zhao, M. S., Reeves, M., & Hashimoto, H. (2004). A continuous satellite-derived measure of global terrestrial primary production. *Bioscience, 54*(6), 547-560. doi: Doi 10.1641/0006-3568(2004)054[0547:Acsmog]2.0.Co;2

Sheffield, J., & Wood, E. F. (2008). Projected changes in drought occurrence under future global warming from multi-model, multi-scenario, IPCC AR4 simulations. *Climate Dynamics, 31*(1), 79-105. doi: DOI 10.1007/s00382-007-0340-z

Thornton, P. E., Thornton, M. M., Mayer, B. W., Wilhelmi, N., Wei, Y., & Cook, R. B. (2012). [Daymet: Daily surface weather on a 1 km grid for North America, 1980 -2008. Acquired online].

Turner, D. P., Ritts, W. D., Cohen, W. B., Gower, S. T., Running, S. W., Zhao, M. S., . . . Ahl, D. E. (2006). Evaluation of MODIS NPP and GPP products across multiple biomes. *Remote Sensing of Environment, 102*(3-4), 282-292. doi: DOI 10.1016/j.rse.2006.02.017

Vicente-Serrano, S. M., Beguería, S., & López-Moreno, J. I. (2010). A Multiscalar Drought Index Sensitive to Global Warming: The Standardized Precipitation Evapotranspiration Index. *Journal of Climate, 23*(7), 1696-1718. doi: 10.1175/2009JCLI2909.1

Walker, S. (1991). *Great Smoky Mountains: The splendor of the southern Appalachians*: Camelback Design Group.

Xiao, J. F., Zhuang, Q. L., Law, B. E., Chen, J. Q., Baldocchi, D. D., Cook, D. R., . . . Wofsy, S. C. (2010). A continuous measure of gross primary production for the conterminous United States derived from MODIS and AmeriFlux data. *Remote Sensing of Environment, 114*(3), 576-591. doi: DOI 10.1016/j.rse.2009.10.013

Zhao, M. S., Heinsch, F. A., Nemani, R. R., & Running, S. W. (2005). Improvements of the MODIS terrestrial gross and net primary production global data set. *Remote Sensing of Environment, 95*(2), 164-176. doi: DOI 10.1016/j.rse.2004.12.011

Zhao, M. S., & Running, S. W. (2010). Drought-Induced Reduction in Global Terrestrial Net Primary Production from 2000 Through 2009. *Science, 329*(5994), 940-943. doi: DOI 10.1126/science.1192666

Zhao, M. S., Running, S. W., & Nemani, R. R. (2006). Sensitivity of Moderate Resolution Imaging Spectroradiometer (MODIS) terrestrial primary production to the accuracy of meteorological reanalyses. *Journal of Geophysical Research-Biogeosciences, 111*(G1). doi: Artn G01002, Doi 10.1029/2004jg000004

CHAPTER 6

SUMMARY, CONCLUSIONS AND FUTURE RESEARCH

6.1 Summary

The Southeastern United States (SEUS) has recently experienced an exceptionally severe drought, with below normal precipitation being recorded for multiple consecutive years, starting in winter 2005/2006. Impacts from widespread hot and dry conditions in the region were significant, including water levels falling to record lows and local terrestrial ecosystems being affected by wildfires. During the extreme 2007 drought, areas used for agriculture in the Southeast (currently approximately 34% of the region's land area) were impacted by reduced rainfall, resulting in economic losses to major field crops surpassing US$1.3 billion Future impacts in the SEUS resulting from extreme hydroclimatic events are expected, as recent literature has presented an increase in frequency of such events in the region, with the potential of becoming even more significant under predicted changes in climate. In this context, this dissertation characterized the spatial and temporal variation of hydroclimatic events in the Southeast, emphasizing severe and extreme events. Further, the work identified relationships between water balance and vegetation status, represented by descriptors derived from remotely-sensed images, including greenness, water content and vegetation primary productivity.

Chapter 2 introduced background information relevant to methodologies and results presented by this set of investigations. The area of study was characterized, including descriptions of its land cover, climate and climatic variability. In addition, remote sensing and the spectral characterization of targets in general, but particularly of vegetation and soil, were presented. Further, the review introduced concepts and challenges related to scaling plant biophysical attributes and processes. In this context, emphasis was given to the spatial domain and to the use

of remote sensing as a scaling tool. In this respect, MODIS, the main remote sensor used by this study, was presented together with additional information and methodologies associated with MODIS products relevant to this work.

Chapter 3 analyzed the historical record of water balance surfaces for the Southeast, computed from 118 years of precipitation and temperature data for the region. Water availability was investigated at multiple time scales and the occurrence of severe and extreme dry and wet events in the area of study was analyzed. In this context, areas and periods when these events were more severe were identified and discussed. The study included the identification of areas where events are more frequent and incorporated the analysis of trends regarding changes in area affected by these events, as well as changes in climatic variability in the region.

Chapter 4 investigated variability in water balance for the 21st century, including relationships between this variability and vegetation status. The work used Enhanced Vegetation Index (EVI) and a modified Normalized Difference Water Index (NDWIm), derived from images acquired by the MODIS sensor and investigated spatiotemporal changes in vegetation photosynthetic potential and water content in the SEUS. Results showed anomalies of greenness and water content over the region and period 2000-2013 and identified relationships between indices and changes in water availability in the Southeast.

Finally, in Chapter 5 the efforts associated with the two previous works were extended, and climatic events in the region following the year 2000 were investigated together with changes in primary productivity in the Southeast. For this purpose, the study used MODIS, climate and flux data to implement and evaluate a light-use efficiency primary productivity model. Productivity, constrained by climate, was used to estimate vegetation primary productivity for multiple biomes over the region of study. Results agree with the vegetation index analysis, and anomalies of productivity were identified. The work further quantified the variability in carbon uptake in the region and discussed linkages between changes in productivity and spatiotemporal variations in water balance.

The studies reported by this dissertation included the design, implementation and testing of multiple methodological approaches to analyze large datasets, including a time series of remotely-sensed images and climate data. As a result, a significant number of software tools were developed during the execution of this research and applications involved the processing of MODIS QA/QC data during gap filling, the implementation of multiple image-derived indices and the computation of light-use efficiency primary productivity.

6.2 Conclusions

Climatic variability is a feature of the climate in the Southeastern United States. Analyses of the historical record indicated multiple instances of dry and wet periods since 1896 over the region. This work represented the history of these events and identified multiple severe and extreme dry and wet periods in the region. Climate analysis in the Southeast also indicated recent increase in climatic variability for time intervals ranging from 5 to 30 years. Further, findings regarding recent upward trends in area affected by severe and extreme droughts in the Southeast are also significant. This work directly addresses current concerns and uncertainties regarding changes in the frequency and areal distribution of climatic events occurring in the Southeast.

Observations of spatiotemporal linkages between climate descriptors and vegetation status, including photosynthetic potential, plant water content and primary productivity, indicate that vegetation responded to changes in water availability during the first years of the 21st century. Considering observed trends and climate projections for the region, it is expected that events of climate will negatively affect the Southeast in the future. The identification and quantification of vegetation responses to these events support the management of natural and man-made resources in the region and are critical for the definition of adaptation strategies.

Our understanding of the complex interactions involving the geobiosphere often requires the consideration of variables and processes across different spatial and temporal scales. Scaling is a complex problem and the comprehension of factors and methods associated with transitioning

from one scale to another can increase our understanding of a transforming environment. In this respect, efforts associated with measuring biophysical properties of vegetation at the regional scale greatly benefit from the continuous acquisition and analysis of remotely-sensed data, including the identification of linkages between these data and natural or anthropogenic phenomena.

6.3 Future Research

Works developed as part of this dissertation can be incorporated into other investigations as baseline data, for regional characterization and representation, or as part of input datasets for time series analysis and data modeling. The studies presented here also can be extended by addressing new research questions and by incorporating data processing steps, including new techniques, into this project's workflow. The following considerations include possibilities for expanding the current research.

- Although MODIS provides powerful tools for environmental characterization, the currently available time series of MODIS data is still relatively short. Works dealing with time analysis at the regional level can benefit from advances in the use of other satellite systems and sensors. In particular, future research may involve extending the current datasets to periods predating the launch of the Terra satellite. One such possibility involves current efforts regarding time series continuity using data from the Advanced Very High Resolution Radiometer (AVHRR) sensor, onboard NOAA satellites.
- It is fundamental to assess and better understand the limits of detectability of environmental phenomena when using remotely sensed data. Due to their nature, events such as droughts and the effects of droughts on biota are particularly challenging to be identified, both in the field as well as by remote sensing. Further research is necessary to improve methods and tools to support a better understanding of these limits.

- Similarly, scaling-up from stand level to orbital level is still a challenge, particularly when involving undersampled areas and the difficulties in identifying relationships and linkages between different scales. In this respect, scaling at the temporal level also should be improved.
- Further efforts are required to understand limits of functioning for different ecosystems and tipping points when these systems collapse. Although the relationships involved are complex and act at multiple spatial and temporal scales, such knowledge can significantly improve our ability to understand the future of important ecosystems on a changing planet.

APPENDIX A

LIST OF ACRONYMS

Table A.1: List of acronyms

	Acronym	Full description
A	ANN	Artificial Neural Network
	APAR	Absorbed Photosynthetically Active Radiation
	AVHRR	Advanced Very High Resolution Radiometer
B	BPLUT	Biome Properties Look-Up Table
	BRDF	Bidirectional Reflectance Distribution Function
	BRF	Bidirectional Reflectance Factor
C	CAI	Climatologically-Aided Interpolation
	CBM	Center for Biosystems Modelling
	CMIP-5	Coupled Model Intercomparison Project Phase 5
	CV-MVC	Constrained View-Maximum Value Composite
E	ENSO	El Niño Southern Oscillation
	EVI	Enhanced Vegetation Index
F	FPAR	Fraction of Photosynthetically Active Radiation
G	GCM	General Circulation Model
	GMAO	Global Modeling Assimilation Office
	GPP	Gross Primary Productivity
I	IPCC	United Nations Intergovernmental Panel for Climate Change
	IRGA	Infrared Gas Analyzer
L	LAI	Leaf Area Index
	LPDAAC	Land Processes-Distributed Active Archive Center
M	MDS	Marginal Distribution Sampling
	MOD12Q1	MODIS Land Cover Product
	MOD13A2	MODIS Vegetation Index product
	MOD15A2	MODIS FPAR/LAI product
	MOD17A2	MODIS Primary Productivity
	MODIS	Moderate Resolution Imaging Spectroradiometer
	MR	Maintenance Respiration
	MVC	Maximum Value Composite
N	NASA	United States National Aeronautics Space Administration
	NCDC	United States National Climatic Data Center
	NDVI	Normalized Difference Vegetation Index
	NEE	Net Ecosystem Exchange
	NOAA	United States National Oceanic and Atmospheric Administration
	NPP	Net Primary Production
	NTSG	Numerical Terradynamic Simulation Group
P	PAR	Photosynthetically Active Radiation
	PDSI	Palmer Drought Severity Index
	PET	Potential Evapotranspiration

	PRISM	Parameter-elevation Regressions on Independent Slopes Model
Q	QA/QC	Quality Assurance/Quality Check
S	SATS	Severity-Area-Time Scale
	SEUS	Southeastern United States
	SLA	Specific Leaf Area
	SPEI	Standardized Precipitation-Evapotranspiration Index
	SPI	Standardized Precipitation Index
U	USGS	United States Geological Survey
V	VPD	Vapor Pressure Deficit

APPENDIX B

CLIMATE NORMALS (1981-2010) FOR THE SOUTHEASTERN UNITED STATES

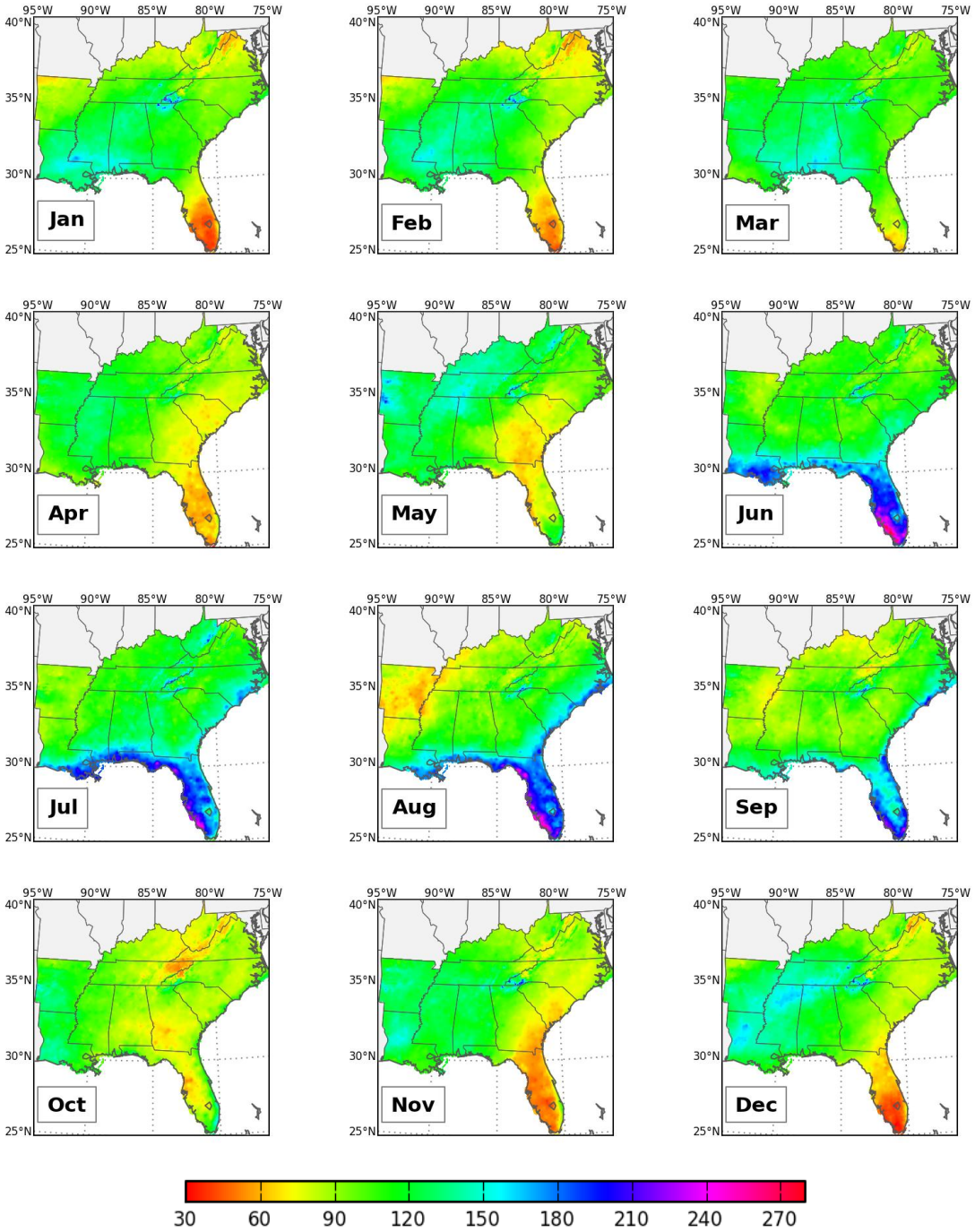

Figure B.1: Monthly total precipitation normals (mm) (data source: PRISM Climate Group)

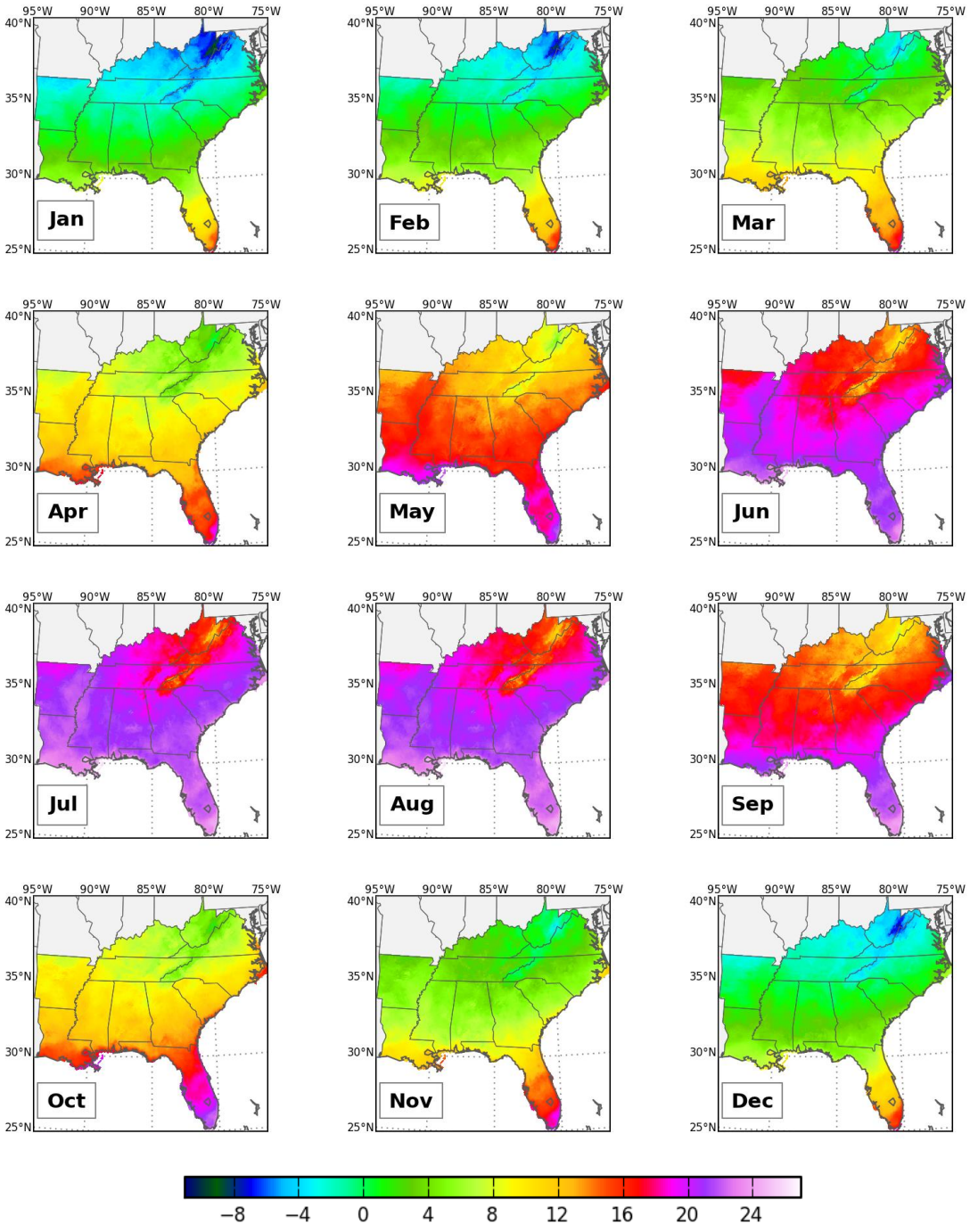

Figure B.2: Monthly minimum temperature normals (^{o}C) (data source: PRISM Climate Group)

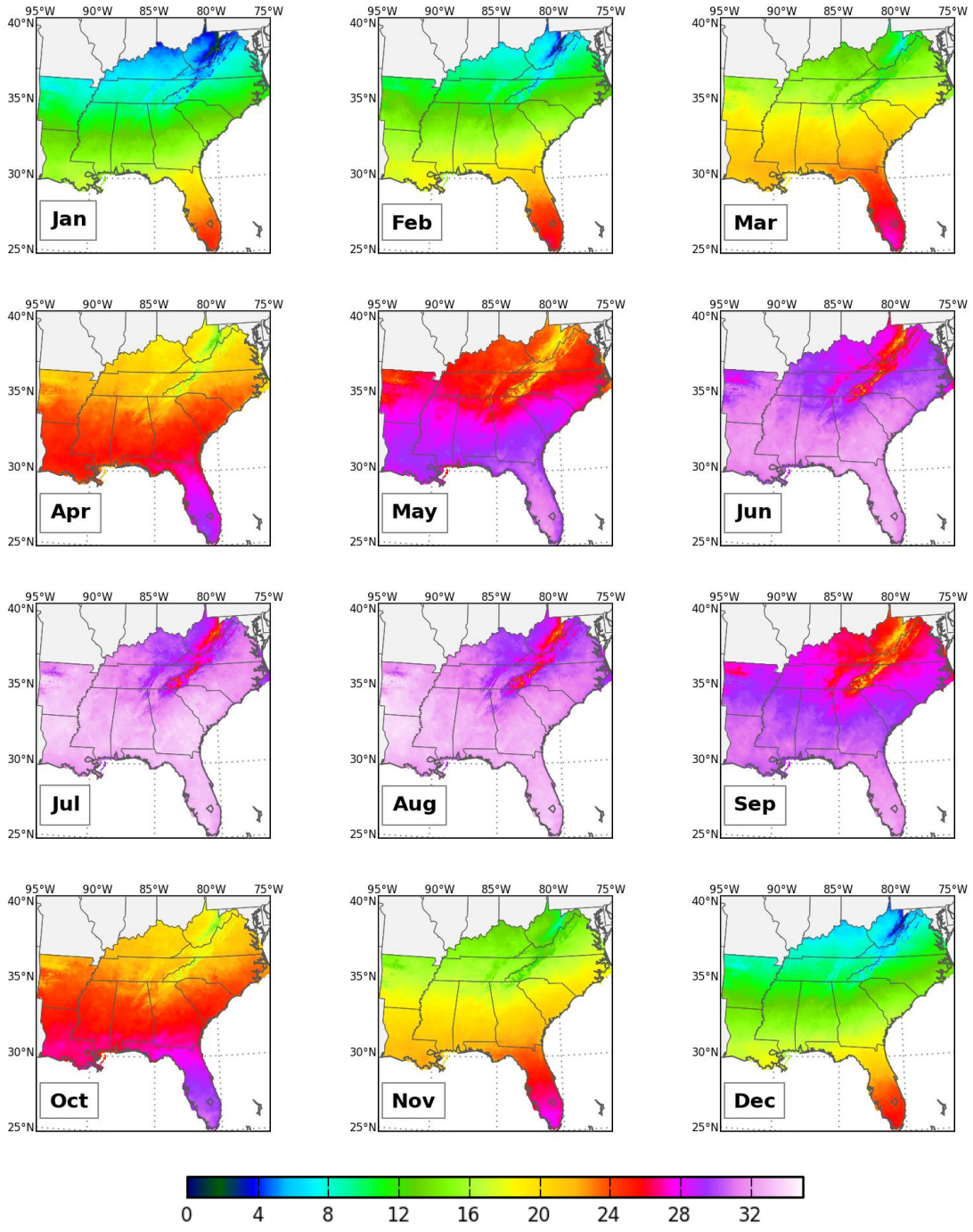

Figure B.3: Monthly maximum temperature normals (^{o}C) (data source: PRISM Climate Group)

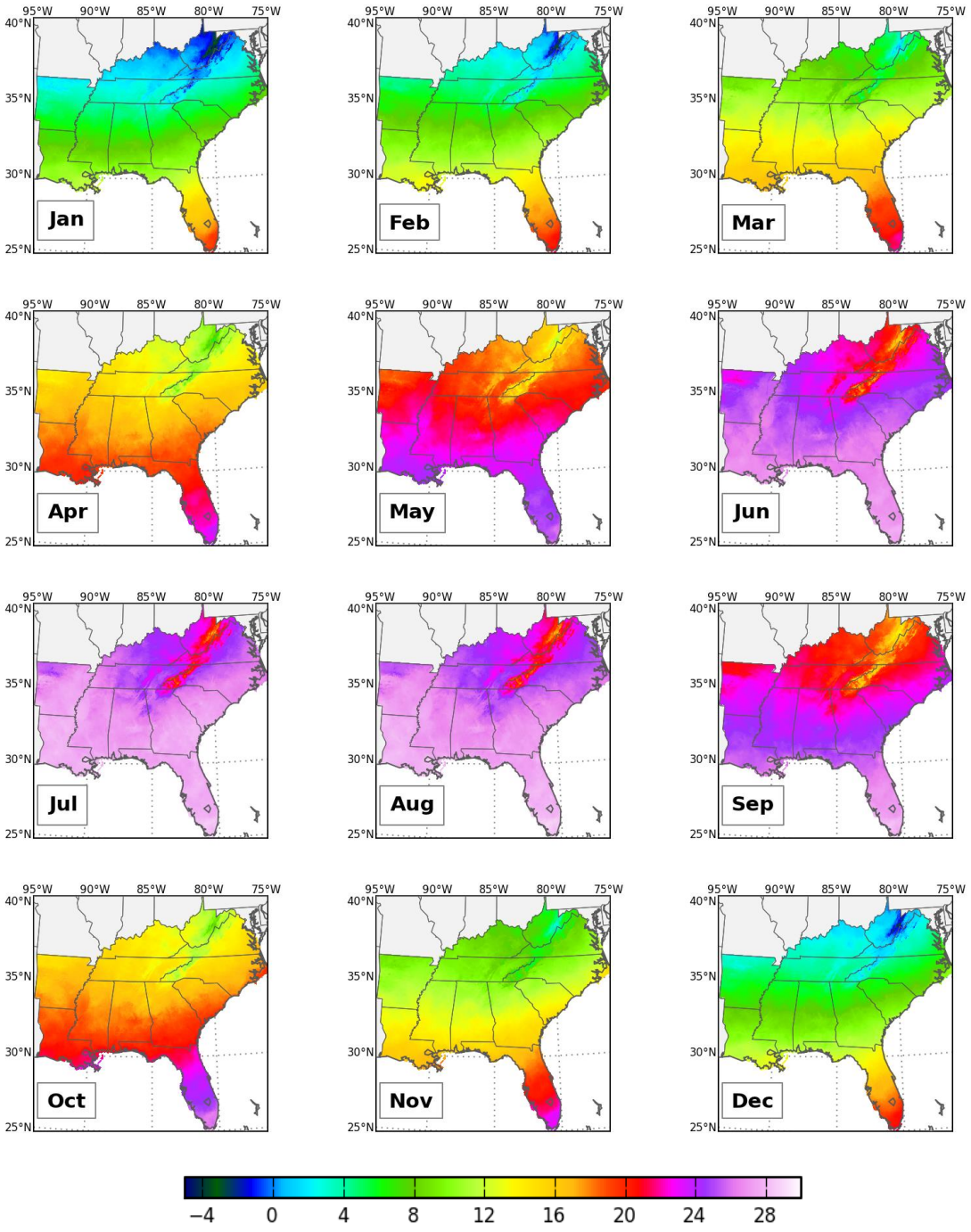

Figure B.4: Monthly mean temperature normals (^{o}C) (data source: PRISM Climate Group)

APPENDIX C

CLIMATE DIVISIONS IN THE SOUTHEASTERN UNITED STATES

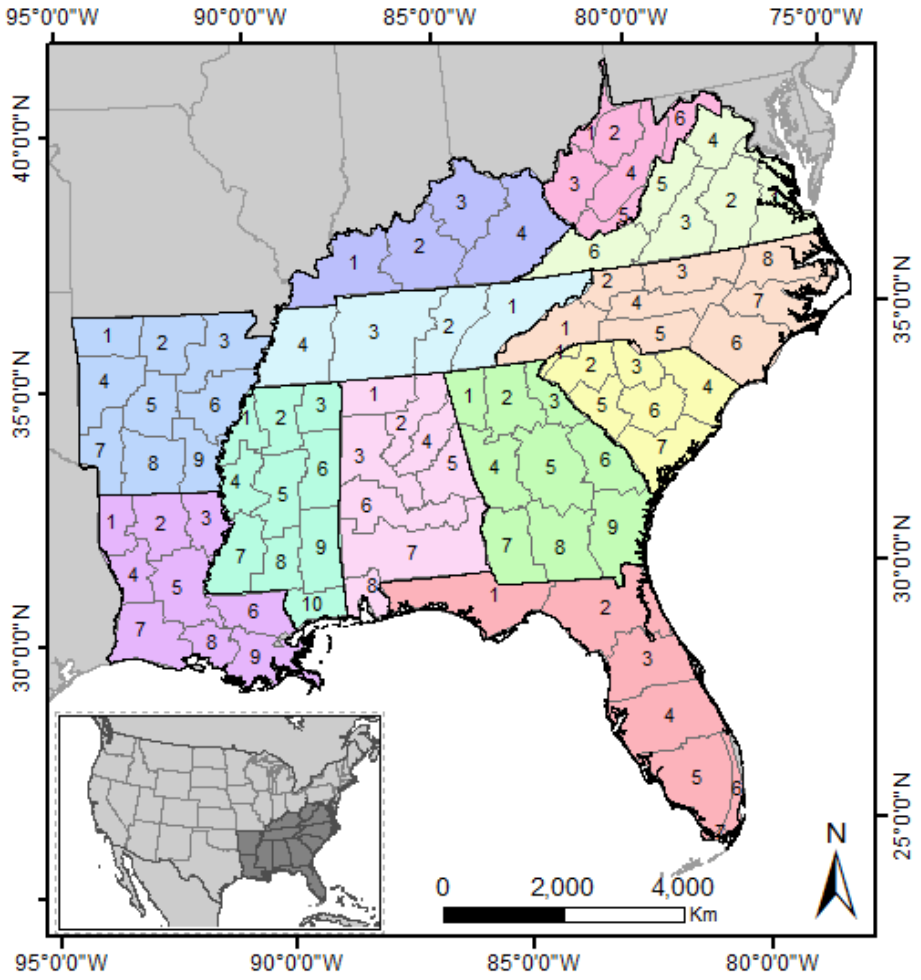

Alabama	1	Northern Valley
	2	Appalachian Mountain
	3	Upper Plains
	4	Eastern Valley
	5	Piedmont Plateau
	6	Prairie
	7	Coastal Plain
	8	Gulf

Mississippi	1	Upper Delta
	2	North Central
	3	Northeast
	4	Lower Delta
	5	Central
	6	East Central
	7	Southwest
	8	South Central
	9	Southeast
	10	Coastal

Arkansas	1	Northwest
	2	North Central
	3	Northeast
	4	West Central
	5	Central
	6	East Central
	7	Southwest
	8	South Central
	9	Southeast
Florida	1	Northwest
	2	North
	3	North Central
	4	South Central
	5	Everglades & Sw Coast
	6	Lower East Coast
	7	Keys
Georgia	1	Northwest
	2	North Central
	3	Northeast
	4	West Central
	5	Central
	6	East Central
	7	Southwest
	8	South Central
	9	Southeast
Kentucky	1	Western
	2	Central
	3	Blue Grass
	4	Eastern
Louisiana	1	Northwest
	2	North Central
	3	Northeast
	4	West Central
	5	Central
	6	East Central
	7	Southwest
	8	South Central
	9	Southeast
North Carolina	1	Southern Mountains
	2	Northern Mountains
	3	Northern Piedmont
	4	Central Piedmont
	5	Southern Piedmont
	6	Southern Coastal Plain
	7	Central Coastal Plain
	8	Northern Coastal Plain
South Carolina	1	Mountain
	2	Northwest
	3	North Central
	4	Northeast
	5	West Central
	6	Central
	7	Southern
Tennessee	1	Eastern
	2	Cumberland Plateau
	3	Middle
	4	Western
Virginia	1	Tidewater
	2	Eastern Piedmont
	3	Western Piedmont
	4	Northern
	5	Central Mountain
	6	Southwestern Mountain
West Virginia	1	Northwestern
	2	North Central
	3	Southwestern
	4	Central
	5	Southern
	6	Northeastern

Figure C.1: Spatial distribution of climate divisions considered by this investigation (source: NOAA)

APPENDIX D

SIGNIFICANT SEVERE AND EXTREME DRY EVENTS IN THE SEUS

FOR THE PERIOD 1896-2012

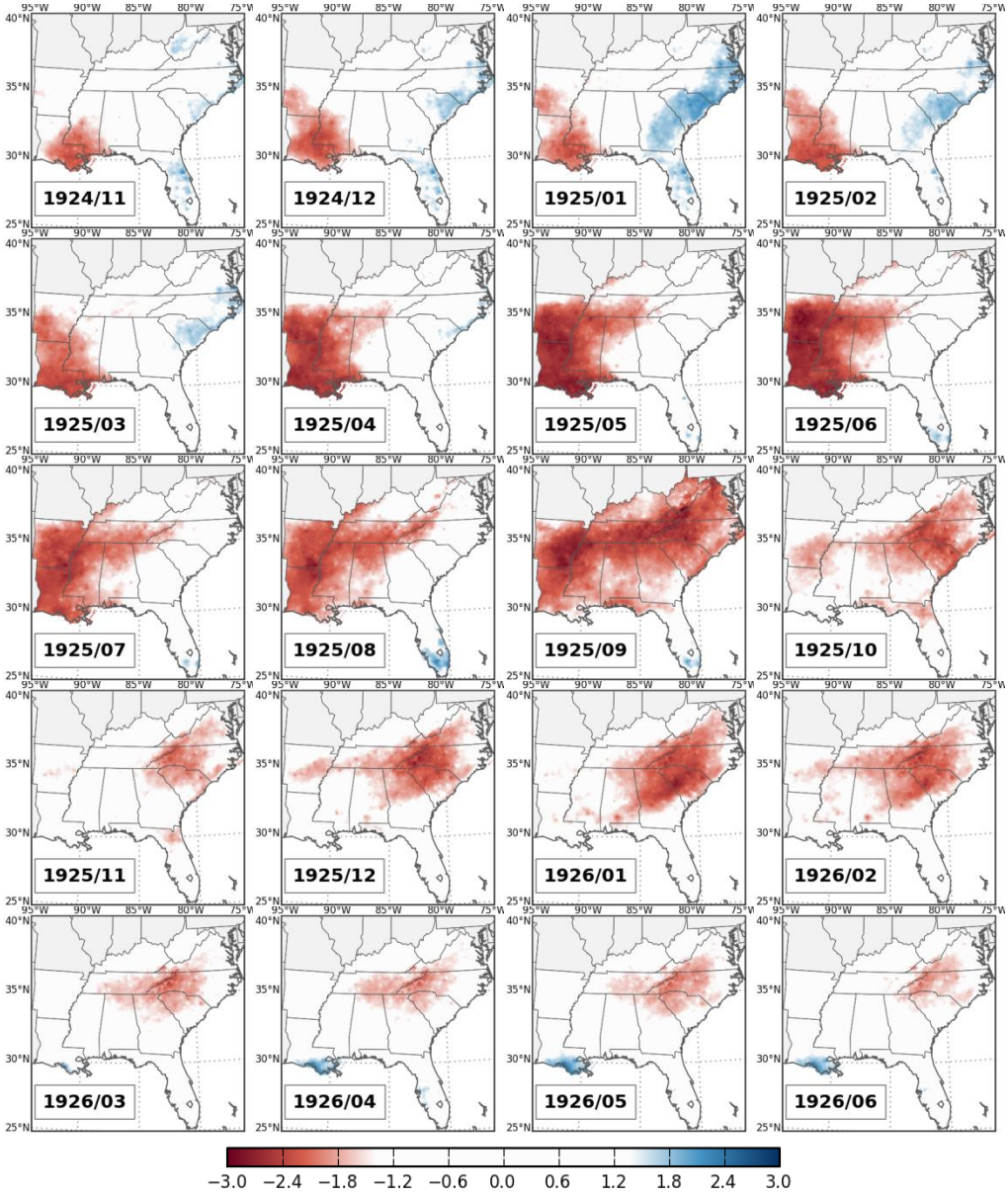

Figure D.1: Area of the SEUS under severe and extreme dry events (SPEI ≤ -1.5, in red) and severe and extreme wet events (SPEI ≥ 1.5, in blue), for 12-month SPEI, for months of 1924-1926.

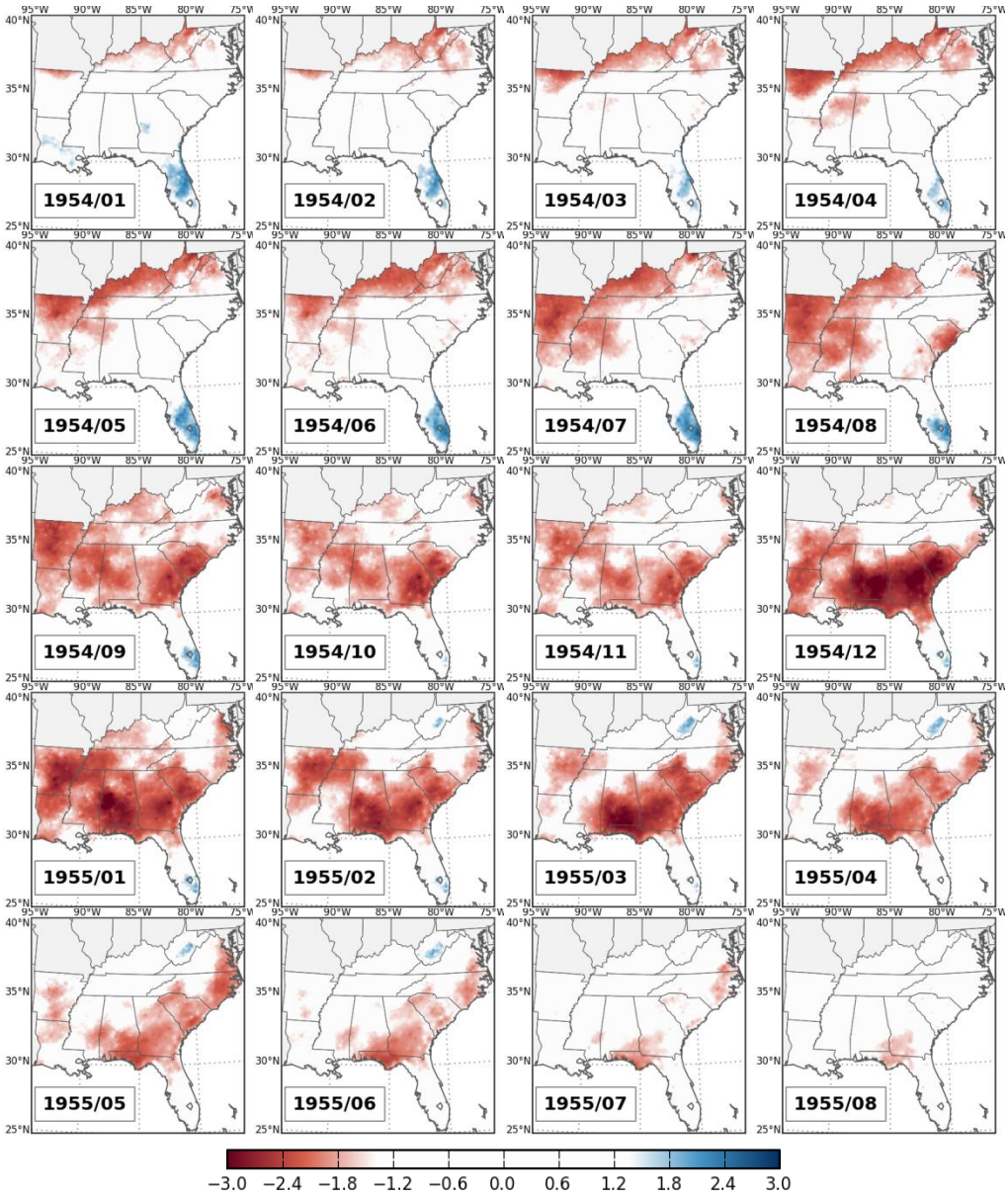

Figure D.2: Area of the SEUS under severe and extreme dry events (SPEI ≤ -1.5, in red) and severe and extreme wet events (SPEI ≥ 1.5, in blue), for 12-month SPEI, for months of 1954-1955.

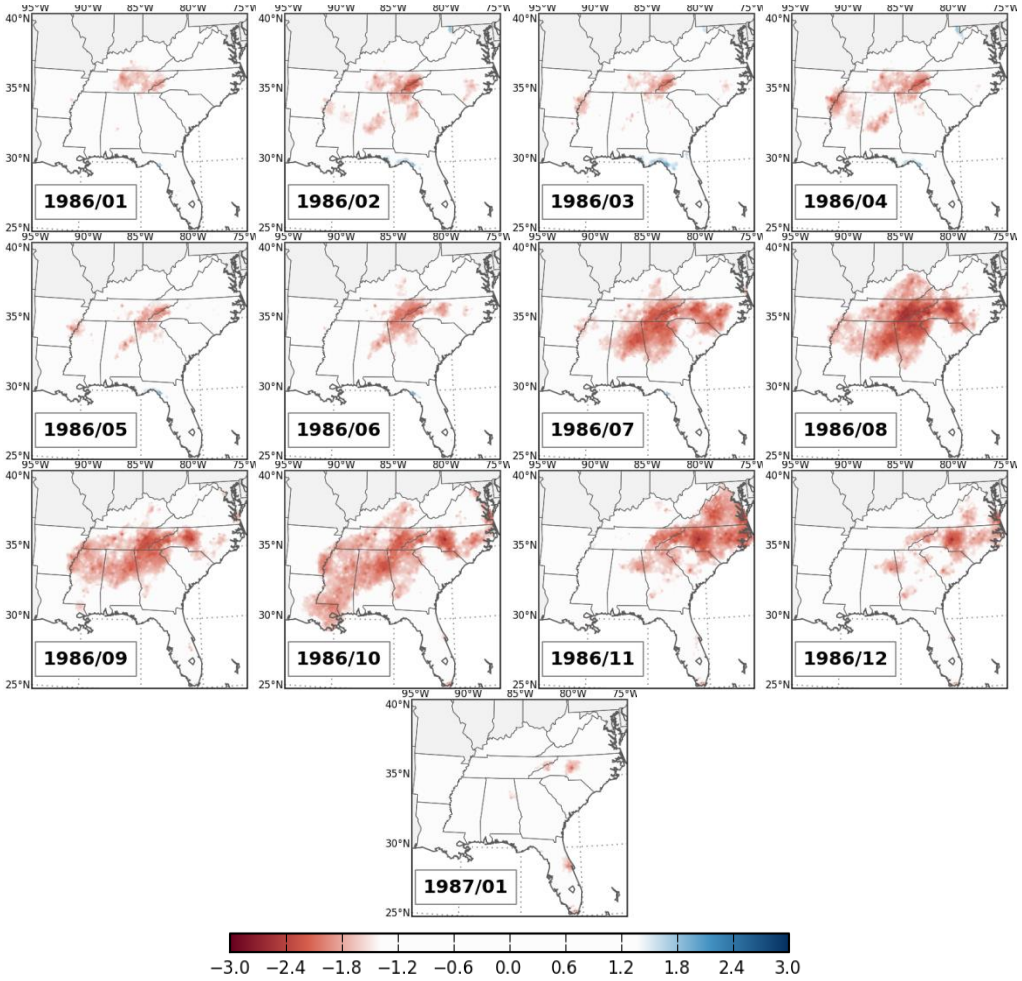

Figure D.3: Area of the SEUS under severe and extreme dry events (SPEI ≤ -1.5, in red) and severe and extreme wet events (SPEI ≥ 1.5, in blue), for 12-month SPEI, for months of 1986-1987.

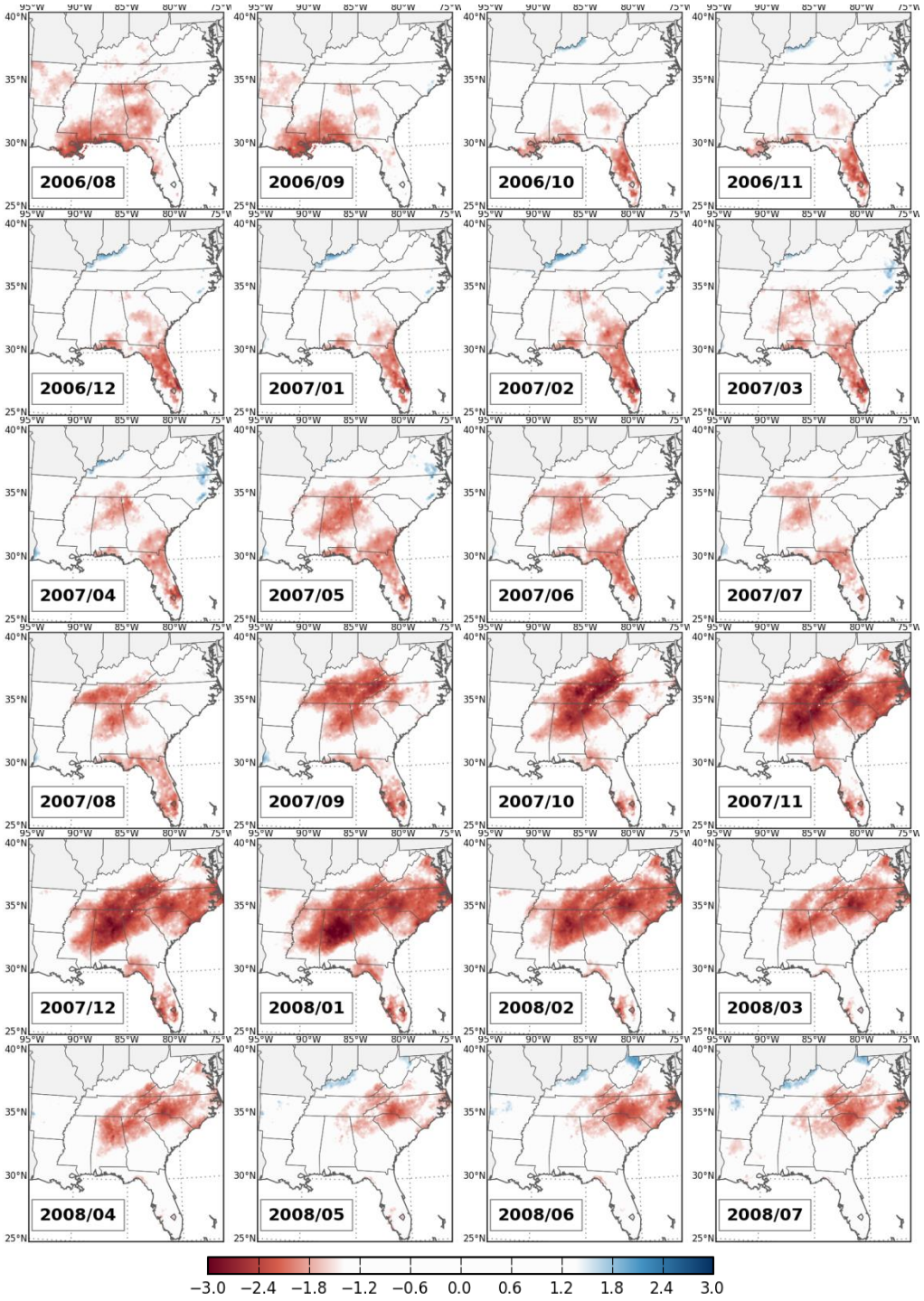

Figure D.4: Area of the SEUS under severe and extreme dry events (SPEI ≤ -1.5, in red) and severe and extreme wet events (SPEI ≥ 1.5, in blue), for 12-month SPEI, for months of 2006-2008.

APPENDIX E

SIGNIFICANT SEVERE AND EXTREME WET EVENTS IN THE SEUS

FOR THE PERIOD 1896-2012

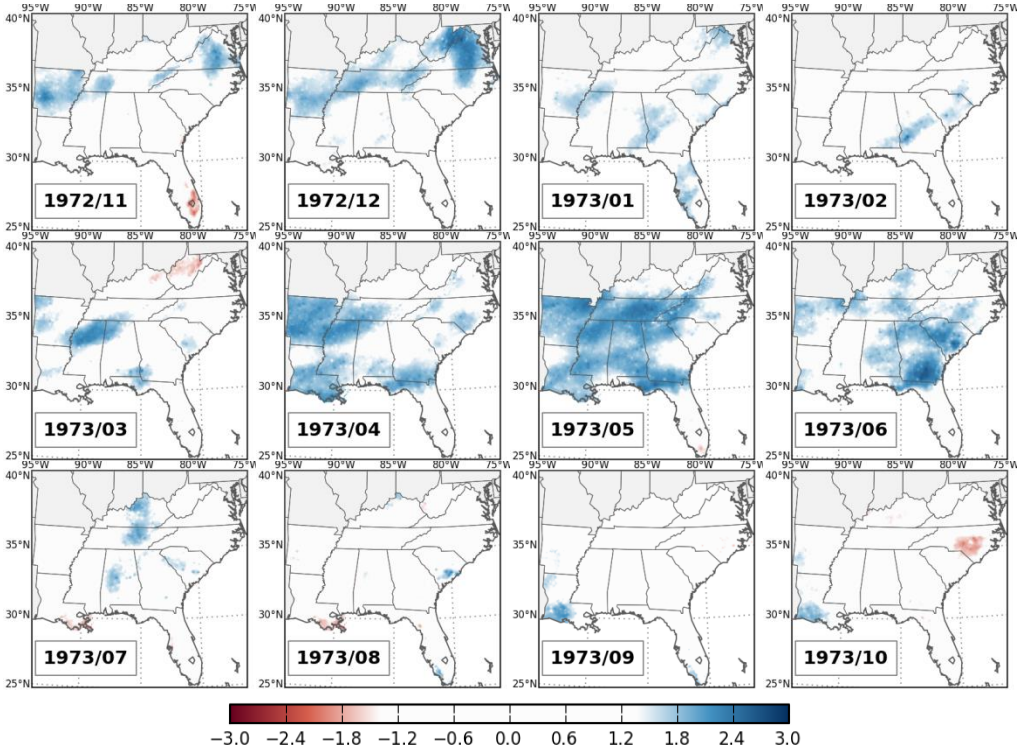

Figure E.1: Area of the SEUS under severe and extreme dry events (SPEI ≤ -1.5, in red) and severe and extreme wet events (SPEI ≥ 1.5, in blue), for 3-month SPEI, for months of 1972-1973.

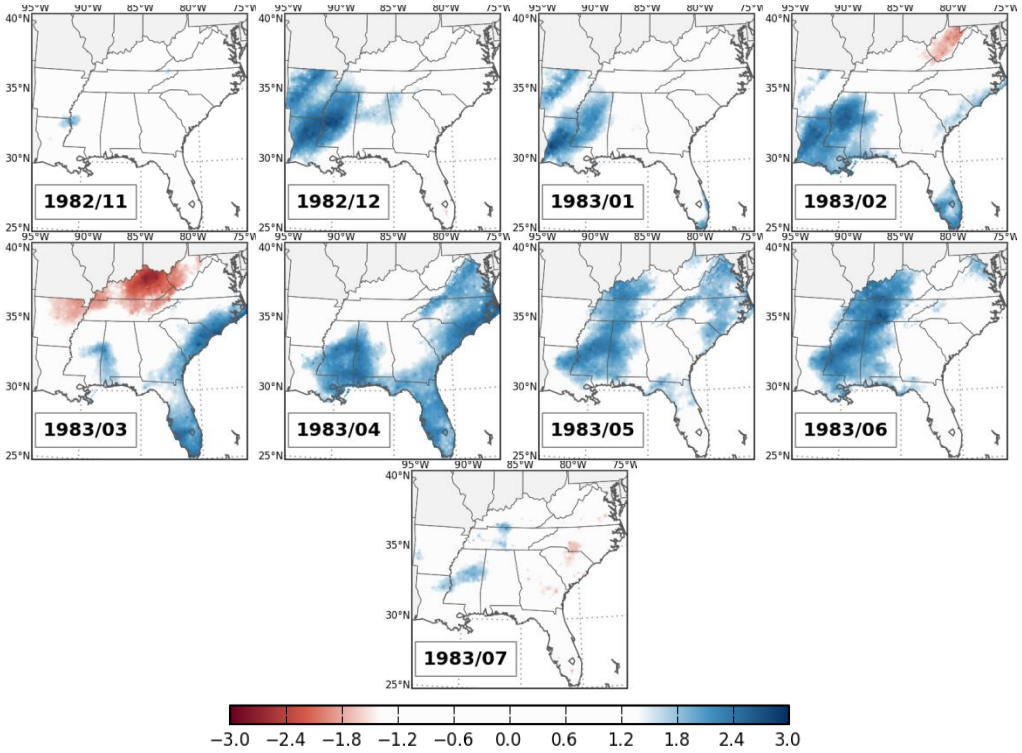

Figure E.2: Area of the SEUS under severe and extreme dry events (SPEI ≤ -1.5, in red) and severe and extreme wet events (SPEI ≥ 1.5, in blue), for 3-month SPEI, for months of 1982-1983.

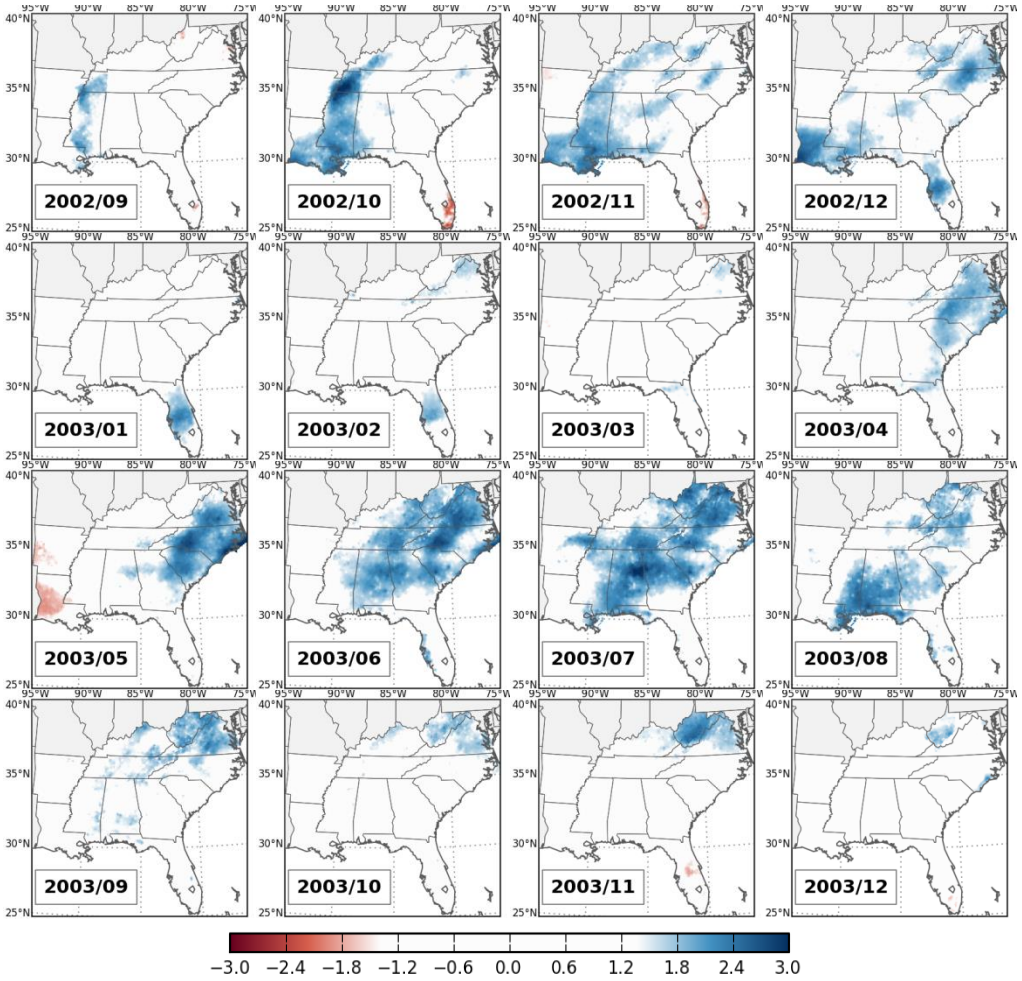

Figure E.3: Area of the SEUS under severe and extreme dry events (SPEI ≤ -1.5, in red) and severe and extreme wet events (SPEI ≥ 1.5, in blue), for 3-month SPEI, for months of 2002-2003.

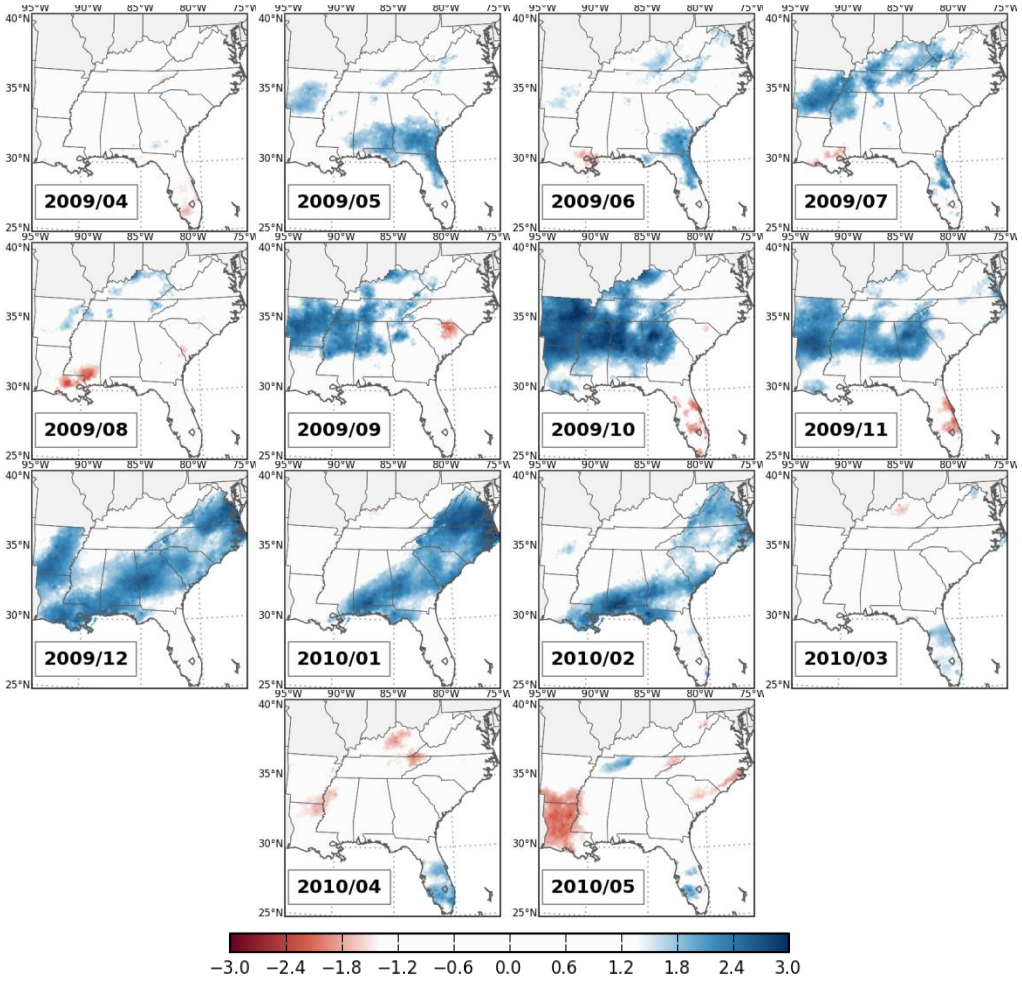

Figure E.4: Area of the SEUS under severe and extreme dry events (SPEI ≤ -1.5, in red) and severe and extreme wet events (SPEI ≥ 1.5, in blue), for 3-month SPEI, for months of 2009-2010.

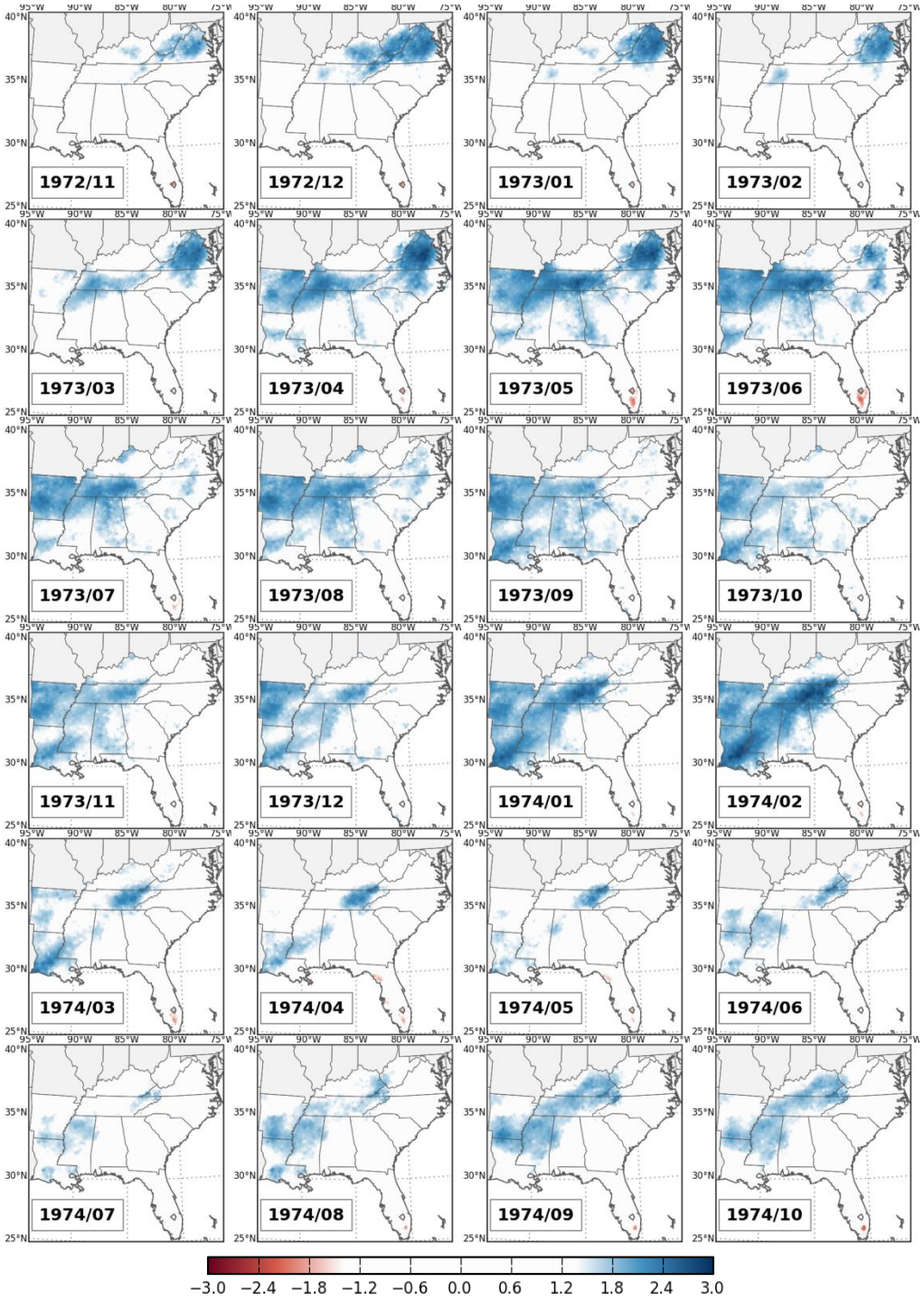

Figure E.5: Area of the SEUS under severe and extreme dry events (SPEI ≤ -1.5, in red) and severe and extreme wet events (SPEI ≥ 1.5, in blue), for 12-month SPEI, for months of 1972-1974.

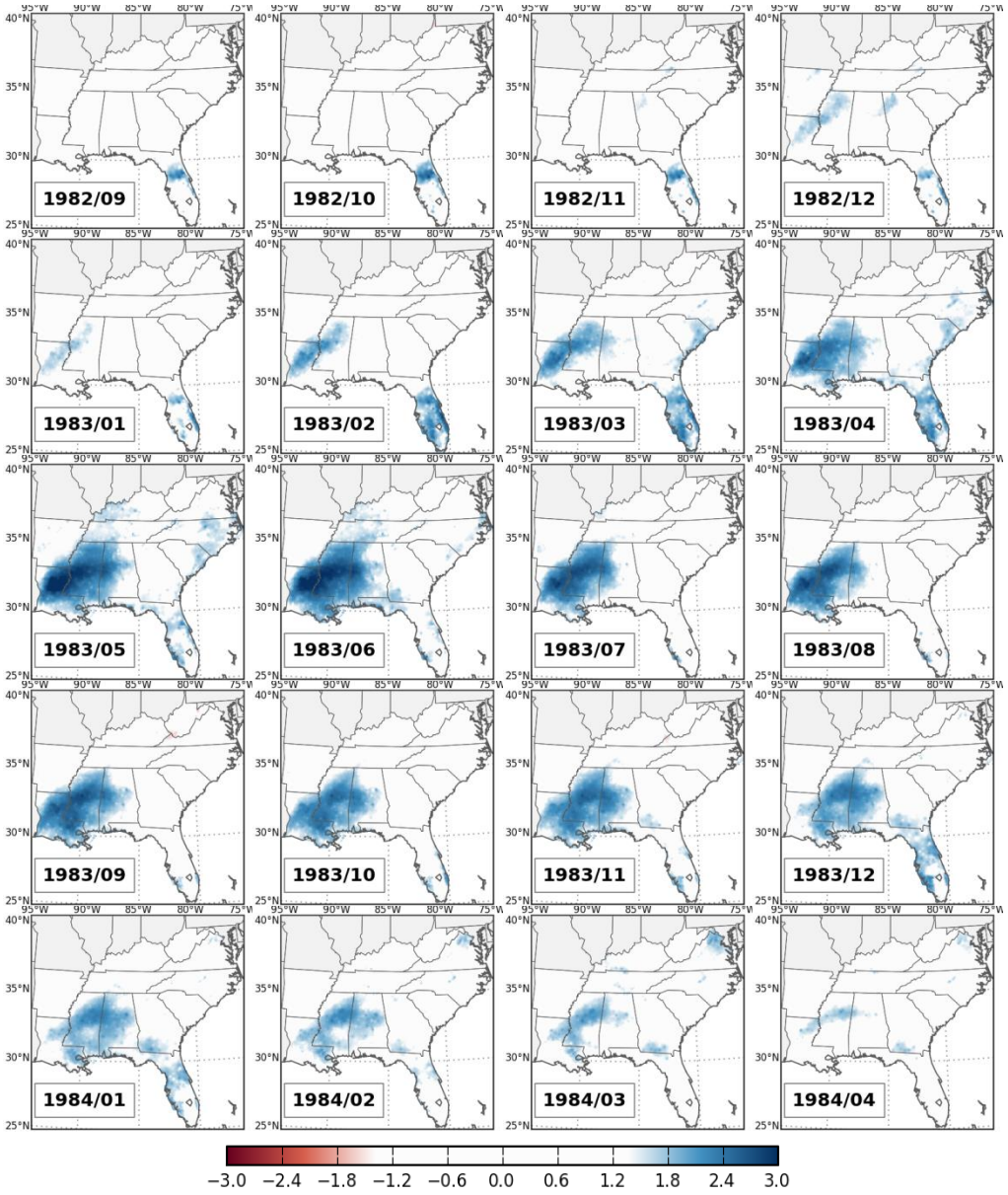

Figure E.6: Area of the SEUS under severe and extreme dry events (SPEI ≤ -1.5, in red) and severe and extreme wet events (SPEI ≥ 1.5, in blue), for 12-month SPEI, for months of 1982-1984.

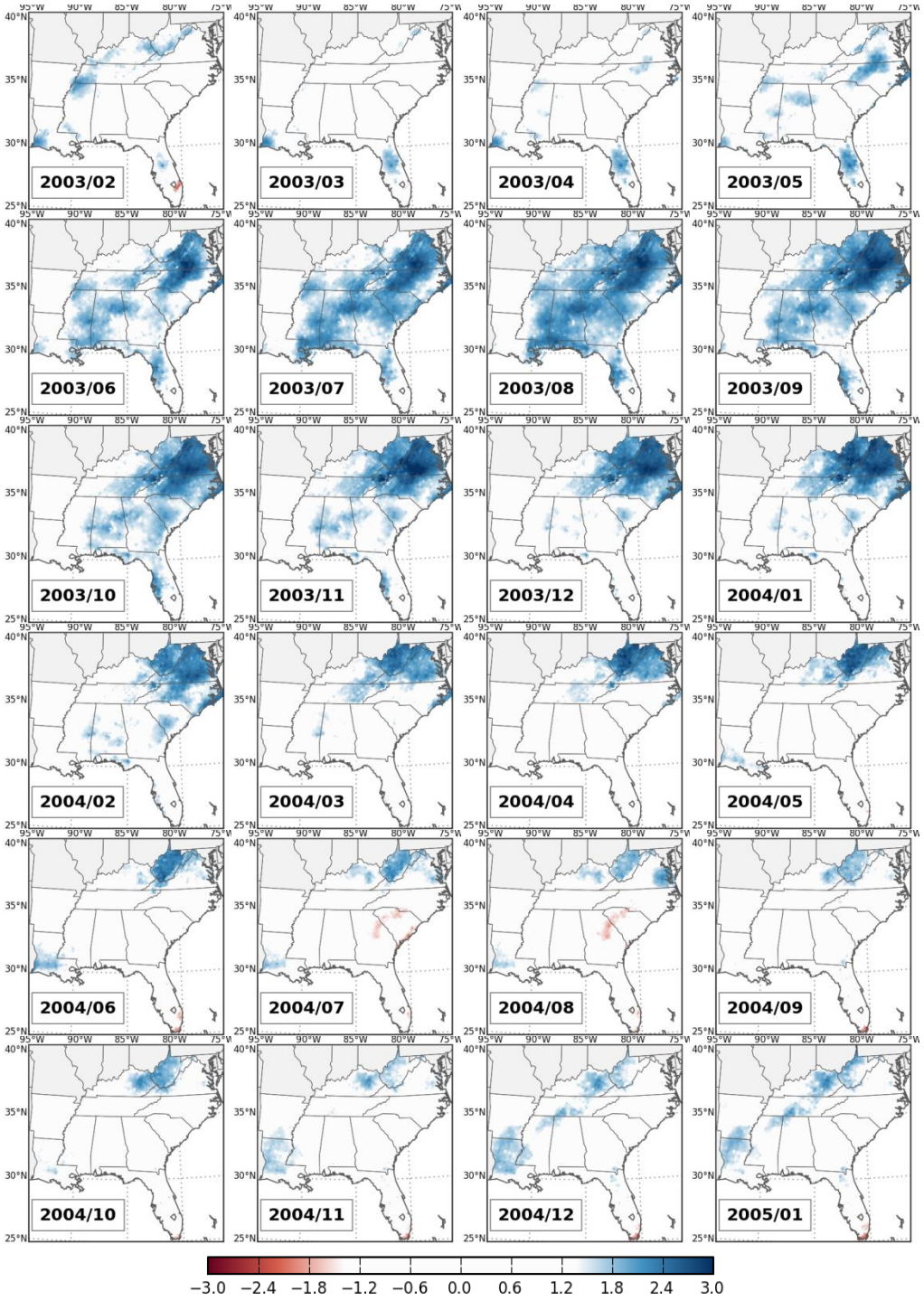

Figure E.7: Area of the SEUS under severe and extreme dry events (SPEI ≤ -1.5, in red) and severe and extreme wet events (SPEI ≥ 1.5, in blue), for 12-month SPEI, for months of 2003-2004.

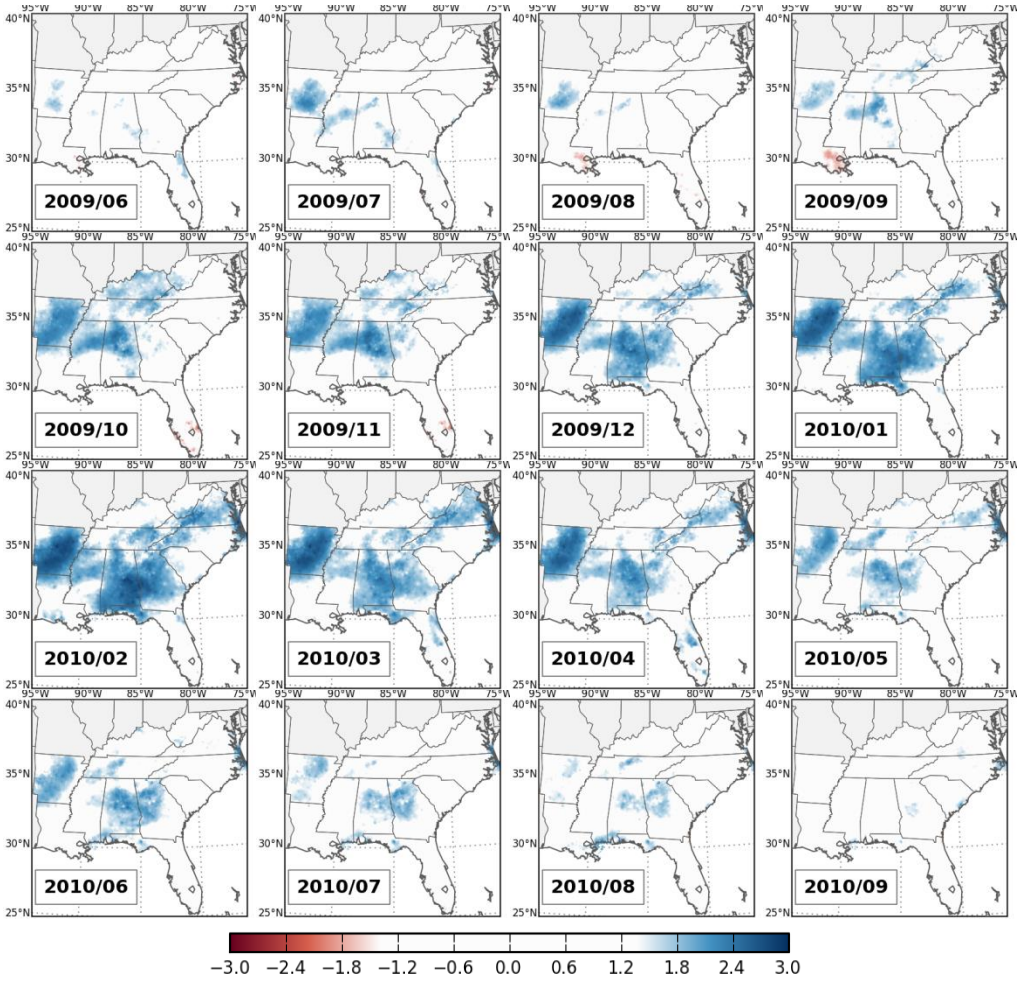

Figure E.8: Area of the SEUS under severe and extreme dry events (SPEI ≤ -1.5, in red) and severe and extreme wet events (SPEI ≥ 1.5, in blue), for 12-month SPEI, for months of 2009-2010.